UFL/COEL-95/020

LABORATORY MOBILE BED MODEL STUDIES ON INLET PART I: MODELING LAW ON PROFILE RESPONSE

---

by

Xu Wang
Lihwa Lin
and
Hsiang Wang

1995

Sponsored by

Florida Sea Grant College
Sea Grant Project No. R/C-S-33
Grant No. NA36RG0070

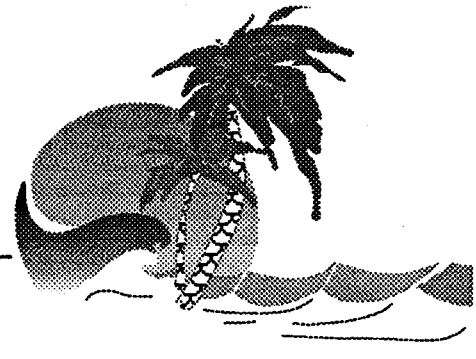

Coastal & Oceanographic Engineering Department
433 Weil Hall • P.O. Box 116590 • Gainesville, Florida 32611-6590

UNIVERSITY OF
FLORIDA

TABLE OF CONTENTS

LIST OF FIGURES iii

LIST OF TABLES ix

1 INTRODUCTION 1

2 LITERATURE REVIEW 4

3 APPROACH TO PHYSICAL MOVABLE-BED MODELING LAW . . . 16
3.1 Principles of Similarity 17
3.1.1 Dynamic Similarity 17
3.1.2 Similarity By Dimensional Analysis 20
3.1.3 Similarity By non-dimensionalizing the governing Equations . 21
3.2 Physical Modeling Laws Of Beach Response 21

4 LABORATORY EXPERIMENTS 29
4.1 Test Facilities 29
4.1.1 Air-Sea Wave Tank 29
4.1.2 Wave Flume Facility 30
4.1.3 Wave Basin Facility 30
4.2 Initial Beach Profile Design 31
4.2.1 Experimental Procedures 37
4.2.2 Test Conditions 38
4.3 Test Results and Data Analysis 42
4.3.1 Profile Classifications of the Test Results 44
4.3.2 Volumetric Changes along the Profiles 44
4.3.3 Beach Erosion 46
4.3.4 Profile Evolution and Bar Migration 48
4.3.5 Eqilibrium Beach Profile 54

5 EVALUATION OF SCALING LAWS 68
5.1 Methodology and Evaluation Criteria 68
5.1.1 Geometrical Scaling and Equilibrium Profile 70
5.1.2 Wave Height and Wave Period Scaling 73
5.1.3 Evaluation of Morphological Time Scale 74
5.1.4 Summary of Two-Dimensional Test Results 92
5.1.5 Test Results from Three-Dimensional Basin 92
5.2 Test Results from Undistorted Model 103

6 SUMMARY AND CONCLUSION 111

APPENDIX

A BEACH PROFILE EVOLUTION AND SEDIMENT TRANSPORT RATE 116

REFERENCES 142

LIST OF FIGURES

4.1	Initial Beach Profile In Prototype	32
4.2	Cumulative Sand Size Distribution	33
4.3	Fall Velocity Of Spherical Grains As A Function Of Size, Rouse (1937)	34
4.4	Designed Initial Beach Profile in Model with $D_{50} = 0.20mm$	36
4.5	Example of Beach Profile with Diffused Bar, $D_{50} = 0.09mm$	45
4.6	Definition Of Net Sediment Transport Rate Across The Beach Profile	47
4.7	Dune Erosion Evolution With Elapsed Time in ASW(1)	49
4.8	Dune Erosion Evolution With Elapsed Time in ASW(2)	50
4.9	Dune Erosion Evolution With Elapsed Time in WF	51
4.10	Dune Erosion Evolution With Elapsed Time in WB	52
4.11	Definition of Longshore Bar With Respect to Initial Profile	53
4.12	Horizontal Movement Of Bar Crest With Horizontal Scale Equal to 20 In ASW	56
4.13	Horizontal Movement Of Bar Crest With Horizontal Scale Equal to 20 In WF	57
4.14	Horizontal Movement Of Bar Mass Center With Horizontal Scale Equal to 20 In ASW	58
4.15	Horizontal Movement Of Bar Mass Center With Horizontal Scale Equal to 20 In WF	59
4.16	Growth of Bar Volume With Horizontal Scale Equal to 20 In ASW	60
4.17	Growth of Bar Volume With Horizontal Scale Equal to 20 In WF	61
4.18	Horizontal Movement Of Bar Crest With Horizontal Scale Equal to 30.	62

4.19	Horizontal Movement Of Bar Mass Center With Horizontal Scale Equal to 30.	62
4.20	Growth Of Bar Volume With Horizontal Scale Equal to 30.	63
4.21	Horizontal Movement Of Bar Crest With Horizontal Scale Equal to 40.	63
4.22	Horizontal Movement Of Bar Mass Center With Horizontal Scale Equal to 40.	64
4.23	Growth Of Bar Volume With Horizontal Scale Equal to 40.	64
4.24	Horizontal Movement Of Bar Crest With $D_{50} = 0.09mm$	65
4.25	Horizontal Movement Of Bar Mass Center With $D_{50} = 0.09mm$	65
4.26	Growth Of Bar Volume With $D_{50} = 0.09mm$	66
4.27	Beach Profile Evolution And Sediment Transport Rate	67
5.1	Definition of The Dune and Bar Regions	69
5.2	Equilibrium Profile Comparison Between Model Test Results and Modeling Laws	72
5.3	ASW Model Tests and Prototype Final Profile Comparison (1)	75
5.4	ASW Model Tests and Prototype Final Profile Comparison (2)	76
5.5	ASW Model Tests and Prototype Final Profile Comparison (3)	77
5.6	WF Model Tests and Prototype Final Profile Comparison	78
5.7	Dune Volume Erosion Error Criterion	79
5.8	The RMS Error of The Bar Profile Criterion	80
5.9	Bar Volume Error Criterion	81
5.10	Bar Location Error Criterion	82
5.11	Summary of ASW Test Results Based On Dune Profile Parameter	85
5.12	Summary of ASW Test Results Based On Bar Profile Parameter	86
5.13	Summary of WF Test Results Based On Dune Profile Parameter	88
5.14	Summary of WF Test Results Based On Bar Profile Parameter	89
5.15	Dune Profile Evolution Scaling from ASW results	90

5.16	Dune Profile Evolution Scaling From WF results	91
5.17	Morphological time scaling of Dune Profile RMS Value from ASW Tests	93
5.18	Morphological time scaling of Dune Profile RMS Value from WF Tests	94
5.19	Morphological time scaling of Bar Crest Location from ASW Tests	95
5.20	Morphological time scaling of Bar Mass Center Location from ASW Tests	96
5.21	Morpholigical Time Scaling of Bar Profile RMS Value from ASW Tests	97
5.22	Morphological time scaling of Bar Volume from ASW Tests	98
5.23	Morpholigical Time Scalings from WF Tests	99
5.24	Initial Profiles Comparison Between 5 Sections for Case 3	101
5.25	Final Profile Comparison Between 5 Sections for Case 3	102
5.26	Comparison of Wave Basin Model Test No.3 with Prototype	104
5.27	Morphological Time Scaling from Wave Basin Test No.1 against Prototype	105
5.28	Morphological Time Scaling from Wave Basin Test No.2 against Prototype	106
5.29	Morphological Time Scaling from Wave Basin Test No.3 against Prototype	107
5.30	Dune Erosion Volume Comparison With Prototype	108
5.31	Dune Profile RMS Comparison With Prototype	109
5.32	Summary of The Undistorted Model Test Results (shore profile)	110
5.33	Summary of The Undistorted Model Test Results (bar profile)	110
6.1	Wave Height Scale as A function of k Value	114
A.1	Beach Profile Evolution and Sediment Transport Pattern of Test No.1	117
A.2	Beach Profile Evolution and Sediment Transport Pattern of Test No.2	118

A.3 Beach Profile Evolution and Sediment Transport Pattern of Test No.3 119

A.4 Beach Profile Evolution and Sediment Transport Pattern of Test No.4 120

A.5 Beach Profile Evolution and Sediment Transport Pattern of Test No.5 121

A.6 Beach Profile Evolution and Sediment Transport Pattern of Test No.6 122

A.7 Beach Profile Evolution and Sediment Transport Pattern of Test No.7 123

A.8 Beach Profile Evolution and Sediment Transport Pattern of Test No.8 124

A.9 Beach Profile Evolution and Sediment Transport Pattern of Test No.9 125

A.10 Beach Profile Evolution and Sediment Transport Pattern of Test No.10 126

A.11 Beach Profile Evolution and Sediment Transport Pattern of Test No.11 127

A.12 Beach Profile Evolution and Sediment Transport Pattern of Test No.12 128

A.13 Beach Profile Evolution and Sediment Transport Pattern of Test No.13 129

A.14 Beach Profile Evolution and Sediment Transport Pattern of Test No.14 130

A.15 Beach Profile Evolution and Sediment Transport Pattern of Test No.16 131

A.16 Beach Profile Evolution and Sediment Transport Pattern of Test No.17 132

A.17 Beach Profile Evolution and Sediment Transport Pattern of Test No.18 133

A.18 Beach Profile Evolution and Sediment Transport Pattern of Test No.19 134

A.19 Beach Profile Evolution and Sediment Transport Pattern of Test No.20 135

A.20 Beach Profile Evolution and Sediment Transport Pattern of Test No.21 136

A.21 Beach Profile Evolution and Sediment Transport Pattern of Test No.22 137

A.22 Beach Profile Evolution and Sediment Transport Pattern of Test No.23 138

A.23 Beach Profile Evolution and Sediment Transport Pattern of Test No.24 139

A.24 Beach Profile Evolution and Sediment Transport Pattern of Test No.25 140

A.25 Beach Profile Evolution and Sediment Transport Pattern of Test No.26 141

LIST OF TABLES

3.1	Summary of Fall Speed Distorted Model Laws	22
3.2	Summary of Wave Breaking Index (γ_b)	27
4.1	Scale Ratios and Physical Dimensions in ASW Tests	35
4.2	Summary of Criteria Governing Beach Classification	39
4.3	Summary of Test Conditions in ASW	40
4.4	Summary of Beach Profile Classification Parameter for ASW . .	41
4.5	Summary of Test Conditions in the WF	42
4.6	Beach Profile Classification Parameter for WF	43
4.7	Test Conditions in Three-Dimensional Wave Basin	43
5.1	Four Fall Speed Distorted Model Laws	70
5.2	Comparison of Model Performances	83

CHAPTER 1
INTRODUCTION

Beach and dune erosion as well as the related beach profile changes that occur under storm waves and high water levels are of basic interest in coastal engineering. Numerous attempts using various techniques have been made to better understand and predict beach and dune responses under storm wave attack. Numerical simulation and laboratory experiments are two of the most commonly employed techniques.

In general, numerical models no doubt have the advantage for their quick and neat answers and usually cost much less than physical models. However, the process of beach and dune erosion is difficult to formulate owing to the inherently complicated nature of sediment fluid interaction and the highly nonlinear unsteady and nonuniform flow condition inside the surf zone. The time varying and irregular bottom changes further complicate the problem. Therefore, current workable numerical models can be considered as the first generation as all of them deal with simple macro-scale gross effects such as the total erosional volume and the final shape of the profile. Even in these terms, the predictive capability already exceeds our fundamental knowledge employed to build these models. For instance, the swash transport mechanism, the beach slope effect and the bar formation are already built in some of the models, mainly based on conjectures with no credible fundamental knowledge. Further model improvement requires better formulas based on improved fundamental understanding.

Physical models, on the other hand, can be used to reproduce the natural condition without a priori knowledge on the basic mechanisms. They also offer the opportunity of improving our understanding and provide useful data for numerical models. One of the major difficulties in physical modeling is the problem of the scale

effects, particularly when sediment transport is involved. Physical models which intend to simulate sediment transport and the associated morphological changes are also known as movable-bed models. The subject of model scaling is a difficult one, as mentioned. Numerous papers have been written proposing various similitude relationships. At present there is no general solution that is also practical. Specific modeling laws are usually only applicable to certain restricted conditions.

The beach response physical modeling has also been studied by a number of investigators. Currently, all the proposed modeling laws for beach response are for two-dimensional application and most of them are based on the main assumption, explicitly or implicitly, that within the surf zone suspended sediment is the dominant mode of transport. These modeling laws can further be classified as distorted and undistorted depending upon whether the horizontal and vertical geometrical scales have the same ratio. The general opinion is that the undistorted model is preferred over distorted model. However, distorted models are more flexible in accommodating wider ranges of variables, both in physical dimensions and other physical parameters, such as wave heights, wave lengths and sand sizes. A common weakness of the existing profile modeling laws, whether distorted or undistorted, appears to be the lack of sufficient information to adequately verify the morphological time scale, i.e., the modeling of beach evolution process as a function of time. This is an important class of problem, particularly if one is to extend the physical modeling to three-dimensional applications such as studying the morphological processes of shoreline changes or nearshore shoaling phenomena.

This study is aimed at evaluating and improving the scaling laws for distorted models guided by the modeling theory and through a series of laboratory experiments carried out at different physical scales. The study is restricted to two-dimensional application although experiments were also carried out in a three-dimensional in addition to the traditional wave tank experiments.

Chapter 2 provides a general review on the development of physical modeling laws concerning coastal sediment transport and that are specifically related to beach profile response modeling. Chapter 3 reviews the basic similitude theorem and summarizes existing beach profile modeling laws and their origins. A modified modeling law based on the work of Wang et al. (1990) was also derived. These modeling laws are evaluated by the results obtained in the subsequent laboratory model tests. Chapter 4 describes the various types of experiments being carried out both in 2-D wave tanks and in the 3-D wave basin. Chapter 5 is the heart of this thesis as it deals with the laboratory data analysis and the evaluation of various modeling laws based on the laboratory data. Finally, summary and conclusion of the study is given in Chapter 6.

CHAPTER 2
LITERATURE REVIEW

Physical modeling is essentially a means of replacing the analytical integration of the differential equations governing a physical process including the often complicated initial and boundary conditions. It is, thereby, considered an important and useful engineering tool. Since physical models are usually conducted at reduced scales, the relationship between the model and the prototype must be clearly established for model design and for extrapolating laboratory results to prototype scales. The literature on the subject of scaling law is vast. This chapter is intended to provide a brief account on the development of movable bed scaling laws for coastal engineering applications, especially those relevant to beach profile modeling.

To the present knowledge, the first known scale-model experiments were conducted by an English engineer (John Smeaton) during the period 1752-53, to determine the performance of water wheels and windmills (Hudson et al., 1979); a French professor (Ferdinand Reech) in 1852, was the first to express what is now known as the Froude criterion of similitude (Rouse and Ince, 1957). The earliest movable bed model was conducted in 1875 by a Frenchman (Louis J. Fargue) and in 1885 by Osborne Reynolds in England. Natural sand was used as bed material and time scale was taken into consideration.

L.P. Vernon-Harcourt, who continued the work of Reynolds, investigated scale models using bed materials of sand as well as lighter weight sediments such as charcoal and pumice. And the principle of movable bed model verification, which means that the model is thought to be verified if it can reproduce all the features of bottom evolution observed in the past, has been proven to be the basic guideline and widely

applied ever since, though there has been no rigorous proof of its sufficiency.

The extremely small scale (horizontal length scale up to 40,000) models with large distortions (up to 100) were used in the early British model studies, which later on tended to use larger scales with smaller distortions so as to reduce the scale effect for more reliable results. Also after the work of Reynolds, movable bed model technology was gradually employed to solving practical engineering problems.

After World War II, experience accumulated over the years through the extensive movable bed scale model studies made by various laboratories all over the world, especially in Europe, the United States, Japan, has advanced the state of the art. And, movable-model studies of coastal engineering problems were routinely conducted in connection with almost all coastal and other hydraulic engineering projects.

Meyer(1936) first conducted the laboratory model of beach profile evolution to investigate scaling effects in movable bed experiments, and derived an empirical relationship between beach slope and wave steepness.

Water(1939) worked on the characteristic response of the beach profile to wave action and classified profiles as ordinary or storm type and led to the conclusion that wave steepness can be used to determine the type of beach profile that developed under certain wave conditions. The process of sediment sorting along the profile was demonstrated in the experiments in which the coarser material remained near the plunge point and finer material moved offshore.

Bagnold (1940) used a wave tank to model the interaction of the waves and beach and presented a thorough discussion of the basic physics of the phenomenon as well as a detailed discussion on the application of using a hydraulic model study for the analysis of the process. Rather coarse sand (0.5-7.0 mm) and waves varied in amplitude between 30 centimeters and 5 centimeters were used to conduct the small-scale laboratory experiments and it was found that the foreshore slope was independent of the wave height and mainly a function of grain size.

By reviewing the literature, one may conclude that the earlier works in 1950s and 1960's were mostly related to beach profile classification and that this topic is well studied and basically understood.

Up to present time, numerous work of the physical processes involved in beach erosion by wave action (Keulegan, 1945, 1948; Bruun, 1954; Saville, 1957; Eagleson and Dean, 1961;; Collins, 1963; Vanoni, 1964; Eagleson, 1957, 1959, 1965 and Galvin,1967; Sumnamura and Horikawa, 1975; Wang, Dalrymple and Shiau, 1975; Dean, 1976, 1977; Inman and Bailard, 1982; Vellinga, 1982, 1986; Kriebel, Dally, and Dean, 1987; etc) would lead us to some conclusions.

Wave breaking generates turbulent motion and provides the necessary mechanism for suspending and keeping sediment in suspension, thus mobilizing the grains for transport by mean currents. Although profile change is highly stochastic on a microscale involving turbulence, movement of individual and collective grains, and various types of organized flows, if viewed on a macroscale, changes in the profile are surprisingly regular and consistent with respect to large features such as bars and berms. And the existence of an equilibrium profile was proven to be a valid concept under laboratory conditions.

For the laboratory scale modeling law for movable-bed models, a number of similitude relations have been developed, each having its own practical assumptions and constraints, and some of them are completely empirical and some completely mathematical, while power laws are the most common type of function employed. But the exact dynamic similitude of the dominant physical processes in two regimes (existing a transition from one basic regime of boundary flow to another as sediment motion outside the surf zone is compared to sediment motion in the surf zone) simultaneously , i.e., using the same model fluid and the same model laws for reproducing the waves, currents, and bottom material for both regimes) is not possible. So far, the attempts to establish the correct scaling law are not really successful due to the lack

of an understanding of the basic mechanism of coastal sediment transport , limited choices of material that can be used in the laboratory resulting in the limited sediment sizes, specific weights, viscosity, and the lack of quality prototype data for verification purposes, etc.

Goddet and Jaffry (1960) derived the basic relations between horizontal scale, vertical scale, sediment diameter scale and relative specific weight scale based on the sediment motion due to combined action of wind waves and unidirectional currents.

$$N_D = N_\delta^{17/20}\Omega^{8/5} \tag{2.1}$$

$$N_{\gamma'} = N_\delta^{3/20}\Omega^{-3/5} \tag{2.2}$$

$$\Omega = N_\delta/N_\lambda \tag{2.3}$$

where N_D is the scale of the sediment size, N_δ is the geometrical vertical scale, and Ω is the distortion, the ratio of the geometrical horizontal scale (N_λ) and vertical scale. The scale relationships proposed by Goddet and Jaffry have not achieved popular use, and were only proposed as a first step towards a reasonable solution.

Yalin (1963) examined model scale selection for sediment transport involving wind waves and tidal currents. The phenomenon was considered to be a function of seven characteristic parameters

$$\rho, \mu, \gamma_s, D, T, u_b, U_b \tag{2.4}$$

where u_b and U_b are typical wave and tide horizontal velocities, at the bottom (immediately above an oscillatory boundary layer) and T is the wave period. These parameters were combined to give a dimensionless expression for two-phase motion in the vicinity of the bed. By assuming that the wave period T does not influence the phenomenon of net sediment transport, and preserving the dimensionless change in bed level and by application of small amplitude wave theory, the relationships as:

$$N_D = N_\delta^{3/4}N_\lambda^{1/2} \tag{2.5}$$

$$N_{\gamma'} N_D^3 = 1 \tag{2.6}$$

were obtained from the dimensional analysis.

Fan and Le Mehaute (1969) preserved the characteristics of sediment transport, i.e., densimetric Froude Number Fr_*, and Reynolds Number for initiation of sediment motion Re_* and used equilibrium beach profile concept.

$$N_{\gamma'} N_D^3 = 1 \tag{2.7}$$

$$N_{\gamma'} = N_\delta^3 N_\lambda^{-3/2} \tag{2.8}$$

or

$$N_D = N_\lambda^{1/2} N_\delta^{-1}$$

The authors reviewed most aspects of coastal mobile bed model technology and concluded the following:

a. Similarity of bottom evolution is a basic requirement for a mobile bed model, which is only possible for a flow regime where the boundary layer is turbulent.

b. A coastal mobile bed model must be geometrically distorted. Geometric distortion should be defined by the ratio of the equilibrium beach slopes as measured in model and prototype.

c. Similarity of wave action is only required to the extent that

$$N_H = N_L = N_\delta \tag{2.10}$$

where L is the short wave length. This prohibits wave height distortion.

Noda (1971) listed seven similitude requirements for profile modeling under equilibrium conditions based on the results of a number of previous investigations, including Fan and Le Mehaute (1969) and Yalin (1963), etc. So far, this is the most comprehensive one in beach profile scale modeling. These eight criteria are as follows:

a. Coastal fluid phenomena are generally dominated by gravitational and inertial forces and hence the Froude number, i.e., $u/(gd)^{1/2}$ is an important parameter. The

requirement that $N_{F_r} = 1$ yields

$$N_u = \sqrt{N_\delta} \tag{2.11}$$

where N_u is the velocity scale.

b. The preservation of the densimetric Froude number, $u/(g\gamma' D)^{1/2}$ based on the grain size and bed shear velocity gives

$$N_{\gamma'} N_D = N_{u_*}^2 \tag{2.12}$$

where u_* is the bed shear velocity, and γ' is the relative specific weight of the material

$$\gamma' = (\gamma_s - \gamma_f)/\gamma_f \tag{2.13}$$

here γ_s is the specific weight of the sediment, and γ_f is the specific weight of the fluid.

c. The requirement of identical grain diameter Reynolds number, i.e., $u_* D/\nu$ produces

$$N_{u_*} N_D = 1 \tag{2.14}$$

d. Bed shear velocity for steady conditions in turbulent flow is proportional to free stream velocity:

$$u_* \propto f^{1/2} u \tag{2.15}$$

f. The scale ratio for the friction factor : $\overline{f}$ related to unidirectional uniform flow.

$$C = (\frac{8g}{\overline{f}})^{1/2} \tag{2.16}$$

$$N_{\overline{f}} = \frac{N_\delta}{N_\lambda} \tag{2.17}$$

and

$$N_C^2 = \frac{N_\lambda}{N_\delta} \tag{2.18}$$

g. Kinematic Similarity:

$$\frac{u}{w} = \frac{x}{y} \tag{2.19}$$

h. Fall velocity in stokes range:

$$w_0 = \frac{D^2 g\gamma'}{18\nu} \tag{2.20}$$

These are all supposed to be pertinent to beach processes, and there are certainly a many of combinations and Noda derived several of the possible scale-model laws from various combinations of seven similitude conditions but failed to sort out the proper ones only based on a limited experiment data.

Based on the assumed equilibrium conditions and limited experiments data sets, Noda (1972) derived a completely empirical modeling law.

$$N_D N_{\gamma'}^{1.84} = N_\delta^{0.55} \tag{2.21}$$

$$N_\lambda = N_\delta^{1.32} N_{\gamma'}^{-0.386} \tag{2.22}$$

Two of the four basic parameters $N_D, N_{\gamma'}, N_\lambda, N_\delta$ can be chosen freely and the other two are automatically constrained. Also, the limiting conditions that if $N_{\gamma'} = N_D = 1$, then, $N_\lambda = N_\delta = 1$ as found experimentally are also satisfied.

This set of modeling laws has been derived from two-dimensional laboratory beach profile data and thus the extrapolation to three-dimensional models is still in question. The wavelength is scaled according to the vertical scale to preserve the refraction pattern, but the number of waves in the model will be smaller in proportion to the distortion when scaled to prototype. Diffraction and reflection processes are not preserved. Also, mass transport, sediment concentration, and material porosity phenomena are not scaled. The region of interest was the beach profile in the breaker zone where the boundary conditions belong to turbulent flow regime. No wind effects have been accounted for.

Dean (1973) reported that the most promising parameter used for the prediction of equilibrium beach slopes and the onshore or offshore sediment transport is the dimensionless fall velocity (H/WT), as this parameter tells whether a sediment particle thrown into suspension by the passage of a wave will settle to the bed during the time that the water particle motion is shoreward or seaward, resulting in onshore or offshore movement of the particle. This parameter actually is the fraction of the drag force in vertical (gravity) and the drag force horizontal (orbital motion of the wave), or the time taken for a sediment particle to fall a distance equal to the wave height.

Dean (1985) reviewed previous movable-bed modeling criteria and considered the dominant physical mechanisms involved in surf zone sediment transport. He argued that the Shield's criterion is not necessary in the surf zone as turbulence, not bed shear, is the dominant cause of sediment mobilization. He argued again that sediment fall path, i.e., the fall speed parameter between the prototype and undistorted model should be preserved. Hydrodynamics scaled according to Froude similarity and the undistorted model are large enough to preclude significant viscous, surface tension, and cohesive sediment effects so that the character of the wave breaking is properly simulated. The scale relationships were proposed as

$$N_{Fr} = 1 \tag{2.23}$$

$$N_T = N_t = (N_\delta)^{1/2} \tag{2.24}$$

$$(\frac{H}{WT})_p = (\frac{H}{WT})_m \tag{2.25}$$

$$N_\delta = (N_W)^{2/3}(N_\lambda)^{2/3} \tag{2.26}$$

$$N_\lambda = N_\delta \tag{2.27}$$

where Fr is the Froude number, W is the particle fall velocity, T the wave period. Dean's empirical relation was established through synthesizing a large number of field profiles.

Kamphuis (1974) listed four different dimensionless parameters as requirements for complete similarity. He proposed a set of four different modeling laws preserving one or more non-dimensional parameters but not all of them and suitable for a specific range of environmental conditions without comparison with laboratory data. And he also did not specify the mode of transport assuming that the sediment transport under two dimensional wave action is related to the four dimensionless parameters and the asymmetry of the wave motion. These criteria for dynamic similarity in modeling movable bed can be summarized as

$$N_{R_*} = \frac{N_{u_*} N_D}{N_\mu} = 1 \tag{2.28}$$

$$N_{F_*} = \frac{N_\rho N_{u_*}^2}{N_{\gamma_s} N_D} = 1 \tag{2.29}$$

$$\frac{N_{\rho_s}}{N_\rho} = 1 \tag{2.30}$$

$$\frac{N_{a_\delta}}{N_D} = 1 \tag{2.31}$$

where D is the particle size, ρ is the fluid density, ρ_s is the particle density and γ_s is the underwater specific weight, i.e., $(\rho_s - \rho)g$, and a_δ is the wave orbital amplitude at the bottom.

The scale effects were also discussed based on the four dimensionless parameters:

a. The Reynolds number scale effect will only be felt at low flows and flow reversals and expected to be small in the short wave models.

b. Incorrect scaling of the densimetric Froude number (Shields parameter) will result in incorrect sediment transport and an undeterminate time scale.

c. The scale effect resulting from the violation of the $N_{\rho_s/\rho} = 1$ is not very serious if mass movement rather than dynamics of individual particles is the interest.

d. The geometric link criterion is normally violated which means that sediment transport is not only incorrect but varies throughout the model with depth.

Vellinga (1978) and Graaff (1977) derived a model law for dune erosion by empirical correlations of tests done at different scale dimensions in the Delft Hydraulic Laboratory in the Netherlands when compared to a single prototype condition. The results of model tests on dune erosion with very fine sand support the validity of the dimensionless fall velocity parameter H/TW for small scale modeling of beach processes. If this parameter cannot be satisfied in the model, a profile distortion based on kinematical similarity $N_\lambda/N_\delta = N_u/N_W = (N_\delta/N_W^2)^\alpha$ with $\alpha = 0.5$, gives good results for the finer sands. For coarser sands values of α ranging from 0.5 to 0.3 were found. The morphological time scale equal to the hydrodynamical time scale and equals to square root of geometrical vertical scale. But Hughes's attempts (1983) to verify the Delft modeling laws using the Hurricane Eloise data proved unsuccessful.

Graaff (1977) and Vellinga (1982) conducted a comprehensive laboratory study by using different scales in attempting to duplicate the beach and dune erosion of the Dutch's coast. The law requires that the wave steepness (H_0/L_0) and Froude number be preserved and takes the morphological time scale into consideration.

Saville (1980) conducted a series of tests that the fall velocity of sediment was scaled correctly and compared the results of these small-scale tests with prototype model tests, finding that profile similarity was best in the surf zone and on the beach-face, where setting velocity might be expected to be a major parameter affecting the modeling.

Hughes (1983) presented a mid-scale modeling law based on consideration of the

inertial forces, represented by the turbulent shear stress, and the gravity force in the nearly horizontal direction of the principal flow, which results in a dynamic scaling relationship for a distorted model. A great number of experiments using both regular and irregular wave trains verified the modeling law by reasonable reproduction of the dune erosion which occurred during prototype event. The scale relationships preserve the dimensionless fall velocity parameter (H/TW) and Froude number.

Wang (1990) derived a relationship based on different argument from the inspection of the basic governing equation instead of from dimensional analysis of physical quantities. Based on the two-dimensional sediment conservation equation and preservation of the surf zone parameter ($Tan\beta/\sqrt{H_0/L_0}$) with $Tan\beta$ the beach slope and the number of incoming waves per unit time, a set of modeling relationships had been derived as:

$$N_T = N_t = \frac{N_\lambda}{N_\delta^{1/2}} \tag{2.32}$$

$$N_H = N_\delta \tag{2.33}$$

$$N_q = N_\delta N_\lambda^{1/2} \tag{2.34}$$

$$N_\delta = (N_S N_W)^{2/5} N_\lambda^{4/5} \tag{2.35}$$

In reviewing these modeling laws a number of issues appear to be unsettled. One important question is the morphological time scale. While most of the profile modeling laws appear to be able to reproduce the final profile between model and the targeted prototype, the morphological time scale usually was not well established owing largely to insufficient time-series data of both prototype and scaled models. Another important parameter which needs attention is the scaling of wave height N_H in distorted models. So far no matter which type of transport mechanism the modeling laws are based on , i.e., bed shear-stress dominated transport or turbulence dominated transport, although the latter was preferred by more investigators, wave height scale is always treat as the geometric vertical scale, which might not be automatically the

case. Wang (1985) argued that in movable bed experiment the water depth at any location is the original depth (which is a geometrical scale) minus (or plus) the sand accretion (or erosion). Such erosion or accretion depth is not a simple vertical scale and, therefore, should not be scaled as such. From this point of view, since wave height also varies with water depth inside the surf zone but not necessarily linearly, then wave height scale might also not be the same as the geometric vertical scale if the model is distorted. The apparent question is why wave height should not be scaled according to horizontal scale so the wave steepness is not distorted. The question of wave height scaling in distorted model must be further explored in the laboratory. Finally, a question can be raised on the criteria of modeling law verification. So far, the performance of modeling is judged by properties in the vicinity of waterline such as the volume of erosion and profile shape in that region. These quantities are of obvious importance in engineering application but may or may not be sufficient for modeling law verification purpose.

In closing this chapter it is reiterated here which has been observed by many authors that the modeling of the coastal problems remains more of an art than a science at this stage. There is general guideline but no general solution. Most of all the model laws are tailored to fit certain restricted circumstances.

CHAPTER 3
APPROACH TO PHYSICAL MOVABLE-BED MODELING LAW

A number of different modelling laws for beach profile response modelling have been proposed in the past; most of them are empirical and can only be applied with certain restricted conditions and there is no clear indication as to which is more preferable than the others.

The laws of hydraulic similitude, which should conform to the principles of fluid mechanics, define the requirements necessary to ensure corespondence between flow conditions of a scale model and its prototype. These requirements can be established on the basis of either dynamical considerations, dimensional analysis or the equations governing the process. However, full correspondence between the model and the prototype is difficult, if not impossible, for most of the hydraulic problems including coastal processes. This is because it is usually not possible to obtain a model fluid that has the required viscosity, surface tension, elasticity and other physical properties to meet the exact similitude requirement unless the linear scale is such that the model is as large, or nearly as large, as the prototype. It is known that complete similitude is not practical and , in most cases not necessary. Then, it is extremely important to select and preserve the parameters that have the dominant effects on the process being examined.

Different investigators based on different interpretations of the coastal processes, may choose to preserve different physical parameters, thus, arrived at different similitude relationships.

In this chapter, the basic principles on similitude is briefly reviewed first. Then follow the work by Wang, et al. (1990) but with different consideration on wave

height scaling based on a general wave breaking criterion, a modified beach response modeling law is derived.

3.1 Principles of Similarity

As stated earlier the requirements for similarity between hydraulic scale model and its prototype can be established on the bases of dynamical considerations, dimensional analysis or the equations governing the process. These three methods are briefly discussed here.

3.1.1 Dynamic Similarity

Similarity between the model and the prototype consists of three categories: geometric similarity, kinematic similarity and dynamic similarity. Geometric similarity means the model and the prototype have similar geometrical and boundary shapes. A basic geometrical scale is then defined as the ratio of linear dimension between the model and the prototype:

$$N_\lambda = \frac{L_p}{L_m} \tag{3.1}$$

where L is the linear dimension and the subscripts m and p refer to model and prototype, respectively. N_λ is called the length scale which dictates the size of the model. If all the linear dimensions are preserved with the same N_λ the model is known as undistorted. The model could also be distorted if different parts of the model have different length scales. They are known as distorted models. A common case is a model with different horizontal and vertical length scales.

Kinematic similarity indicates a similarity of motion between model and prototype. Kinematic similarity of two systems is obtained if homologous particles are at homologous points at homologous times (American Society of Civil Engineers, 1942). The time intervals in the two systems must have a constant ratio,

$$N_T = \frac{T_p}{T_m} \tag{3.2}$$

Where N_T is time scale.

In geometrically similar models, kinematic similarity is assured when there is dynamic similarity. Following Newton's second law of motion, dynamic similarity can be achieved when the ratio of inertial forces (F_i) between model and protyotype equals the vector sums of the ratios of active forces, which are recognized as gravitational forces (F_g), viscous forces (F_μ) , elastic forces (F_e), surface tension forces (F_{st}), and pressure forces (F_{pr}) in general fluid mechanics problems, i.e.,

$$\frac{(F_i)_p}{(F_i)_m} = \frac{(F_g + F_\mu + F_{st} + F_e + F_p)_p}{(F_g + F_\mu + F_{st} + F_e + F_p)_m} \tag{3.3}$$

A more restrictive requirement that guarentees Eq.(3.3) to be true is that the ratios of each and every force be equal, or,

$$\frac{(F_i)_p}{(F_i)_m} = \frac{(F_g)_p}{(F_g)_m} = \frac{(F_\mu)_p}{(F_\mu)_m} = \frac{(F_{st})_p}{(F_{st})_m} = \frac{(F_e)_p}{(F_e)_m} = \frac{(F_p)_p}{(F_p)_m} \tag{3.4}$$

The above equation can also be written as,

$$1 = \frac{(F_g)_p/(F_i)_p}{(F_g)_m/(F_i)_m} = \frac{(F_\mu)_p/(F_i)_p}{(F_\mu)_m/(F_i)_m} = \frac{(F_{st})_p/(F_i)_p}{(F_{st})_m/(F_i)_m} = \frac{(F_e)_p/(F_i)_p}{(F_e)_m/(F_i)_m} = \frac{(F_p)_p/(F_i)_p}{(F_p)_m/(F_i)_m} \tag{3.5}$$

The above equation consists of five non-dimensional force ratios. If both model and prototype are under the same atmospheric pressure condition as often to be the case, the non-dimensional pressure force ratio will be preserved if other force ratios are preserved. Therefore, full dynamic similarity, in general, require the other four force ratios all to be unity. Except with a one to one scale model, it is generally not possible to achieve such full dynamic similarity. Therefore, it is important to examine which forces are dominant in the prototype that are to be preserved in the model. The others which contribute little to the phenomenon under consideration are then ignored in the model simulation. Familiar examples are the Froude similitude which preserves only the non-dimensional gravitational force ratio and the Reynolds similitude that preserves only the non-dimensional viscous force ratio.

These forces can be expressed in basic physical quantities of length (L), mass (M), gravitational accelation (g), density (ρ), dynamic viscosity (μ), modulus of elasticity (E), surface tension (σ), and pressure (p), that is,

$$F_i = mass \times acceleration = (\rho L^3)(V^2/L) \tag{3.6}$$

$$F_g = mass \times gravitationalacceleration = \rho L^3 g \tag{3.7}$$

$$F_\mu = viscosity \times \frac{velocity}{distance}\ area = \mu V L \tag{3.8}$$

$$F_{st} = unitsurfacetension \times length = \sigma L \tag{3.9}$$

$$F_e = modulusofelasticity \times area = EL^2 \tag{3.10}$$

$$F_p = unitpressure \times area = pL^2 \tag{3.11}$$

Based on these expressions, the ratio of gravitational force to inertial force can be readily obtained as $\frac{\sqrt{gL}}{V}$, the inverse of which is known as the Froude number. The preservation of gravitational force is equivalent to preserve the Froude number between the model and the prototype. Similarly, the ratio of viscous force to inertial force given by $\frac{LV}{\mu/\rho}$ is known as Reynolds number. The modeling law that preserves the Reynolds number is called Reynolds similitude.

Other similitude creteria can be derived if one of the other non-dimensional force ratios is preserved. When surface tension force predominates, the force ratio is given by Weber's number, $We = \frac{V}{\sqrt{\sigma/\rho L}}$. Similarly, the elastic force to inertial force ratio is known as Mach or Cauchy number,$Ma = \frac{V}{\sqrt{E/\rho}}$.

Usually, for problems in coastal engineering field where gravity wave plays an important role, Froude similitude needs to be preserved and every effort should be made in the model design to either compensate or minimize the effects of viscous force.

3.1.2 Similarity By Dimensional Analysis

The methods of dimensional analysis were developed primarily by Rayleigh (1899), Buckingham (1914), and Bidgman (1922). The best method of analyzing fluid-flow problems is by direct mathematical solution. However, many physical problems are complex and direct mathematical solutions are not possible. For such cases, laboratory model experiments are one of a few available alternatives. Dimensional analysis is a means to organize test parameters and scale the test results without the knowledge of the governing equations. Buckingham's theorem, generally known as the π theorem, is used quite commonly.

Any correct mathematical equation which governs the physical process must be dimensionally homogeneous and each term in the equation must contain identical powers of each of the fundamental dimensions when the terms are reduced to basic dimensions of mass, length, and time (M,L,T) or force, length, and time (F,L,T). If n variables are connected by an unknown dimensionally homogeneous equation, the equation can be expressed in the form of a relationship among n-k dimensionless products, where k is the number of fundamental dimensiona in the problem and n-k is the number of products in a complete set of dimensionless products (π terms) of the variables, and each π term will have k+1 variables of which one must be changed from term to term. The general function can be written in the form

$$A_1 = f(A_2, A_3, A_4, ..., A_n) \tag{3.12}$$

which can also be written

$$f'(A_1, A_2, A_3, ..., A_n) = 0 \tag{3.13}$$

or

$$f''(\pi_1, \pi_2, \pi_3, ..., \pi_{n-k}) = 0 \tag{3.14}$$

And the form of the function and values of the constant, for different types of flow

conditions, must be determined by analytical reasoning, experiment, or a combination of reasoning and experiment.

3.1.3 Similarity By non-dimensionalizing the governing Equations

The mathematical equations that govern a phenomenon may give more insight into the laws of similarity than the use of dimensional analysis of the variables influencing or being suspected of influencing the phenomenon. If a phenomenon can be described with sufficient accuracy by differential equations, the equations, after being converted to dimensionless form, provide the basis of determining transfer parameters between model and prototype. This is simply an extension of the dynamic similitude techniques described earlier. There are several ways to convert the differential equations to dimensionless forms. For the details , the reader may refer to Langhaar (1951), Duncan (1953), Keulegan (1966), and Young (1971).

3.2 Physical Modeling Laws Of Beach Response

A number of modeling laws have been proposed for beach response modeling. A summary can be found in Wang et.al (1990) and Hughes (1993). In both texts, it was pointed out that the scale criteria dependent on fall velocity appeared to be most promising. Table 3.1 summarizes some of the modeling laws given in the texts mentioned above. Of these formulas, the Dean's criterion is gemotrically undistorted whereas all the others permit geometrical distortions. It was pointed out by both authors that all these criteria converge to the same undistorted condition.

Although an undistorted model is preferred, it lacks flexibility and limits the range of tests that can be performed either due to facility limitation or material limitation. Therefore, in this study, the main concern is the devlopment of criteria that permit scale distortion.

Hughes (1993) made a general assessment on the tests of distorted modeling criteria and remarked that the body of experimental evidence presently supports either

Table 3.1: **Summary of Fall Speed Distorted Model Laws**

Author	Geometric Distortion	Hydrodynamic Time Scale	Morphological Time Scale
Le Mehaute (1970))	$\frac{N_\lambda}{N_\delta} = (\frac{N_g N_\delta}{N_W^2})^{1/2}$	$N_T = \sqrt{\frac{N_\delta}{N_g}}$	$N_{t_m} = \sqrt{\frac{N_\delta}{N_g}}$
Vellinga (1982)	$\frac{N_\lambda}{N_\delta} = (\frac{N_g N_\delta}{N_W^2})^{0.28}$	$N_T = \sqrt{\frac{N_\delta}{N_g}}$	$N_{t_m} = \sqrt{\frac{N_\delta}{N_g}}$
Hughes (1983))	$\frac{N_\lambda}{N_\delta} = (\frac{N_g N_\delta}{N_W^2})^{1/2}$	$N_T = \frac{N_\lambda}{\sqrt{N_\delta N_g}}$	$N_{t_m} = \frac{N_\lambda}{\sqrt{N_\delta N_g}}$
Wang, et.al (1990))	$\frac{N_\lambda}{N_\delta} = (\frac{N_g N_\delta}{(N_{\rho'} N_W)^2})^{1/4}$	$N_T = \sqrt{\frac{N_\delta}{N_g}}$	$N_{t_m} = \sqrt{\frac{N_\delta}{N_g}}$
Wang,et.al (1994)	$\frac{N_\lambda}{N_\delta} = (\frac{N_g N_\delta}{(N_{\rho'} N_W)^2})^{1/4}$	$N_T = \sqrt{N_\lambda}$	$N_{t_m} = \sqrt{N_\lambda}$

Vellinga's relationships or Wang, et.al.'s guidance. The geometrical relationships of these two set of criteria are very similar but the time scale is different. Vellinga's approach is largely empirical based on dimensional analysis of physical quantities. Wang (1990) took a slightly different approach by the inspection of the basic governing equation to deal with a restricted case, here the two dimensional beach profile changes under the influence of wave action. Since their approach is based on the actual sediment transport equation it offers the major advantage that the modeling laws can be rationally modified to accommodate different hypotheses. These modeling laws, in turn, can be used to explain the physical process that is being modelled, not simply producing match scales between model and prototype. Therefore, the approach by Wang et.al is adopted here with a brief derivation of their results then followed by a proposed variation.

The basic equation, which balancing the spatial change of sediment transport rate and the temporal change of beach profile, is the two-dimensional sediment conservation equation:

$$\frac{\partial h}{\partial t} = \frac{\partial q}{\partial x} \tag{3.15}$$

where h is the bottom elevation, q is the volumetric sediment transport rate in the direction x. Non-dimensionalize the equation:

$$\frac{\partial \bar{h}}{\partial \bar{t}} = \frac{q_n t_n}{\delta \lambda} \frac{\partial \bar{q}}{\partial \bar{x}} \tag{3.16}$$

where the overbar refers to non-dimensional quantities and $q_n, t_n, \delta, \lambda$ represent the reference values of sediment transport rate, the morphorogical time scale, vertical and horizontal geometrical scale respectively.

To maintain similitude between the model and prototype requires

$$\frac{N_q N_t}{N_\delta N_\lambda} = 1 \tag{3.17}$$

where N refers to the ratio of prototype to model.

It is assumed that suspended load transport mode predominates the sediment transport inside the surf zone which is approximated by the following equation,

$$q_s = hVc \tag{3.18}$$

where h is depth, V is mean transport velocity and c is mean sediment concentration.

The suspended sediemnt concentration is then assumed to be directly proportional to the ratio of stirring power due to turbulence and the settling power due to gravity and can be expressed as (Hattori and Karvamata, 1980):

$$c \propto \frac{\rho u'}{(\rho_s - \rho)\overline{W}} \propto \frac{u'}{SW} \tag{3.19}$$

where u' is the turbulent intensity, W is the particle settling velocity and S is the submerged specific weight.

The ratio of turbulent velocity and wave induced velocity is a function of surf zone parameter as suggested by Thorton (1978), i.e.,

$$\frac{u'}{u} = f(\xi) \tag{3.20}$$

The surf zone parameter is defined as $Tan\beta/\sqrt{H_b/L_0}$ with $Tan\beta$ the beach slope, H_b the breaking wave height, and L_0 the deep water wave length.

Physically, this equation states that if the surf zone property is similar, the turbulent intensity should be proportional to the mean velocity scale provided the surf zone parameter is preserved. Since in a wave field u is proportional to H/T, combining Eqs. (1.17), (1.18) and (1.19) with Eq. (1.16) gives the following scaling law,

$$\frac{N_V N_{f(\xi)} N_t N_H}{N_\lambda N_W N_T N_S} = 1 \tag{3.21}$$

where the subscripts correspond to various physical quantities given earlier. It should be noted here N_V is the scale ratio of the mean transport velocity which must not be confused with the wave-induced particle velocity, u. This mean net transport velocity is assummed to be proportional to wave celerity inside the surf zone. Therefore, N_V is scaled as $(N_g N_\delta)^{1/2}$.

By requiring $N_{f((\xi)} = 1$, i.e.,

$$(g^{1/2}T \cdot Tan\beta/H_0^{1/2})_m = (g^{1/2}T \cdot Tan\beta/H_0^{1/2})_p \tag{3.22}$$

the hydrodynamic time scale, or here the wave period scale, is obtained as,

$$N_T = \frac{N_\lambda N_H^{1/2}}{N_g^{1/2} N_\delta} \tag{3.23}$$

In the modeling law proposed by Wang et.al. (1990), it was stated that the wave height is treated as a vertical parameter which leads to the following hydrodynmaic time scale,

$$N_T = \frac{N_\lambda}{N_g^{1/2} N_\delta^{1/2}} \tag{3.24}$$

From here after, the N_g term will be dropped from all the formulas since all of the coastal models are carried out in the same gravity field. Wang et.al further examined two possibilities for geometric modeling. The first case was by letting the morphological time scale to be the same as the distorted hydrodynmaic time scale which is equivalent to preserve the number of waves in determining morpholical time scale. The second alternative is to preserve the sediment particle fall trajectory. The first possibility leads to the following pair of morpholical time scale and geometrical scaling laws,

$$N_T = N_t = \frac{N_\lambda}{N_\delta^{1/2}}$$
$$N_\delta = (\frac{N_s}{N_\gamma})^{2/3} N_W^{2/3} N_\lambda^{2/3} \tag{3.25}$$

The second case offers the following scaling equations,

$$N_T = \frac{N_\lambda}{N_\delta^{1/2}}$$
$$N_t = \frac{N_\delta}{N_V} = N_\delta^{1/2}$$
$$N_\delta = (\frac{N_s}{N_\gamma})^{2/5} N_W^{2/5} N_\lambda^{4/5} \tag{3.26}$$

Therefore, geometric distortion is permissible by both scaling laws. Wang et.al. indicated that the second pair is perferred by comparing with experimental results. The distorted modeling law offers a major advantage over undistorted modeling laws in that it greatly relaxes the requirment of laboratory facilities.

It has been noted that in this modeling law, the wave height is treated as a vertical scale. This assumption is re-examined here. Clearly, in modeling beach profile change, wave height inside the surf zone should be similar between model and prototype. By treating wave height as a vertical geometrical scale in essence implicitly assumes that wave height is proportional to the local water depth, i.e., $H = \gamma_b h$ with the γ_b a constant value. This relationship was orginally proposed by McCowan (1984) as a breaking criterion and has been widely used. To maintain wave height similitude for

the region to be simulated, here the surf zone, however, also requires that the same criterion be true for the entire surf zone. This may or may not be case. therefore, a more general wave height scaling law is proposed here with the following form,

$$N_H = N_\gamma N_\delta \tag{3.27}$$

with N_γ being the scale ratio of the breaking index, γ_b. This is the major difference from the one proposed by Wang, et.al. Substituting the above equation into Eqs. (3.21) and (3.23) give the modified modeling laws,

$$N_T = N_\gamma^{1/2} \frac{N_\lambda}{N_\delta^{1/2}} \tag{3.28}$$

and

$$N_\delta = \left[\frac{N_T}{N_t} \frac{N_S N_W N_\lambda}{N_\gamma} \right]^{2/3} \tag{3.29}$$

A guideline on determining N_γ is proposed here by examining the functional form of γ_b as developed by various investigators. A summary of different empirical formulas for γ_b is given in table 3.2 (from Wang, 1990). From this Table it can be seen that the breaking index γ_b could be affected by beach slope and deepwater wave steepness. Inside surf zone, the effect of deepwater wave steepness is likely to be minimal. Therefore, a general power law functional form of N_γ is proposed as,

$$N_\gamma = \left[\frac{N_\delta}{N_\lambda} \right]^k \tag{3.30}$$

From examining the equations given in Table 3.2, one may conclude that the value of k is likely in the range from 0 to 1. In the case, k=0, the proposed modeling law reduces to that of Wang's. On the other extreme if k=1, or N_γ is linearly proportional to the local beach slope, then,

$$N_\gamma = \frac{N_\delta}{N_\lambda} \tag{3.31}$$

and Eqs. (3.28) and (3.29) become

$$N_T = N_\lambda^{1/2} \tag{3.32}$$

Table 3.2: **Summary of Wave Breaking Index (γ_b)**

Author	γ_b	note
McCowan (1894)	$\gamma_b = 0.78$	solitary
Munk (1949)	$\gamma_b = 10/3(\frac{H_0}{L_0})^{1/3}$	solitary
Galvin (1968)	$\gamma_b = 1.087 m_i$ $\gamma_b = \frac{1}{1.40-6.85m}, m < 0$	laboratory
Collins and Weir(1969)	$\gamma_b = 0.72 + 5.5m$	linear
Komar and Gaughan(1972)	$\gamma_b = 1/0.56(\frac{H_0}{L_0})^{1/5}$	linear
Weggel (1972)	$\gamma_b = b(m) - a(m)\frac{H_b}{gT^2}$ $a(m) = 43.8(1.0 - e^{-19m})$ $b(m) = 1.56(1.0 + e^{-19.5m})^{-1}$	laboratory
Singamsetti and Wind(1980)	$\gamma_b = 0.568 m^{0.107}(\frac{H_0}{L_0})^{-0.237}$	laboartory
Sunamura (1980)	$\gamma_b = 1.1[\frac{m}{(H_0/L_0)^{1/2}}]^{1/6}$	laboratory
Moore (1982)	$\gamma_b = b(m) - a(m)(\frac{H_0}{2\pi L_0})^{4/5}$ a and b same as Weggel	hybrid
Larson and Kraus(1989)	$\gamma_b = 1.14[\frac{m}{(H_0/L_0)}]^{0.21}$	
Smith and Kraus(1990)	$\gamma_b = b(m) - a(m)(\frac{H_0}{L_0})$	$\frac{1}{80} < m \leq \frac{1}{10}$ $0.007 < \frac{H_0}{L_0} \leq 0.0921$
Wu (1990)	$\gamma_b = 0.85 + 0.35 log(\frac{m}{H_0/L_0})$	laboratory
Hansen (1990)	$\gamma_b = 1.25 m^{0.2}$	laboratory
Kampuis (1991)	$\gamma_b = 0.56 e^{3.5m}$	laboratory

and

$$N_\delta = (\frac{N_T}{N_t})^{2/5}(N_S N_W)^{2/5} N_\lambda^{4/5} \tag{3.33}$$

Again, by using the two different hypotheses proposed by Wang on morphological time scaling, two different scaling laws can be obtained. First, by assuming that the number of incoming waves per unit time is preserved for the similitude of erosion rate, we obtain,

$$\begin{aligned} N_t &= N_T = N_\lambda^{1/2} \\ N_\delta &= (N_S N_W)^{2/5} N_\lambda^{4/5} \end{aligned} \tag{3.34}$$

Second, if one perserves the fallen particle trajectory, the following modeling laws are arrived at,

$$\begin{aligned} N_T &= N_\lambda^{1/2} \\ N_t &= N_\delta^{1/2} \\ N_\delta &= (N_S N_W)^{1/3} N_\lambda^{5/6} \end{aligned} \tag{3.35}$$

In summary, a new set of profile modeling law have been derived by using the same approach of Wang et.al. This new modeling law contains an additional scale ratio of wave height. It seems that Wang et.al's law represents one limiting condition of the proposed law. The other limiting condition is also derived here and the modeling law is also included in the Table 3.1.

CHAPTER 4
LABORATORY EXPERIMENTS

4.1 Test Facilities

Laboratory experiments were carried out in three different facilities all located in the Department of Coastal and Oceanographic Engineering, University of Florida. The main series of experiment was conducted in what is referred to as the air-sea wave tank (ASW) and a limited number of cases were repeated in a different wave tank, hereto referred to as the wave flume (WF). Finally, a set of experiment was carried in a three-dimensional basin (WB) with varying input wave angles. The results under normal wave incident angle were also reported in this thesis for comparision. Brief discriptions of each facility is givn here.

4.1.1 Air-Sea Wave Tank

The ASW tank is 1.8-meter wide and 45.7-meter long. The wave generator section occupies 3.4 meter and the wave absorbing beaches is 5.8 meter long. The remaining 36.6 meters are divided into two bays, each 0.86-meter wide and 1.9 meters deep. The maximum allowable water depth is about 0.9 meters. The wave tank can be filled from a well at the rate of 500 gallons per minute.

Wave generation in the Air-Sea tank is controlled electronically, hydraulically driven wave paddle measuring 1.8-meter wide and 1.2-meter high. The wave genarator bulkhead is mounted on acarriage and is driven by two hydraulic rams governed by hydraulic servo-valves. The system provides independent control of the top and bottom rams in such a way that the bulkhead can move either as a piston on the carriage or as a paddle. Any combination of piston and paddle motion is possible.

For the beach response modelling law verification tests, the piston type is used.

A moving instrument carriage was mounted on the railing system traversing on top of the tank. The rails for the carriage was installed with a horizontal tolerance of ± 0.03 mm, providing an leveled reference platform from which precision beach profile measurement can be performed. The carriage also serves to carry various sensing instruments. The carriage drive train is powered by a 1/2HP electric motor capable of moving the carriage at variable speed between 0 to 6.1 meters per second. A hand-held remote control unit is used to start or stop the drive motor. A hand-operated optic probe is used in this series of tests to measure beach profile elevations.

4.1.2 Wave Flume Facility

A limited number of experiments were repeated in the Wave Flume which is considerably smaller than ASW. It is 0.6-meter wide, 0.9-meter high and 15.5-meter long with one side of the wall made of glass panel and the other side of steel. The tank is equipped with a piston type wave maker driven by a mechanically controlled electric motor. A manually operated ponit gage was installed for profile measurement. In order to avoid penetrating into the sand at the point of contact the gage was constructed of light aluminium and the tip was modified by replacing the point with a small rectangular base which rests flat on the sand.

4.1.3 Wave Basin Facility

Three-dimensional model tests were carried out in the wave basin of the Coastal and Oceanographic Engineering Department, University of Florida. The dimension of the basin is approximately 28 m x 28 m x 1 m. The basin is equipped with a snake-type wave-maker, which consists of 88 independent wavepaddles of 24 cm width each. By adjusting the phase of each individual paddle motion, it can generate waves of various oblique angles. Also the amplitude can be adjusted individually to meet different needs with wave heights ranging from 1 centimeter to 15 centimeter and wave periods from 0.89 to 1.89 seconds.

4.2 Initial Beach Profile Design

In this laboratory study, a test series obtained from the Grosser Wellenkanal (GWK) facility in Hannover, Federal Republic of Germany (Dette and Uliczka,1987) was selected as the prototype-scale target condition. This was chosen on the basis that GWK is among the largest tank facilities in the world and the experiments carried out thereout can be considered as near prototype scale. The experiments were also well documented with rather comprehensive time histories of profile evolution and the associated wave transformation data. The GWK experiments, hereto referred as prototype, used sand with a median diameter of 0.33 mm molded to a composite slope of 1 on 4 on the upper portion of the slope and 1 on 20 on the lower portion of the slope. This initial prototype profile is shown in figure 4.1. The tests were conducted at water depth of 5.0 meters under the input wave condition of 1.5 meters wave height and 6.0 seconds wave period.

In the ASW tank model tests, two types of sediment were used, one of natural fine sand with median diameter (D_{50}) of 0.20 mm, hereon referred to as natural sand and the other a well sorted very fine quartz sand, hereon referred to as fine quartz sand, with D_{50} equal to 0.09 mm. The former was used in the bulk of the experiments. The latter was used only in one series of tests at undistorted model scale to see whether very fine sand can be used in the model as this is one option to increase the geometrical scale ratio between prototype and model without resorting to distorted models. The size distributions of the two sand sizes obtained by sieve analysis are given in Figure 4.2. The sediment fall velocities corresponding to $D_{50} = 0.09$ mm and $D_{50} = 0.2$ mm are, respectively, 0.675 cm/sec and 1.90 cm/sec at a water temperature 20^0C (see Figure 4.3 after Rouse, 1937).

The modeling laws listed in Table 3.1 do not dictate the same geometrical distortion ratio. The geometrical distortions based on LeMehaute's and Hughes' laws are identical whereas the geometrical distortions based on Vellinga's, Wang's the newly

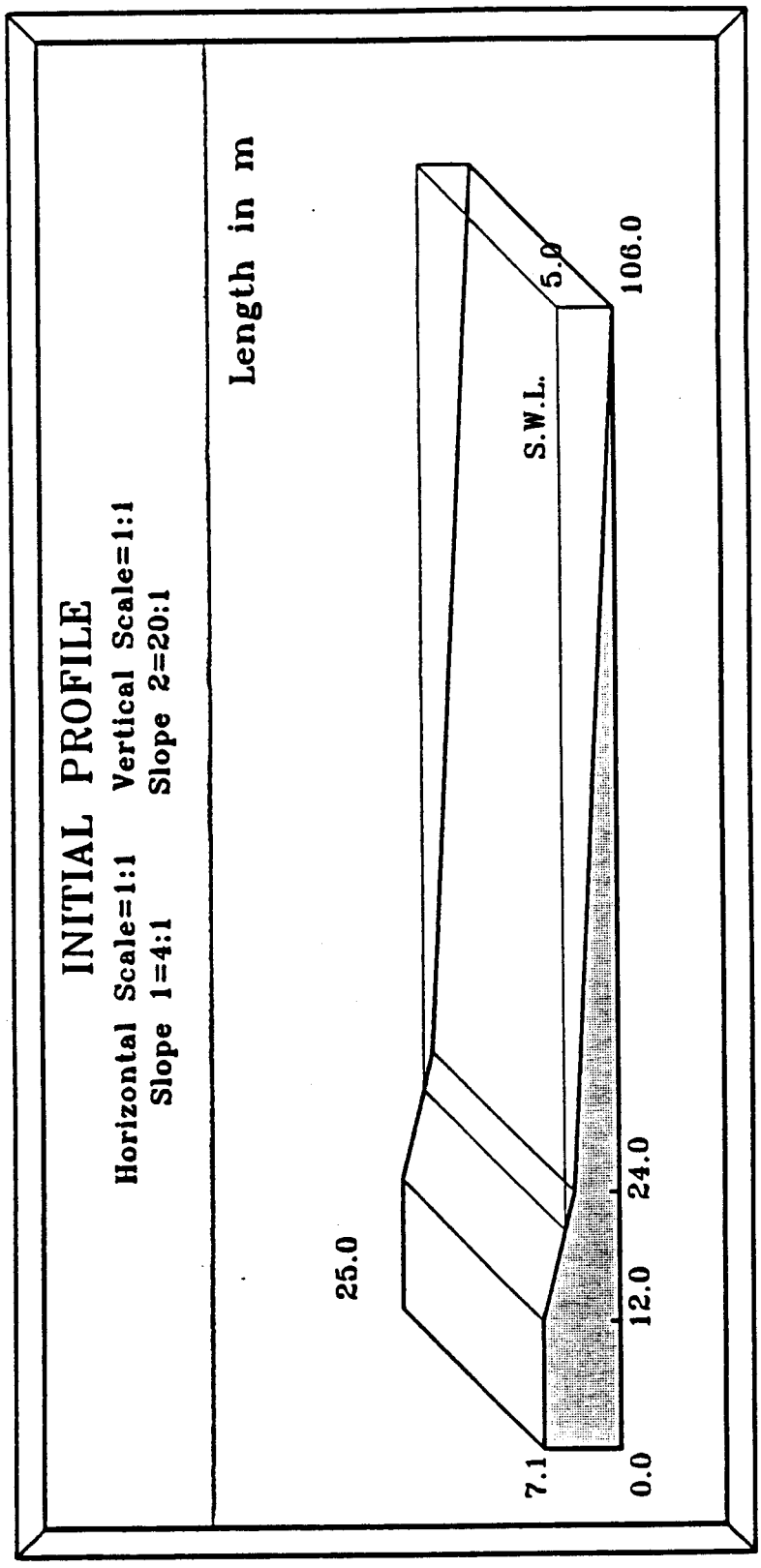

Figure 4.1: Initial Beach Profile In Prototype

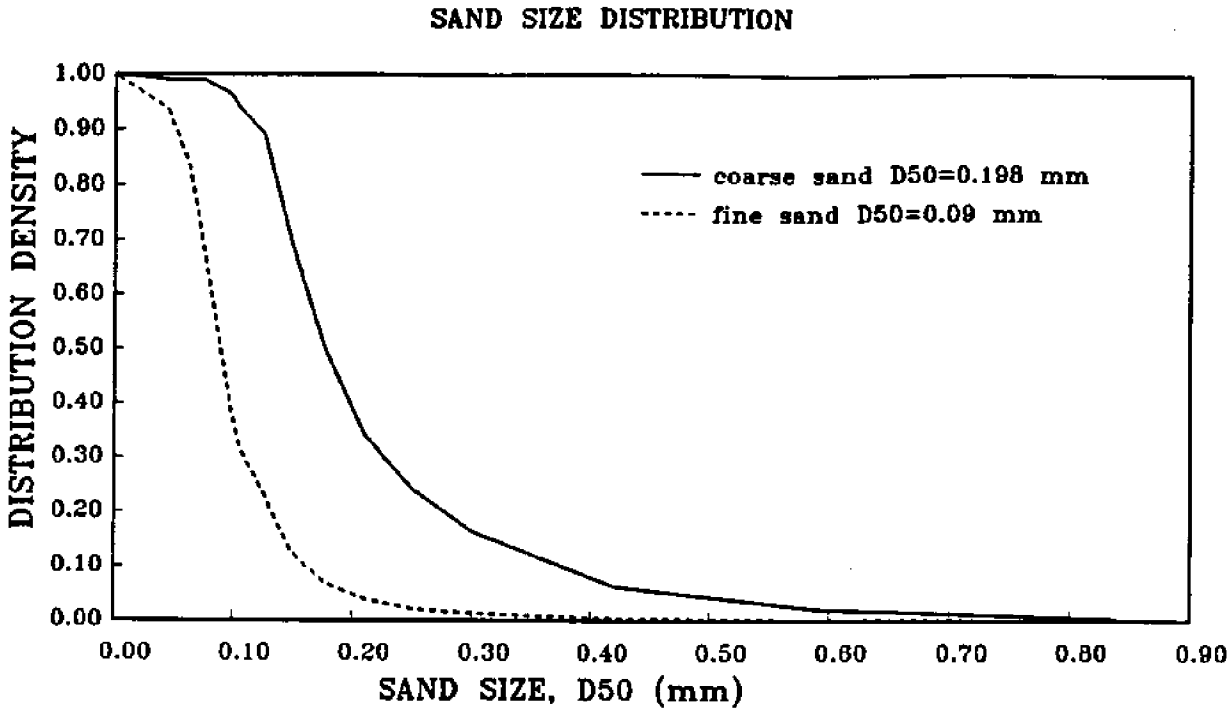

Figure 4.2: Cumulative Sand Size Distribution

proposed one are nearly the same. A choice has to be made here for the laboratory initial profile design. The geometrical distortion based on the latter group, or the Wang's modeling law is adopted. This is because the existing field and laboratory data seemed to have better agreement using either the Vallinga's or the Wang's criterion (Hughes, 1993), which are nearly the same in terms of geometrical distortion. It should also be pointed out here that the geometrical distortion criteria of all the modeling laws listed do no actually differ significantly from each other and that the final test profile is not particularly sensitive to the initial profile.

The geometrical distortion law proposed by Wang is,

$$N_\delta = N_\lambda^{4/5} N_W^{2/5} \tag{4.1}$$

The initial test profile is shaped according to the above equation based on the prototype profile dimensions. Three different horizontal scales $N_\lambda = 20$, 30 and 40 were selected in the test. The relevant geometrical scale ratios and some of the

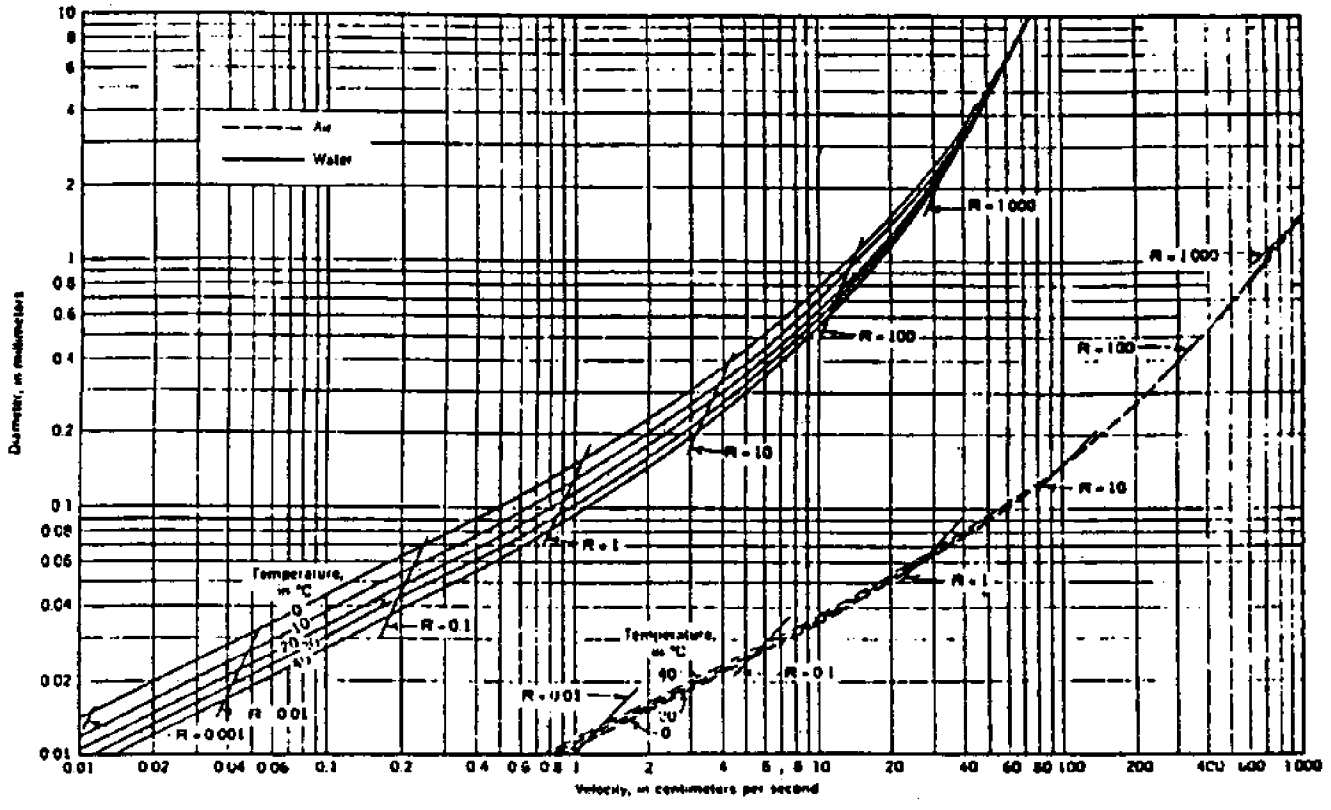

Figure 4.3: Fall Velocity Of Spherical Grains As A Function Of Size, Rouse (1937)

Table 4.1: **Scale Ratios and Physical Dimensions in ASW Tests**

Median Sand Size D_{50}	0.20 mm			0.09 mm		
Median Fall Velocity W_s	1.9 cm/s			0.675 cm/s		
Fall Velocity Scale N_W	2.08			6.62		
Horizontal Length Scale N_λ	20.0	30.0	40.0	20.0	30.0	40.0
Vertical Length Scale N_δ	14.46	20.00	25.18	20.00	30.00	40.00
Distortion ($N_\delta : N_\lambda$)	1:1.38	1:1.5	1:1.59	1:1	1:1	1:1
Water Depth	34.6cm	25.0cm	19.9cm	25.0cm	16.7cm	12.5cm
Corresponding "A" Parameter	0.092			0.065		

physical dimensions at different scale models are listed in Table 4.1. The physical dimensions of these initial profiles are also shown in Figure 4.4 for the natural sand models. As can be seen from Table 4.1, the fine quartz sand models are all close to undistorted. Or, in other words, to achieve undistorted modeling very fine material has to be used. To avoid too shallow water due to the increased scale ratios, shift the whole profile to maintaining the water level around 40.0 centimeters but keep the shape of the profile unchanged as designed.

The WF tank tests were design to repeat part of the experiment carried out in the ASW, namely only the cases with 20:1 horizontal scale. A planar beach of initial slope 1:2.9 at upper segment and :14.46 at the lower segment was formed such as given in Figure 4.4. The beach material used here was well-sorted fine quartz sand with a mean diameter of 0.21 mm (close to that used in the ASW) with a sorting coefficient of 0.58. The corresponding fall velocity is approximately 2.0 cm/sec. The

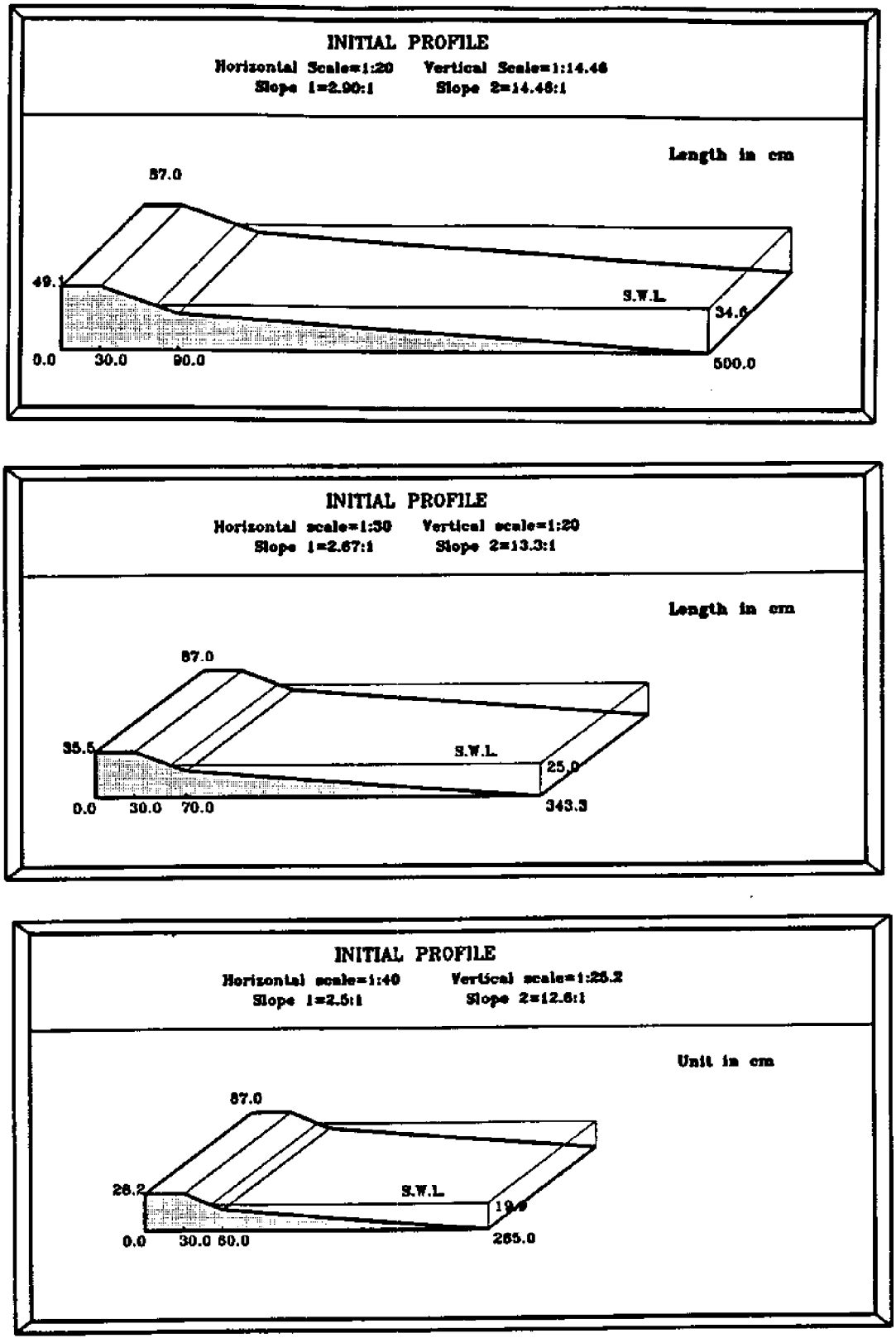

Figure 4.4: Designed Initial Beach Profile in Model with $D_{50} = 0.20mm$

grain size distributions range between 0.1 mm and 0.5 mm. The water depth is 35.3 cm. A total 10 experiments was conducted with test conditions summarized in the table 4.5.

Finally, in the 3D wave basin tests, the sediment used in the model was also fine quartz sand with median diameter of 0.20 mm with size distribution given in Figure 4.2. The corresponding fall velocity is 1.9 cm/sec at water temperature 20^0C; this yields a N_w=2.0 which is the same as the natural sand experiment in the ASW tank. The horizontal scale was again selected at 20 and the corresponding vertical scale is 14.46 according to the modeling law.

The beach built in the basin has a total length of 19 m with a width of 14 m and contained 125 tons of quartz sand. Both ends of the beach were confined by rigid block walls. The entire beach was molded into initial shape by wooden templates cut into the desired shape.

4.2.1 Experimental Procedures

It is desirable to have set a standard procedure before conducting the experiments so that the results from the three different setups can be consistent and to reduce the operating error as much as possible. Hopefully the procedure will also be helpful for future experiments of a similar nature. This procedures are outlined in the following:

Step 1. Mark the design profile and water level on the outside of the tank glass wall. Close the drainage valves and fill air-sea tank with water to the required depth and adjust the wave generating machine to the design test conditions including wave height and wave period .

Step 2. While filling the tank with water, a wooden board cut to just slightly less than the tank width is used to mold the profile from offshore to beach face according to the profile line. The uniformity of the profile across the width of the tank is checked with a leveler.

Step 3. Survey the initial profile after the beach attends saturation at the test

water level. Record the water level.

Step 4. The beach is first stablized by a series of small waves. The wave height is gradually increased to the designated test height.

Step 5. In most of the two-dimensional tests, beach profiles are surveyed only along the centerline of the tank at time intervals of 5 minutes, 10 minutes, 20 minutes, 40 minutes, 80 minutes. In the three-dimensional wave basin experiments, 5 profies were regularly surveyed at any time interval.

A number of experimental errors are evident. The seaward position of closure where sand transport stopped sometimes was difficult to define as a verneer of sand was often transported beyond the end of the initial profile and deposited as a thin layer over the horizontal floor of the tank. Also, profile variations across the tank were common. Uniform sand compaction was also difficult to achieve. These errors together with survey inaccuracy could lead to erroreous results that did not conserve the total volume of material. In general, this errors was small. Nevertheless, caution must be exercised in accepting the data.

4.2.2 Test Conditions

The test conditions were determined by the requirment that the beach should be erosional under the given wave input. Various criteria have been proposed in the past, some of them are given in Table 4.2.

From this table it can be seen that three non-dimensional parameters are often used: the wave steepness parameter, H_0/L_0, the relative fall velocity parameter, $\pi W/gT$ and the surf zone parameter, $tan\beta/\sqrt{H_0/L_0}$.

The test conditions for the two-dimensional and three-dimensional experiments as well as the values of these three key paramters were given in Tables 4.3 to 4.7. The ASW tank tests were the most comprehensive conisting of 26 cases at 3 different horiziontal geometrical scales whereas 10 tests were performed in WF with a horiziontal scale of 20. In the three-dimensional basin, 4 sets of experiments were

Table 4.2: **Summary of Criteria Governing Beach Classification**

Authors	Parameters	Erosional Criterion
Johnson, 1952	$\frac{H_0}{L_0}$	$\frac{H_0}{L_0}$ >0.025-0.030
Dean, 1973	$\frac{H_0}{L_0}; \frac{\pi W}{gT}$	$\frac{H_0}{L_0} > 1.7\frac{\pi W}{gT}$
Sunamura and Horikawa, 1974	$\frac{H_0}{L_0}; Tan\beta; \frac{d_{50}}{L_0}$	$\frac{H_0}{L_0} = C(Tan\beta)^{-0.27}(\frac{d_{50}}{L_0})^{0.67}$
Wang and Yang, 1980	$\frac{H_b}{\sqrt{gTTan\beta}}; \frac{\pi W}{gT}$	$\frac{H_b}{\sqrt{gTTan\beta}} > 0.5(\frac{\pi W}{gT})^{1/3}$
Hattori and Kawamata, 1980	$\frac{H_0}{L_0}Tan\beta; \frac{W}{gT}$	$\frac{H_0}{L_0}Tan\beta > 0.5\frac{W}{gT}$
Kraus, 1991	$(H_0/L_0)/(\frac{\pi W}{gT})^{3/2}$	$(H_0/L_0)/(\frac{\pi W}{gT})^{3/2} < 184$

Table 4.3: **Summary of Test Conditions in ASW**

Test No.	Wave period (sec)	Wave height (cm)	Water depth (cm)	Grain size (mm)	Horizontal scale	Vertical scale
1	1.00	11.50	52.0			
2	1.14	10.50	34.6			
3	1.20	11.25	52.0			
4	1.20	12.75	52.0			
5	1.33	10.00	52.0			
6	1.33	11.00	35.3			
7	1.33	11.25	35.3	0.20	20.0	14.46
8	1.33	12.00	52.0			
9	1.33	12.75	52.0			
10	1.33	13.00	35.3			
11	1.33	17.50	52.0			
12	1.45	10.50	52.0			
13	1.45	13.50	52.0			
14	1.45	18.00	52.0			
16	1.33	10.00	40.0			
17	1.15	9.50	40.0	0.20	30.0	20.0
18	1.00	9.50	40.0			
19	0.80	5.50	40.0			
20	1.00	9.00	40.0	0.20	40.0	25.2
21	1.15	9.50	40.0			
22	1.34	7.50	40.0		20.0	20.0
23	1.34	7.50	40.0		20.0	20.0
24	1.10	5.00	40.0	0.09	30.0	30.0
25	1.10	5.00	40.0		30.0	30.0
26	1.054	3.75	40.0		40.0	40.0

Table 4.4: **Summary of Beach Profile Classification Parameter for ASW**

Test No.	Wave period (sec)	Wave height (m)	Wave Length (m)	Wave Steepness $(\frac{H_0}{L_0})$	Relative Fall Velocity $\frac{\pi W}{gT}$	Surf Zone Parameter $\frac{Tan\beta}{\sqrt{H_0/L_0}}$	Kraus Parameter $(\frac{H_0}{L_0})/(\frac{\pi W}{gT})^{3/2}$
(GWK)	6.00	1.50	56.18	0.0267	0.00239	0.3060	228
1	1.00	0.115	1.56	0.0737	0.00689	0.2547	129
2	1.14	0.105	2.03	0.0517	0.00604	0.3041	110
3	1.20	0.1125	2.25	0.0500	0.00574	0.3093	115
4	1.20	0.1275	2.25	0.0567	0.00574	0.2904	130
5	1.33	0.10	2.76	0.0362	0.00518	0.3635	97
6	1.33	0.11	2.76	0.0399	0.00518	0.3462	107
7	1.33	0.1125	2.76	0.0408	0.00518	0.3424	109
8	1.33	0.12	2.76	0.0435	0.00518	0.3316	117
9	1.33	0.1275	2.76	0.0462	0.00518	0.3217	124
10	1.33	0.13	2.76	0.0471	0.00518	0.3187	126
11	1.33	0.175	2.76	0.0634	0.00518	0.2747	170
12	1.45	0.105	3.28	0.0320	0.00475	0.3866	97
13	1.45	0.135	3.28	0.0411	0.00475	0.3411	126
14	1.45	0.18	3.28	0.0549	0.00475	0.2952	168
16	1.33	0.10	2.76	0.0362	0.00518	0.3942	97
17	1.15	0.095	2.06	0.0461	0.00600	0.3493	99
18	1.00	0.095	1.56	0.0609	0.00689	0.3039	120
19	0.80	0.055	1.00	0.0550	0.00861	0.3384	69
20	1.00	0.09	1.56	0.0577	0.00689	0.3304	101
21	1.15	0.095	2.06	0.0461	0.00600	0.3696	99
22	1.34	0.075	2.81	0.0267	0.00161	0.3060	413
23	1.34	0.075	2.81	0.0267	0.00161	0.3060	413
24	1.10	0.050	1.89	0.0265	0.00197	0.3071	303
25	1.054	0.0375	1.73	0.0217	0.00205	0.3394	233
26	1.10	0.050	1.89	0.0265	0.00197	0.3071	303

Table 4.5: **Summary of Test Conditions in the WF**

Test No.	Wave period (sec)	Wave height (cm)	Water depth (cm)	Grain size (mm)	Horizontal scale	Vertical scale
1	1.30	11.50				
2	1.30	11.50				
3	1.30	12.00				
4	1.30	12.50				
5	1.30	12.50	35.3	0.21	20.0	14.46
6	1.30	13.00				
7	1.30	13.00				
8	1.60	15.00				
9	1.30	16.50				
10	1.65	16.50				

carried.

All the test conditions listed above should, in theory, satisfy the erosional conditions given in Table 4.2, however, some cases dropped to the region of the accretional profile according to one or two parameters, especially for the undistorted model tests the profiles suppose to be accretional according to the Kraus parameter.

4.3 Test Results and Data Analysis

The experimental data consisted of a set of measured profiles for the three test series. This data set is too voluminous to be included in this thesis. However, they are archived on computer disks in the Department of Coastal and Oceanographic Enginnering, University of Florida. In this thesis only reduced information related to the specific study subject is reported.

Data anaylsis was performed for two objectives: a primary objective of establishing the modeling law as stated in the "Introduction" and a secondary objective of documenting profile evolution process under laboratory condition. To fulfill the first

Table 4.6: **Beach Profile Classification Parameter for WF**

Test No.	Wave period (sec)	Wave height (m)	Wave Length (m)	Wave Steepness $(\frac{H_0}{L_0})$	Relative Fall Velocity $\frac{\pi W}{gT}$	Surf Zone Parameter $\frac{Tan\beta}{\sqrt{H_0/L_0}}$	Kraus Parameter $(\frac{H_0}{L_0})/(\frac{\pi W}{gT})^{3/2}$
1	1.30	0.13	2.63	0.0494	0.00468	0.311	154
2	1.30	0.11	2.63	0.0418	0.00468	0.338	131
3	1.30	0.115	2.63	0.0418	0.00468	0.338	131
4	1.30	0.12	2.63	0.0456	0.00468	0.324	142
5	1.30	0.10	2.63	0.0380	0.00468	0.354	119
6	1.30	0.135	2.63	0.0513	0.00468	0.305	160
7	1.30	0.105	2.63	0.0399	0.00468	0.346	125
8	1.30	0.1125	2.63	0.0428	0.00468	0.337	134
9	1.30	0.165	2.63	0.0627	0.00468	0.276	196
10	1.65	0.165	4.24	0.0389	0.00370	0.350	173

Table 4.7: **Test Conditions in Three-Dimensional Wave Basin**

Test No.	Wave Height (cm)	Wave angle	Wave Period (sec)	Vertical Scale
1	10.5	normal	1.14	17.05
2	10.5	normal	1.14	14.16
3	12.5	normal	1.33	14.16
4	12.5	oblique	1.33	14.16

objective, various quantities that can be used for comparisions between prototype and model are computed; such quantities include the profiles themselves, the volume of erosion and the bar charecteristics. The procedures of computing these quantities and the results are given here. The subject of modeling law will be treated separately in the next chapter. The secondary objective, however, is more descriptive and will be discussed here as an integral part of the data analysis process.

4.3.1 Profile Classifications of the Test Results

As stated earlier that all the test conditions were selected on the permise that the beach should be erosional. An erosional beach generally is also associated with the development of a bar-type of profile. This has been the case for practically all the cases tested. Berm and foreshore erosion occurred in every cases. The development of breaking bar also occurred, but in certain cases the breaking bar is not as prominent but rather diffused; an example is shown in Figure 4.5. In the very fine sand experiments (D_{50}=0.09 mm), no prominent breaking bar was formed in any of the test case.

4.3.2 Volumetric Changes along the Profiles

The basic equation to compute the volumetric change along the profile is the two-dimensional sediment conservation given by

$$\frac{\partial h}{\partial t} = -\frac{\partial q}{\partial x} \tag{4.2}$$

where h is the elevation of the profile at a given point x and time t; x is on-off shore direction pointing offshore and z-axis orients upward from an origin located at the still water shoreline; q is the time-averaged volumetric sediment transport rate per unit length of shoreline.

Integrate equation (4.2) from the landward reference, x_0, to any other position, x, gives the net volume change per unit time:

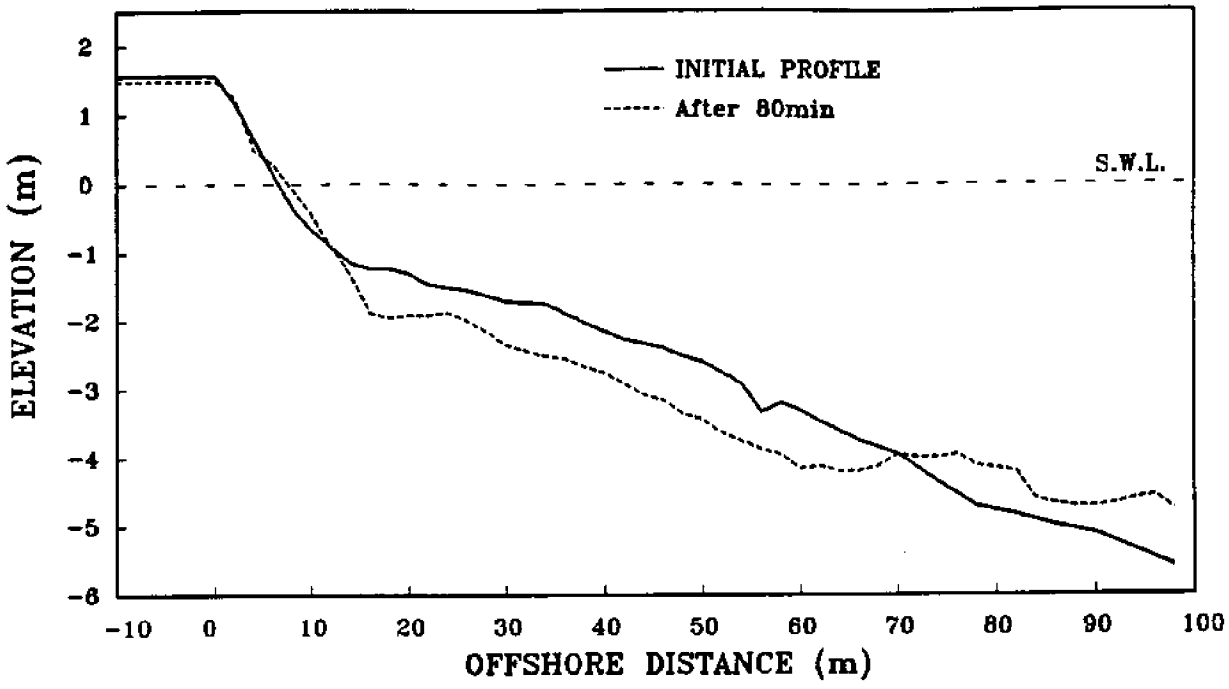

Figure 4.5: Example of Beach Profile with Diffused Bar, $D_{50} = 0.09mm$

$$\int_{x_0}^{x} \frac{\partial q}{\partial x} dx = -\int_{x_0}^{x} \frac{\partial h}{\partial t} dx \tag{4.3}$$

Let $q(x_0) = 0$ at landward closure we have:

$$q(x) = -\int_{x_0}^{x} \frac{\partial h}{\partial t} dx \tag{4.4}$$

with

$$\frac{\partial h}{\partial t} = \frac{[z(x,t_2) - z(x,t_1)]}{t_2 - t_1} \tag{4.5}$$

The quantites on LHS are measured. Thus, the spatial variation of transport rate between any two time levels can be computed from Equation 4.4 and 4.5. In theory, this transport rate should become zero at the offshore closure depth. Figure 4.6 illustrates a typical spatial variation of the transport rate for the erosional beach and bar-type profile. In the computation transport to the offshore direction is defined as positive.

The cumulative volumatric difference per unit width along the profile between two type steps defined as VD(volumetric difference) is simply the integration of Δh along the profile:

$$V.D. = \int_{x_0}^{x_c} \Delta h dx \tag{4.6}$$

$$\Delta h = z(x, t_2) - z(x, t_1) \tag{4.7}$$

If the profile is truly two dimensional and the sediment bulk density is unchanged VD should be zero when the integration is carried out to the closure depth to conserve the mass. In the experiments, non-zero values were often obtained owing to the combined effects sediment losses to the offshore region and the three dimensional tank effect.

The beach profiles evolution at different elasped time, the computed transport rate and V.D. values are presented graphically in Appendix A.

4.3.3 Beach Erosion

There are a number of ways to define beach erosion. The two common ones are shoreline retreat and volumetric sand loss. The former is clearly more direct and the latter may be or more engineering concern. In the experiments, the shoreline is not always easy to define in the final profile as the profile may undulate near mean water level thus resulting in multiple intersects. To compute volumetric loss, one must define an offshore cutoff point which also is not necessarily easy. In the present experiment setups, the initial profile was composite and has a natural break. This artifical point is chosen as the offshore limit in the volumetric integration based on Equation 4.6. This volume is defined as the dune volume erosion and the results are presented in Figure 4.7 to 4.10. As can be seen, most of the erosion took place in the early period and the erosion rate decreased rapidly on later times. However, not all cases had reached non-erosional state at the end of the tests (in most cases 80

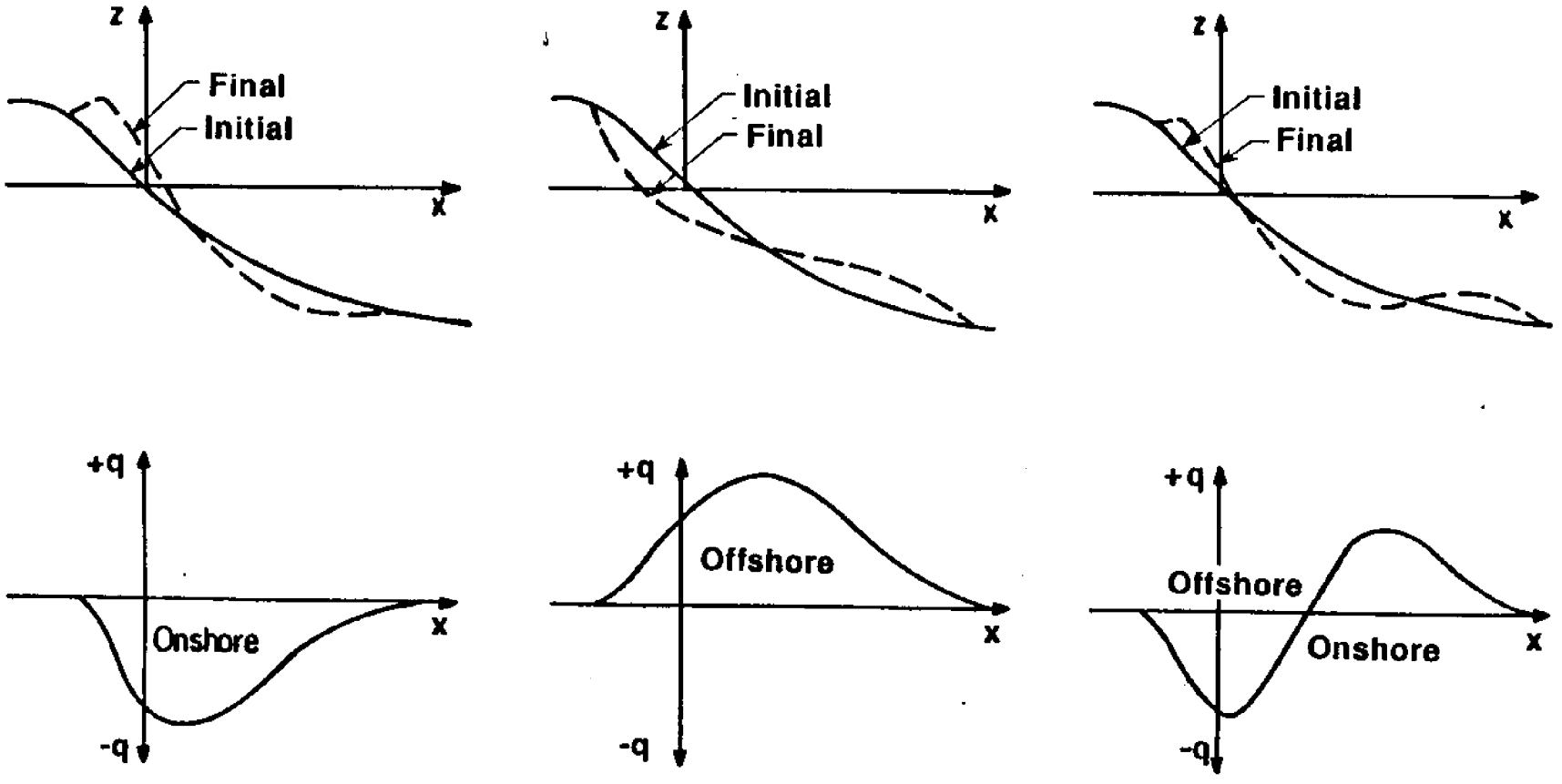

Figure 4.6: Definition Of Net Sediment Transport Rate Across The Beach Profile

minutes test time). In fact, the general trend as evidenced from the figures appeared to indicate otherwise.

4.3.4 Profile Evolution and Bar Migration

As mentioned earlier, most of the profiles evolved into bar-type with erosion at near the shore face and dune region. Initially the material eroded from the beach face was deposited just seaward of the plunging point to form a breaking bar. A trough would develop immediatedly landward of the breaking bar. As the bar grew, waves started to break farther offshore, causing the location of the bar also to move offshore. The volume of the bar would also grow as the bar elevation is mainly controlled by the water depth. The material supply was taken from the region inshore of the bar. Secondary bar(s) could also be developed shoreward of the breaking bar. The breaking bar developed rather quickly in the early stage of the test. But the process of bar migration was more gradual and the rate of offshore migration also slowed down as time progressed. Analysis was performed here to quantify the process of bar development and to examine whether a stable profile had been reached at the end of the test.

First a definition of a bar feature is needed. In the laboratory a convienent reference is the initial profile and a bar can be defined as material accumulated above the initial profile. The limits of the bar can be expressed by the intersects with the initial profile. A number of indices can be defined to charecterize the bar such as the bar volume, the bar crest location and the mass center. These definions are given in Figure 4.11. A number of difficulties were encountered in handling the actual test profiles. The most frequent problem was that there existed no clear intersecting point at the seaward end, and, at other occasions, the bar appeared reached beyond the toe of the beach profile. The same problem was also encountered at the landward end but of fewer cases. For these cases, the intersects were determined subjectively.

Each profile survey was, thus, visually examined for bar feature. The following

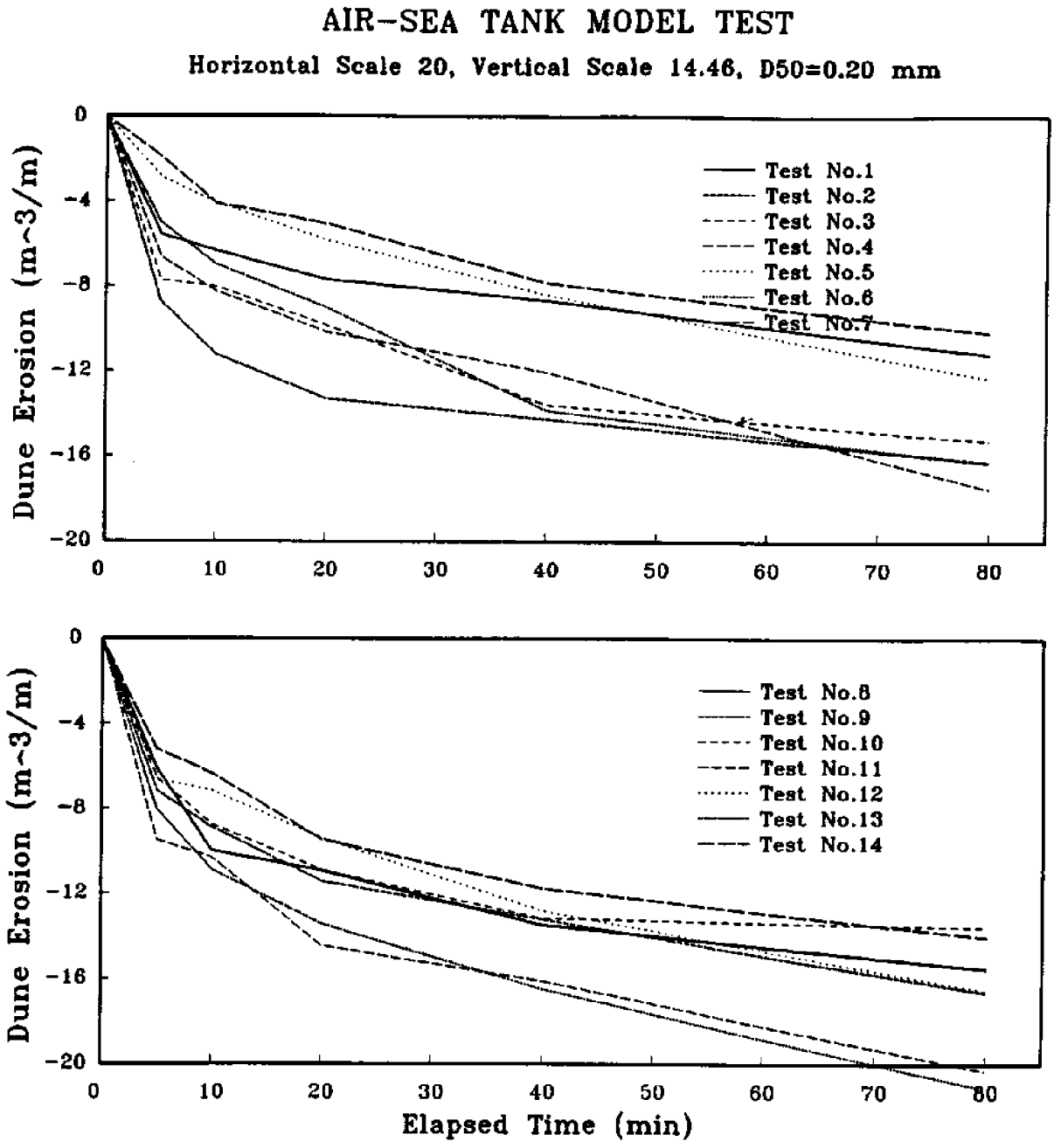

Figure 4.7: Dune Erosion Evolution With Elapsed Time in ASW(1)

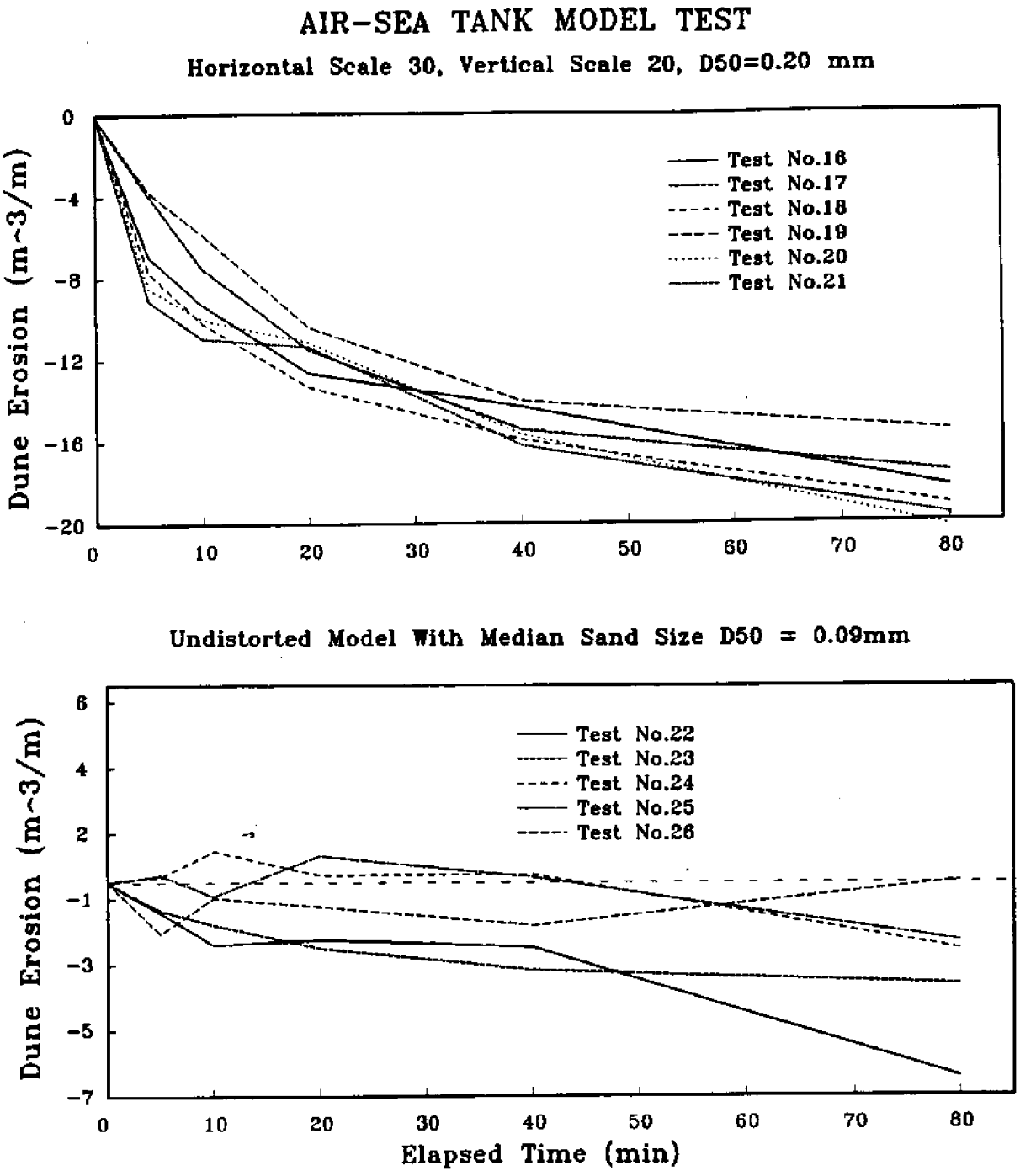

Figure 4.8: Dune Erosion Evolution With Elapsed Time in ASW(2)

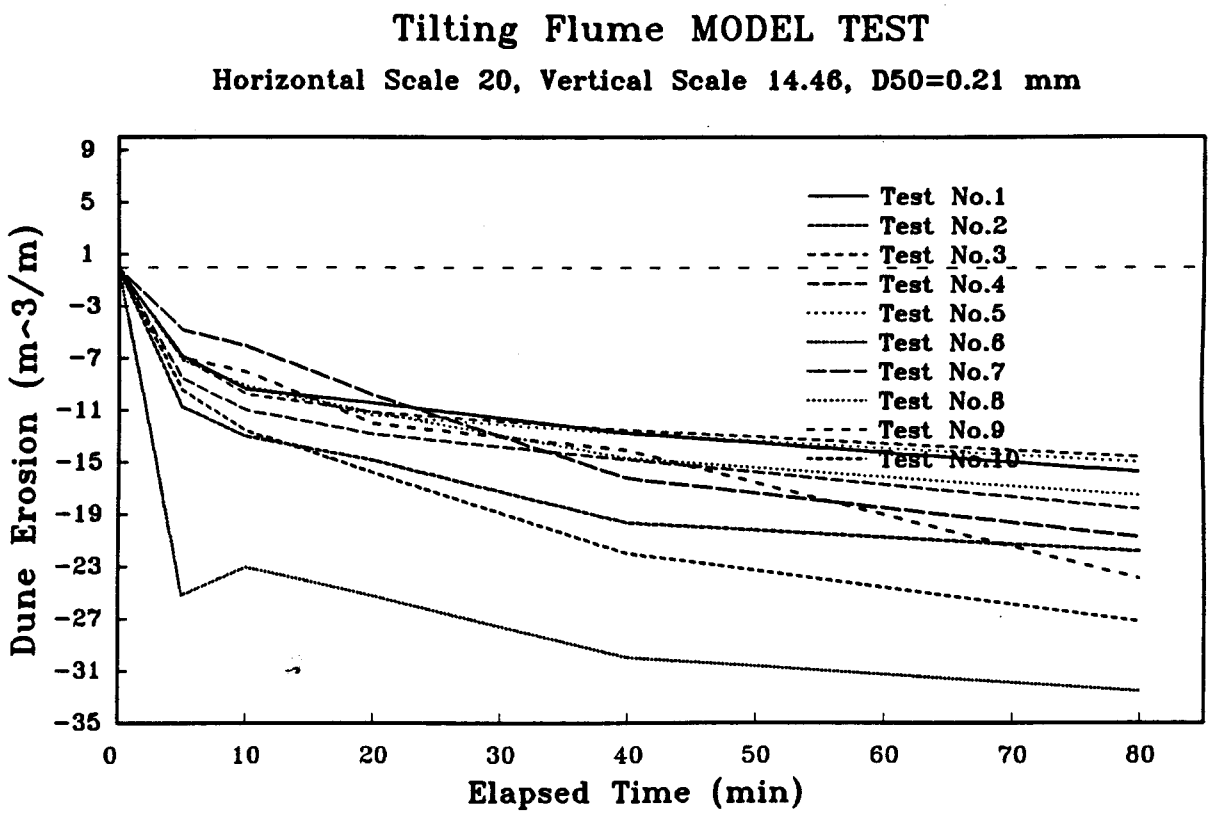

Figure 4.9: Dune Erosion Evolution With Elapsed Time in WF

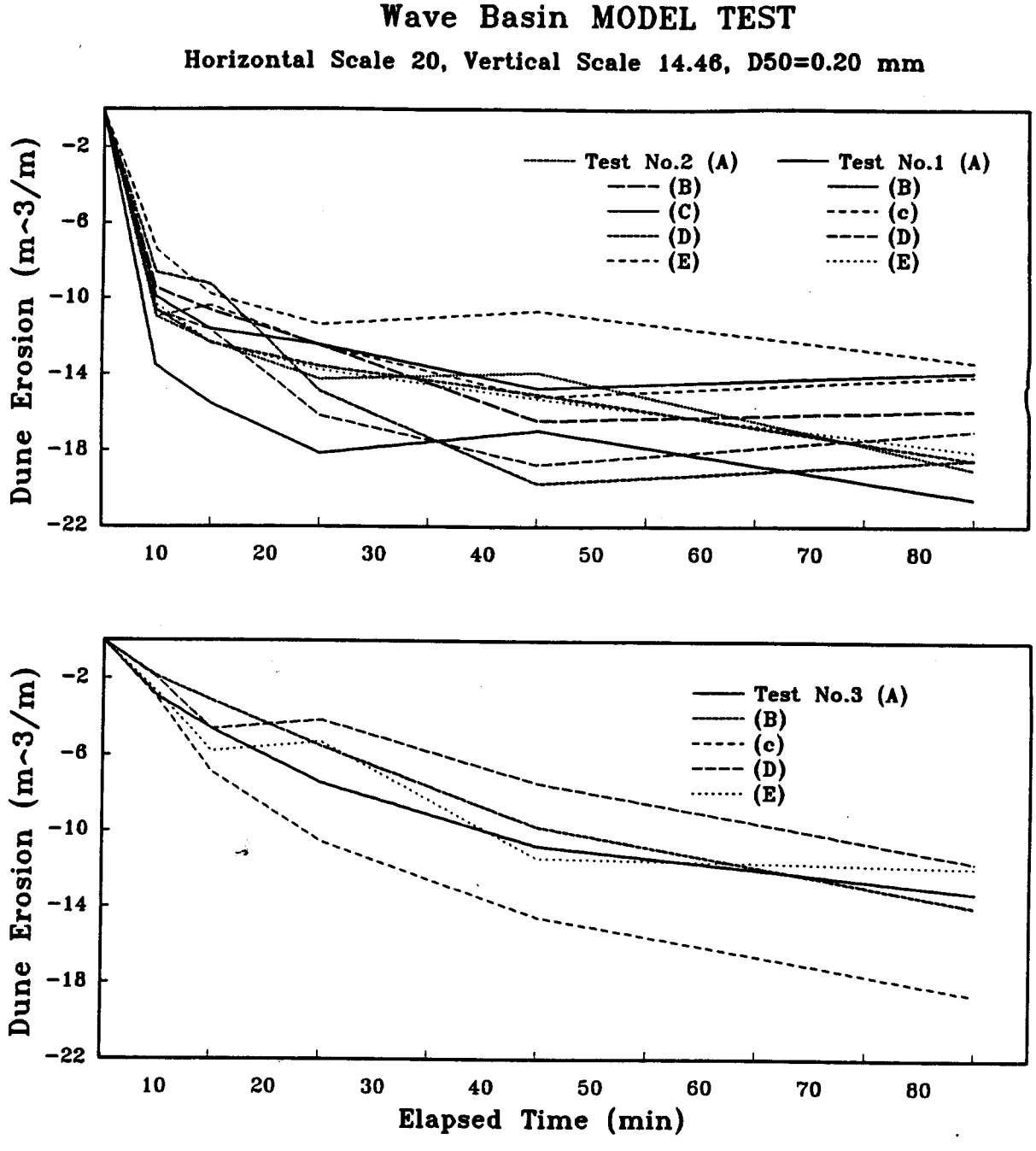

Figure 4.10: Dune Erosion Evolution With Elapsed Time in WB

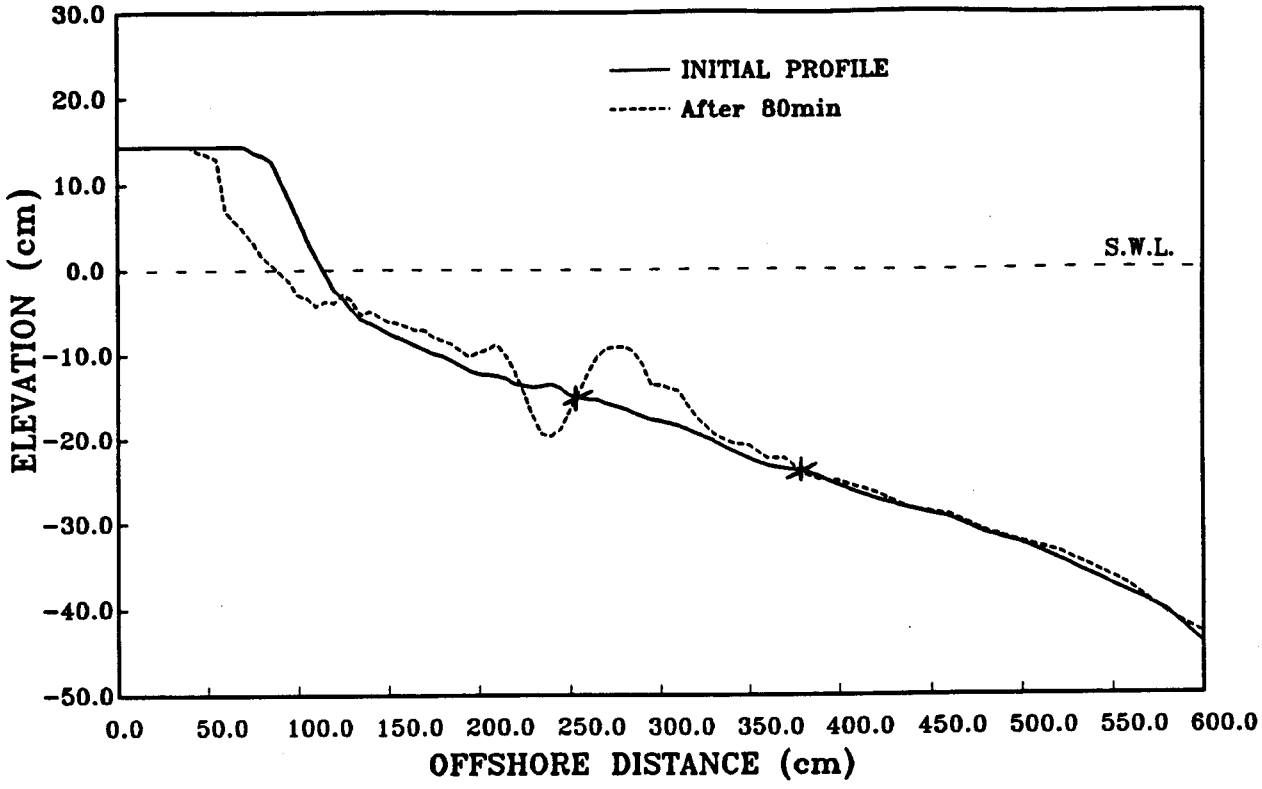

Figure 4.11: Definition of Longshore Bar With Respect to Initial Profile

properties are then calculated for every identified breaking offshore bar from the profiles: bar voulume = V_b, location of bar center of mass = x_{cm}, location of bar crest =x_c.

The results of these computed values are given in Figure 4.12 to 4.23 for the natural fine sand ($D_{50} = 0.20mm$). As can be seen from the above figures, breaking bar development can be broken down into two distinctive stages: the formation stage and movement stage. During the formation stage the breaking bar grew rapidly as can be seen from the growth curves of both bar crest and bar volume. The bar quickly reached a stable condition usually within the first 10 to 20 minutes of the test. Once the bar reached this mature stage it remained rather stable and only moved at a very slow rate in the offshore while bar volume also grew. This can be witnessed from the distinct breaks of the curves shown in the above figures. In most of cases, the bar and the profile appeared to gradually reach a stationary condition near the end of the

tests. There were cases, however, the bar seemed to extend beyond the end of the initial profile and an offshore intersecting point could not be established; consequently , the bar volume could not be clearly defined. For these cases, a stationary condition may or may not have been reached. It is also observed here that as indicators of bar development, the bar crest and the bar mass center, particularly the bar crest, appeared to be more stable than bar volume. Part of reason may be that the bar crest is mainly controlled by the wave breaking point whereas the bar volume could be rather diffused at times for lack of clear boundaries. As a consequence, the bar crest usually approached to a stationary position in the test whereas the volume still was undergone changes.

Similar anayalsis was performed for the very fine quartz sand ($D_{50} = 0.09$ mm)tests. The results were shown in Figure 4.24 to 4.26. In most of these cases, a clean bar-profile such as evidenced in the natual sand tests was not obtained. The bar(s), if any, was rather diffused. This was likely due to the fact that the very fine material which when suspended by the wave motion settled over a wider aera.

4.3.5 Eqilibrium Beach Profile

Equilibrium beach profile is an idealized stable beach profile under a given stable wave condition. The permise is that under a constant wave condition, the profile will eventually evolve into a shape such that the net sediment tranport at any point along the profiile is zero, or in other words, the destructive and constructive forces reached local balance. This idea is widely accepted and applied in coastal engineering In the field, since the enviornmntal forces change constantly, the equilibrium profile, if exists, should also be "dynamic" that might change its shape or shift its location from time to time and are, therofore, more difficult to define or verify. In theory, the idea of equilibrium profile can best be tested in a laboratory enviornment under controlled test conditions. Therefore, although testing the concept of equilibrium profile is not the main objective of this thesis analysis was performed here to contribute to this

topic. Basically, there are two issues; whether equilibrium condition is attainable or has been attained in the tests and, if it is, what is the final shape?

Based on the analysis given above, one can clearly identify that the time-averaged sediment transport rate along the profile deceased monotonically with increasing time. This is illustrated here by the test case 8 which was tested for an extended period up to 240 minutes. The profile change as well as transport rate are shown in Figure 4.27.

For most of test cases, the transport rate quickly approached to negilible value after 40 to 80 minutes run time. This can be seen from the plots in A.1 to A.26. Another stable feature is the bar profile which was generally achieved before the end of 80 minutes test time after which the breaking bar maintained its shape with little or no movement.

The quantity that appeared to have not reached stable condition at the end of the tests were the dune erosion volume which still showed a trend of increasing. This suggested that even when the profile appeared to have reached a stable form it may shift as a whole.

As to the shape of the equilibrium profile, the results will be presented in chapter 5.

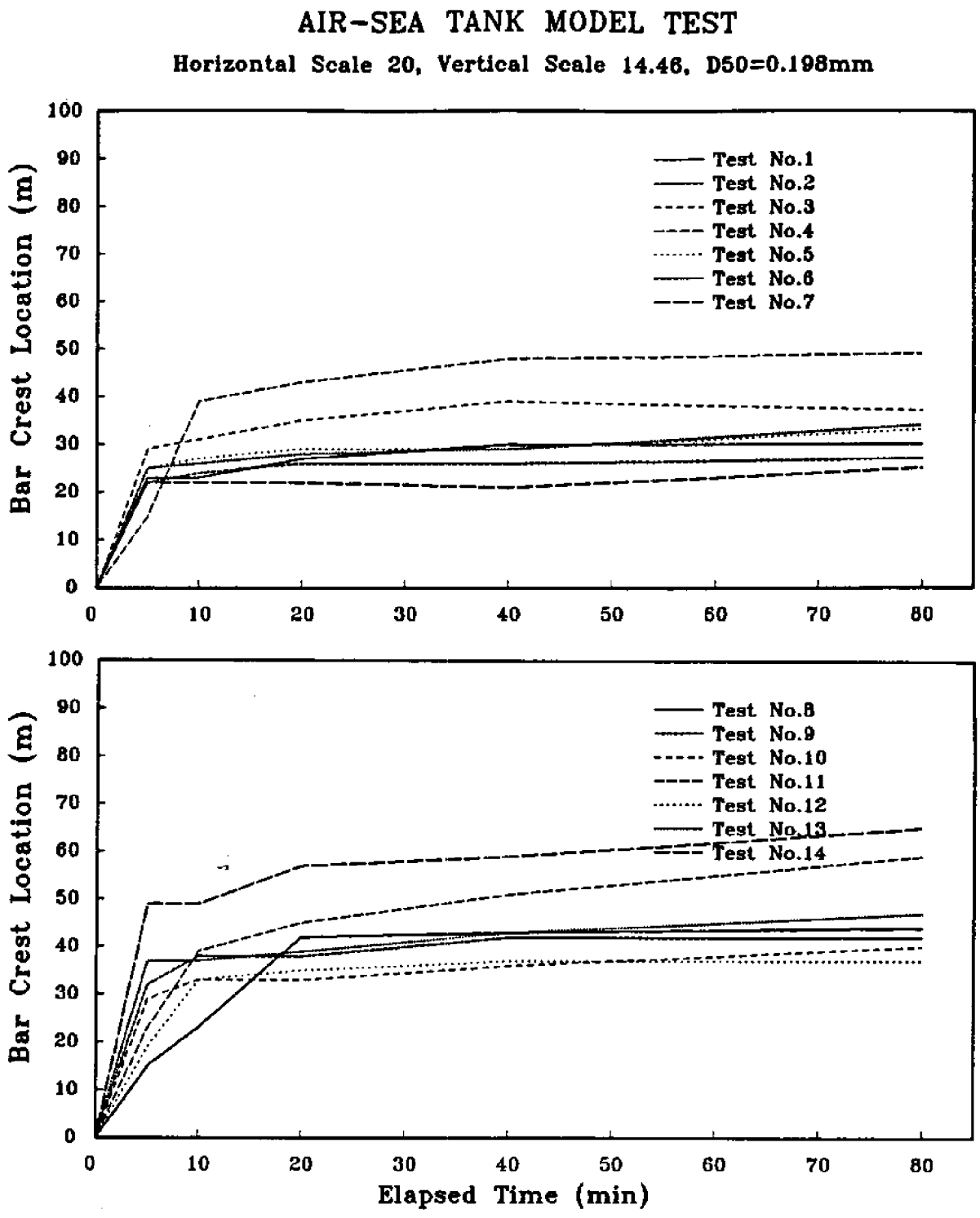

Figure 4.12: Horizontal Movement Of Bar Crest With Horizontal Scale Equal to 20.

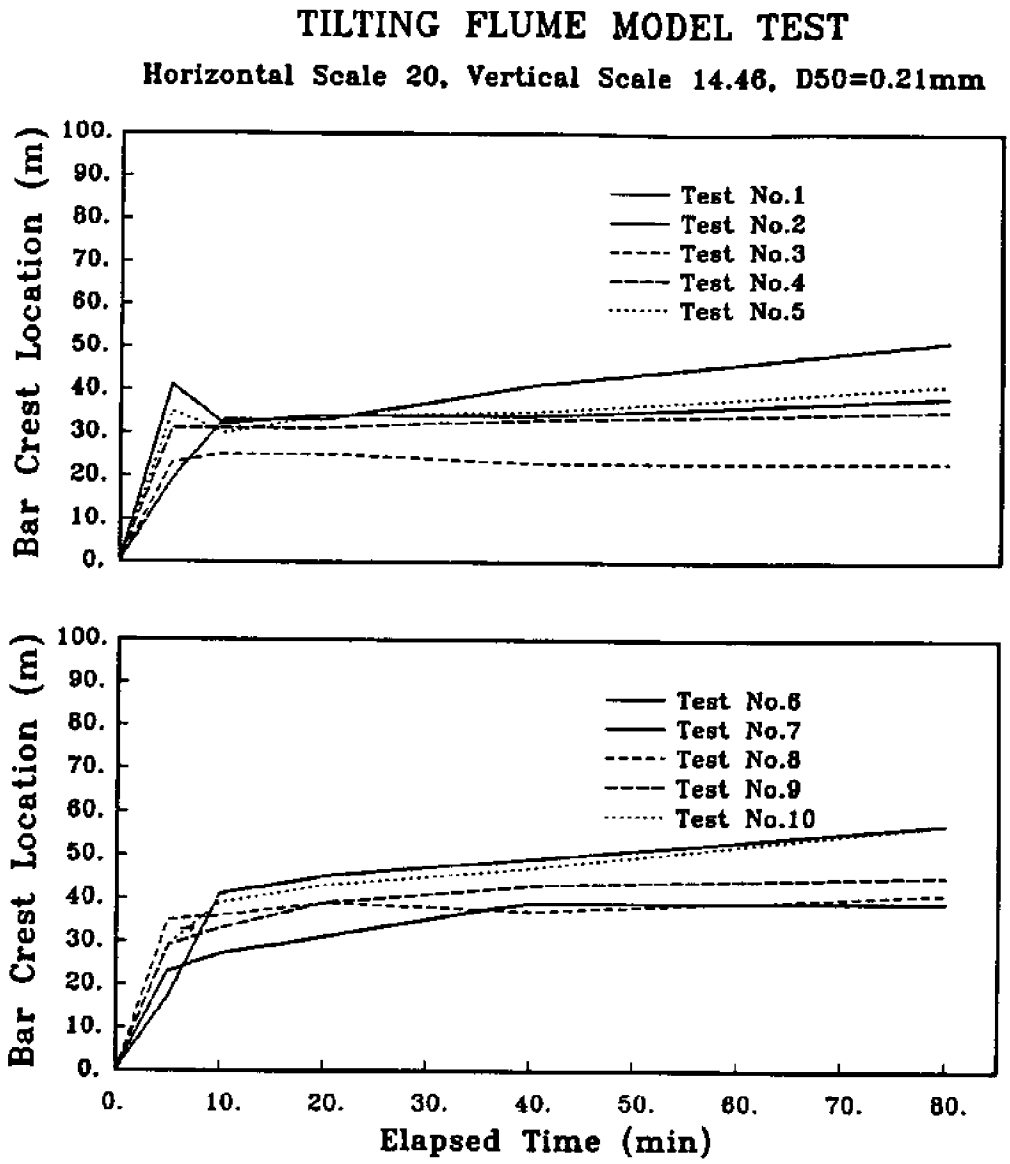

Figure 4.13: Horizontal Movement Of Bar Crest With Horizontal Scale Equal to 20 In WF

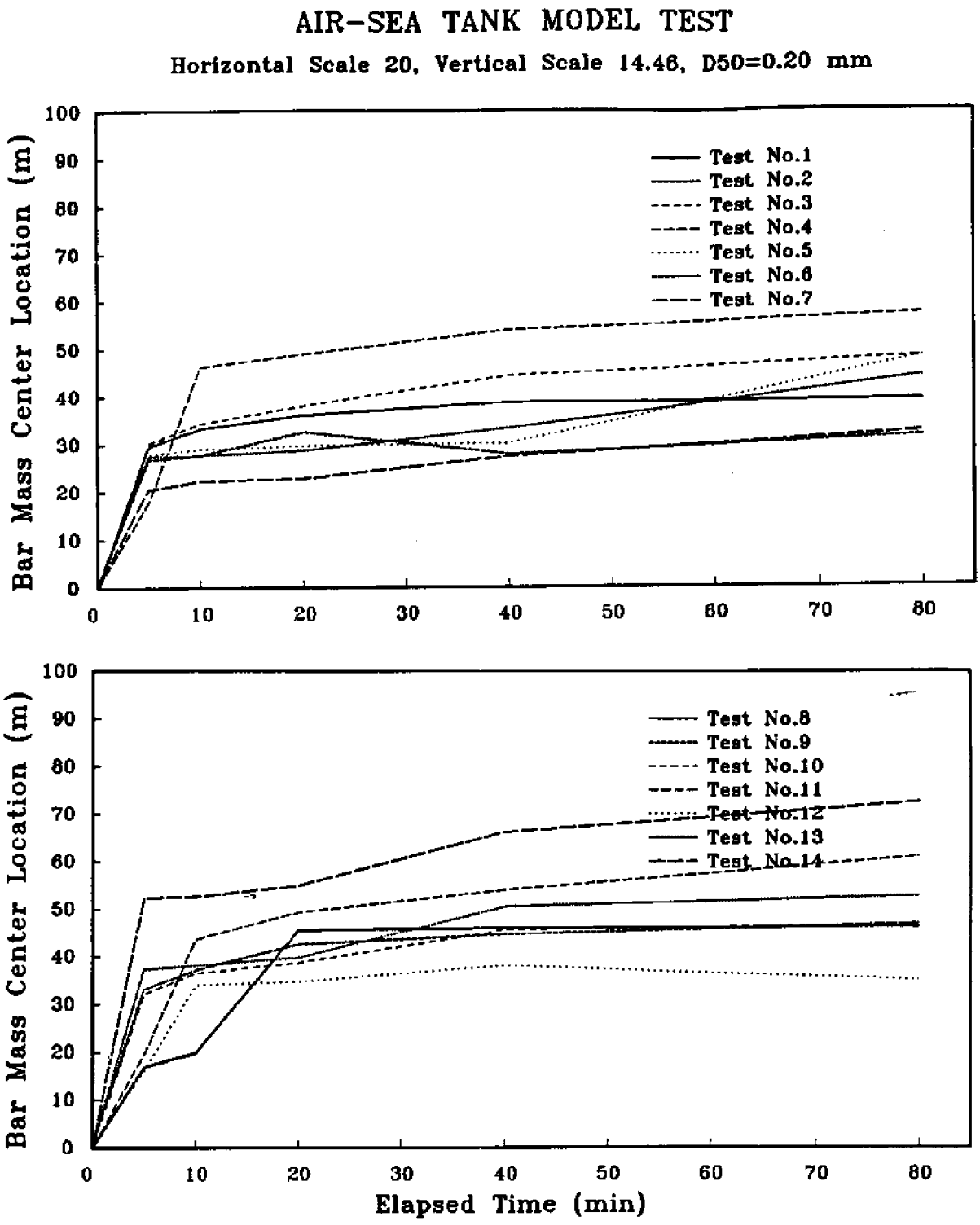

Figure 4.14: Horizontal Movement Of Bar Mass Center With Horizontal Scale Equal to 20 In ASW

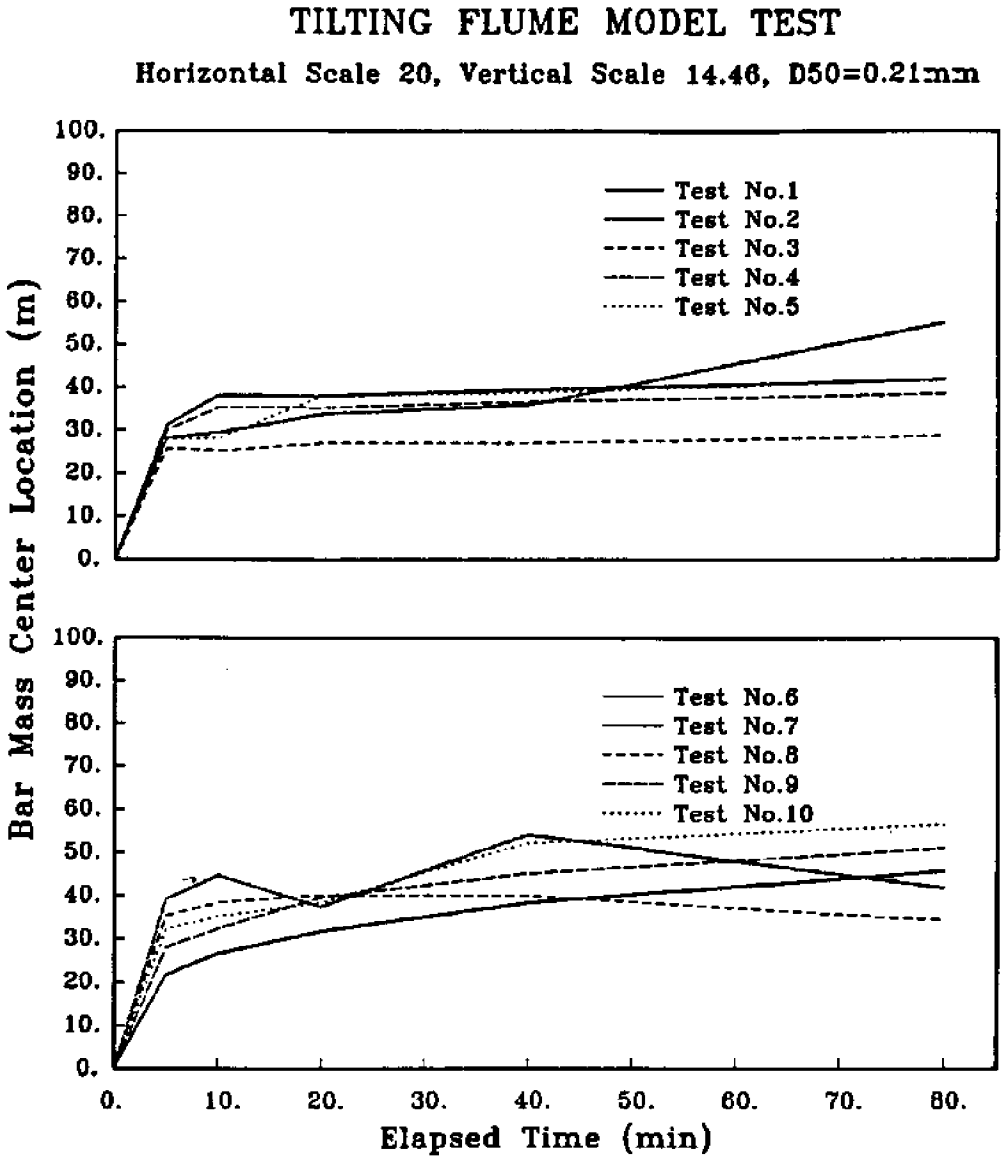

Figure 4.15: Horizontal Movement Of Bar Mass Center With Horizontal Scale Equal to 20 In WF

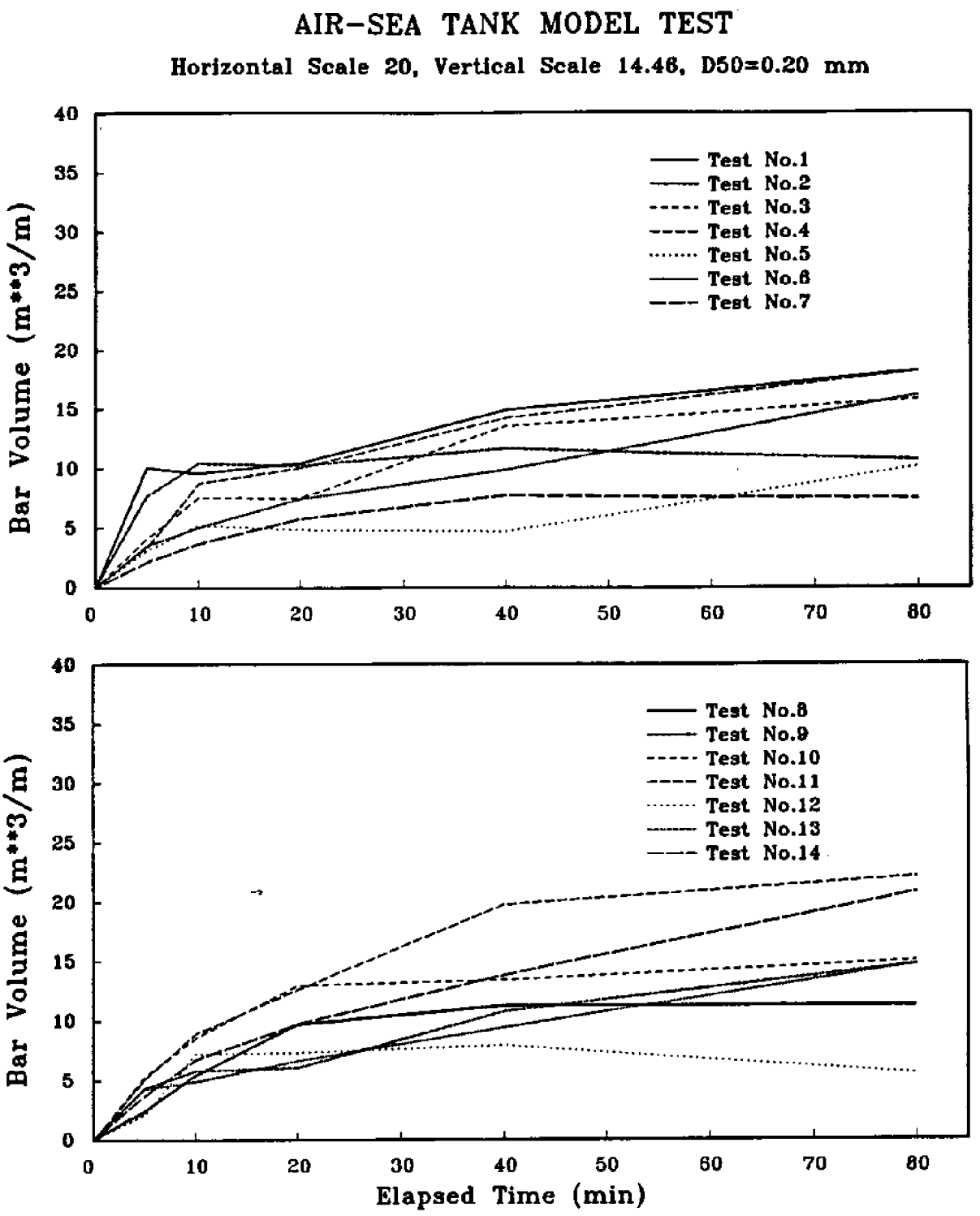

Figure 4.16: Growth of Bar Volume With Horizontal Scale Equal to 20 In ASW

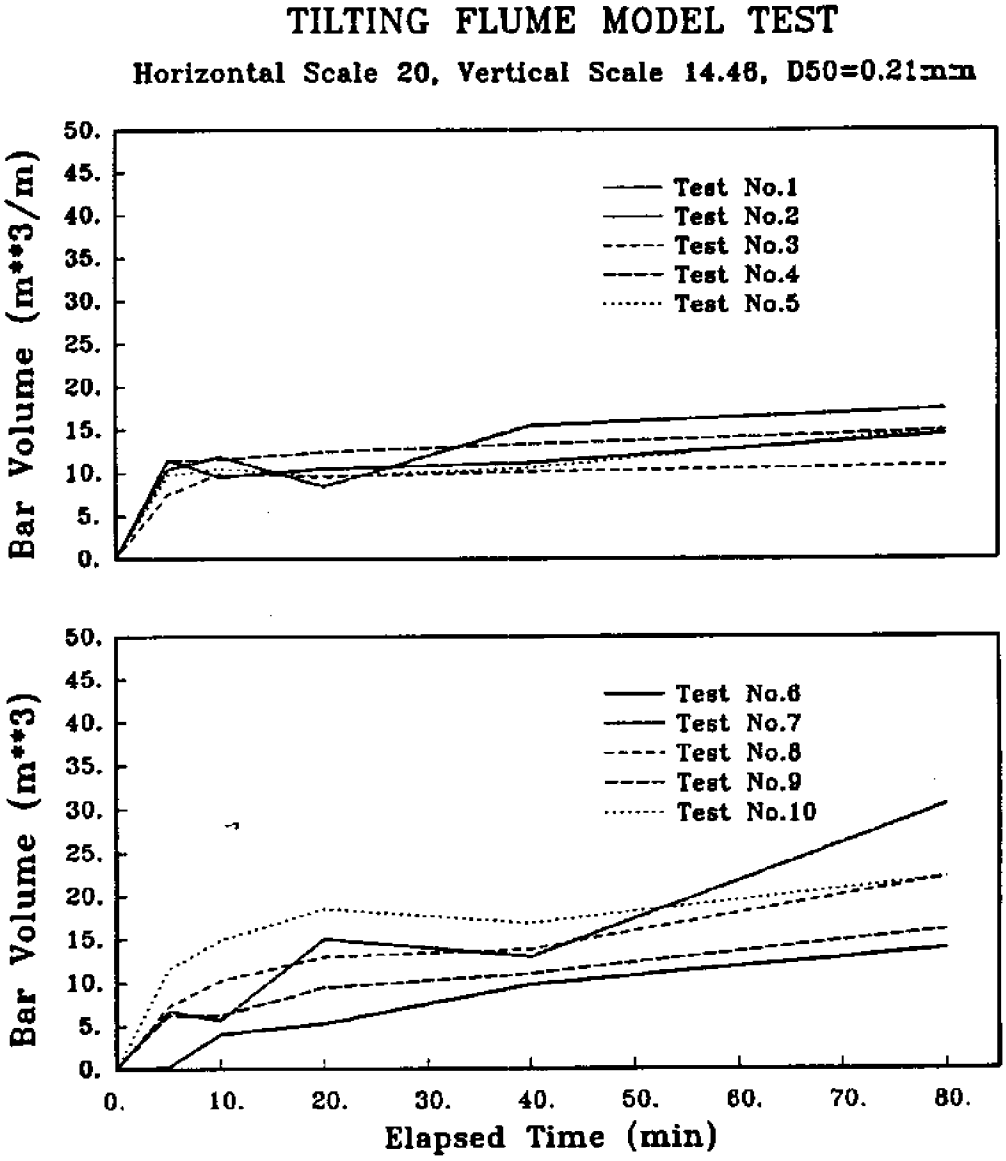

Figure 4.17: Growth of Bar Volume With Horizontal Scale Equal to 20 In WF

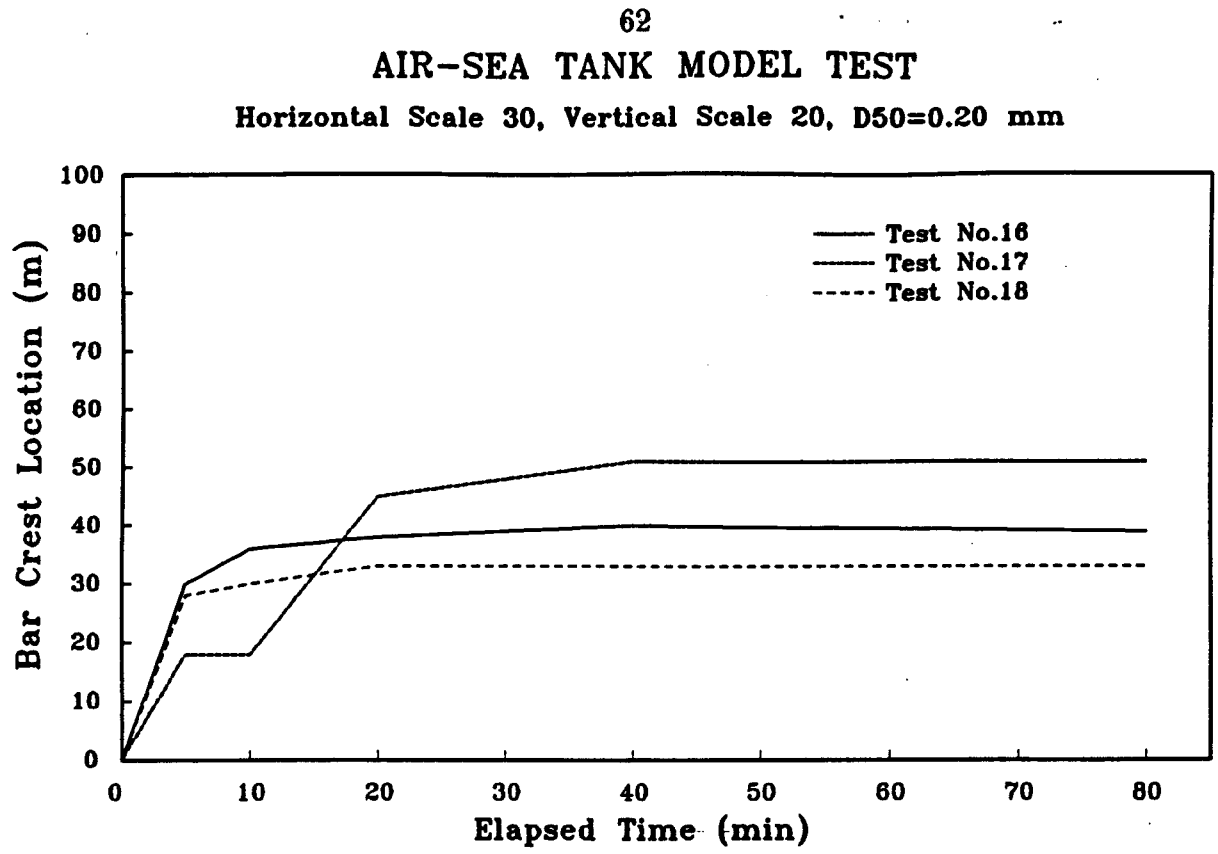

Figure 4.18: Horizontal Movement Of Bar Crest With Horizontal Scale Equal to 30.

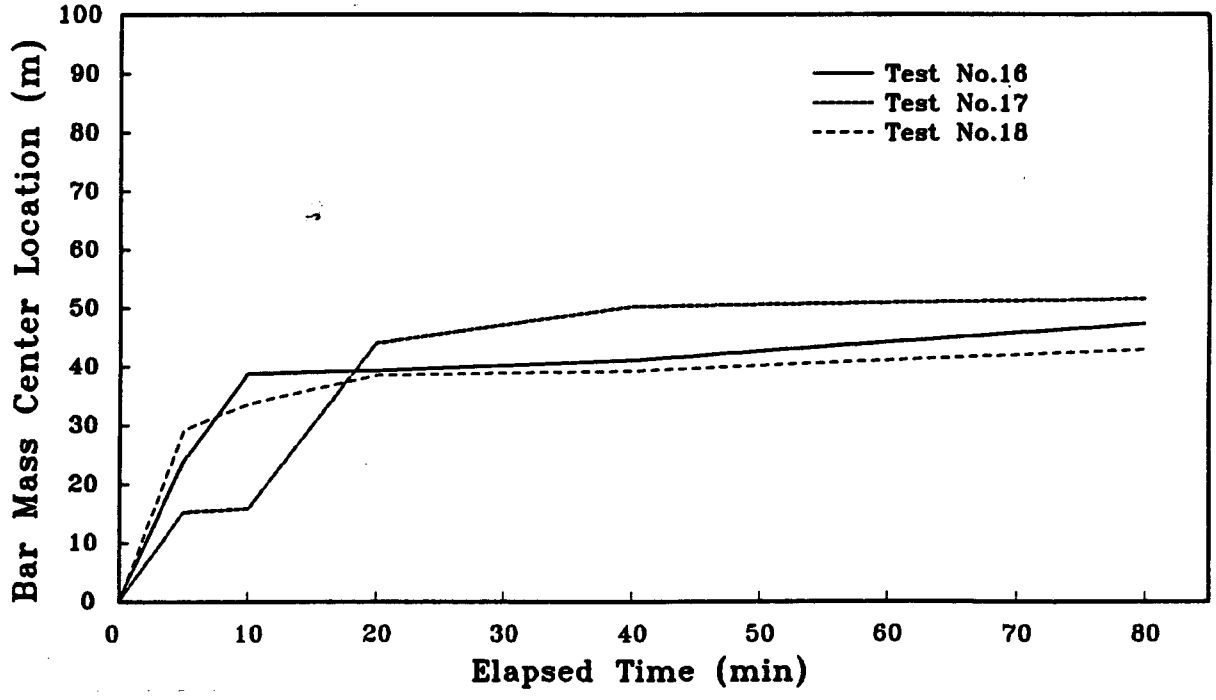

Figure 4.19: Horizontal Movement Of Bar Mass Center With Horizontal Scale Equal to 30.

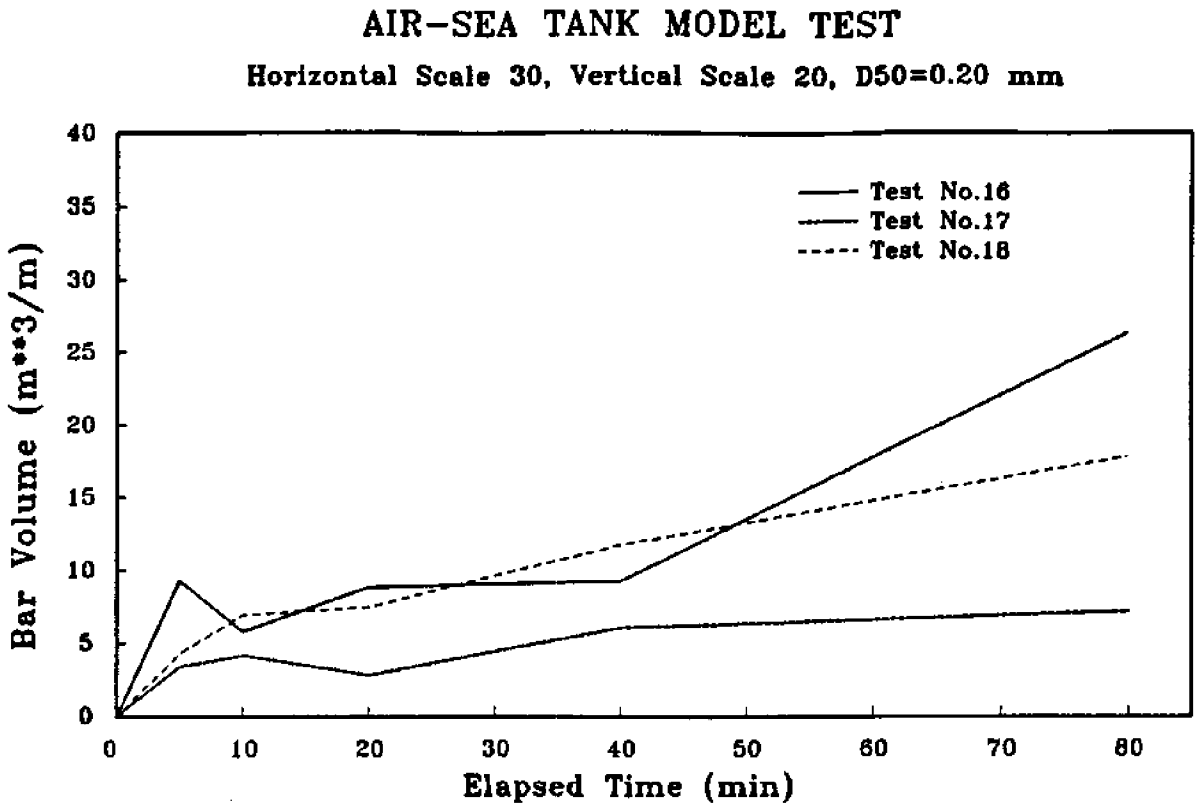

Figure 4.20: Growth Of Bar Volume With Horizontal Scale Equal to 30.

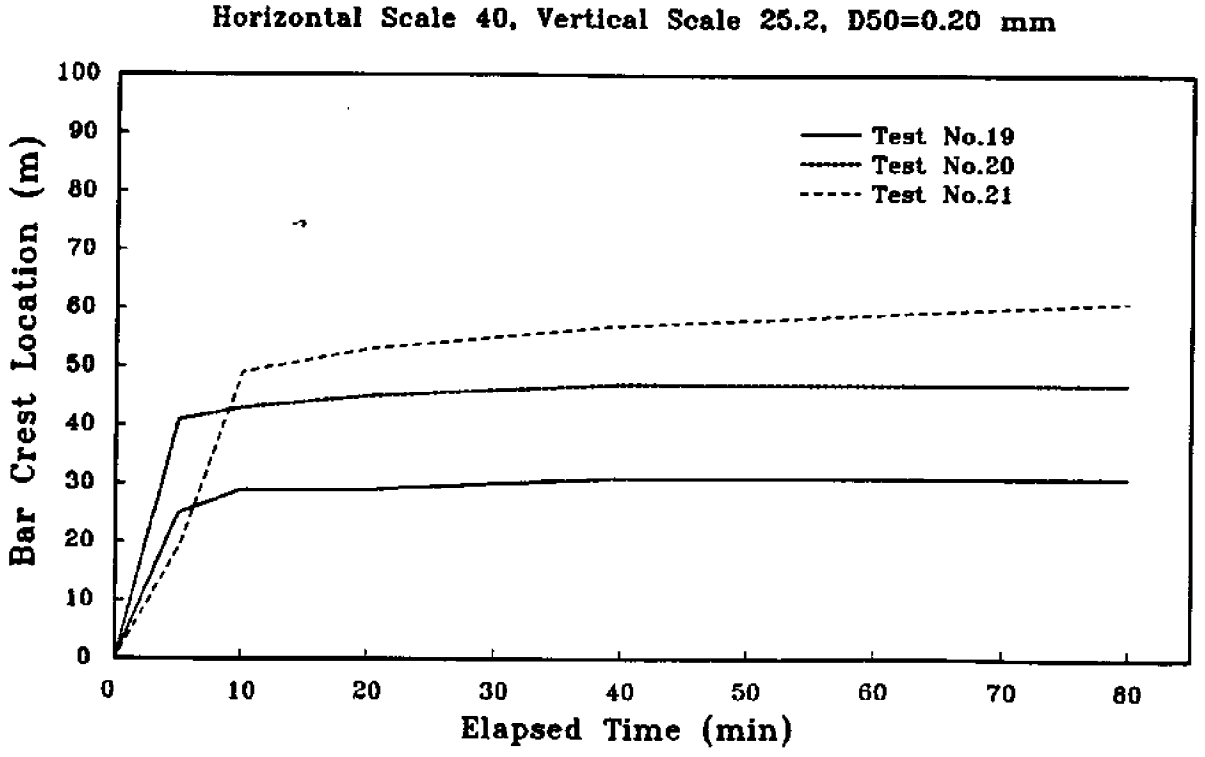

Figure 4.21: Horizontal Movement Of Bar Crest With Horizontal Scale Equal to 40.

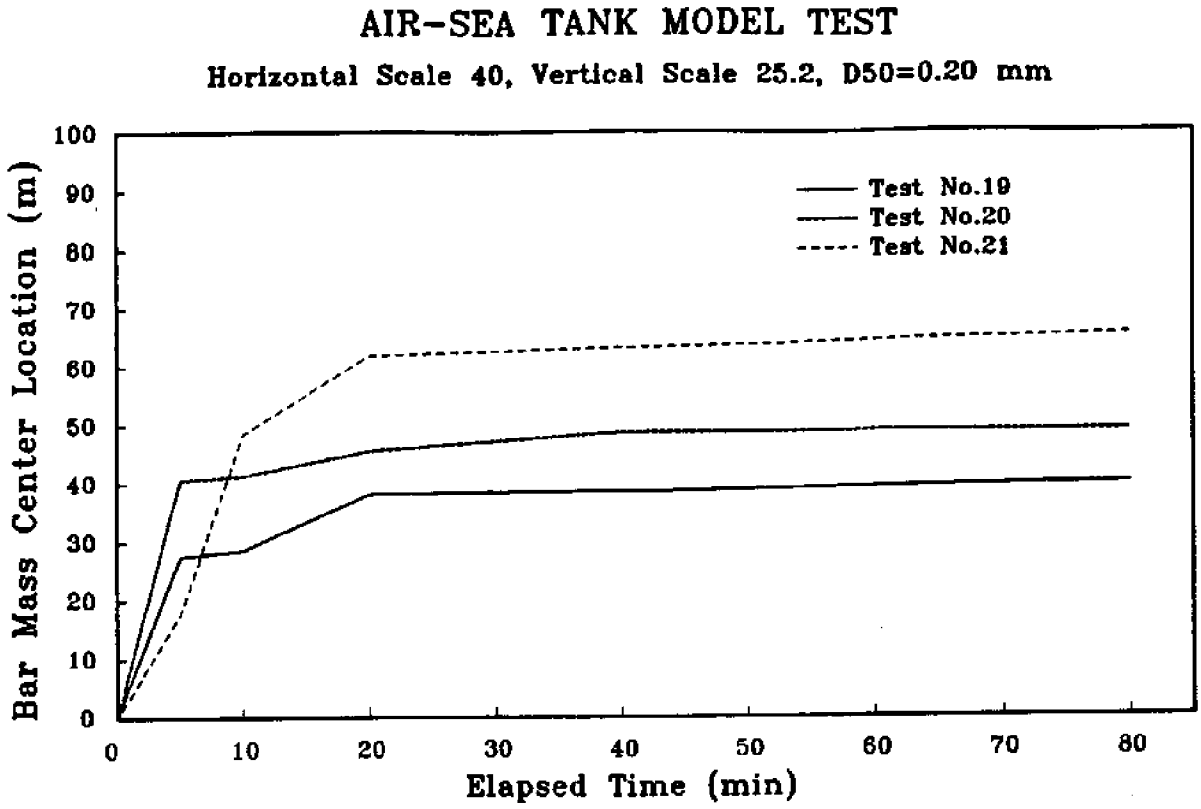

Figure 4.22: Horizontal Movement Of Bar Mass Center With Horizontal Scale Equal to 40.

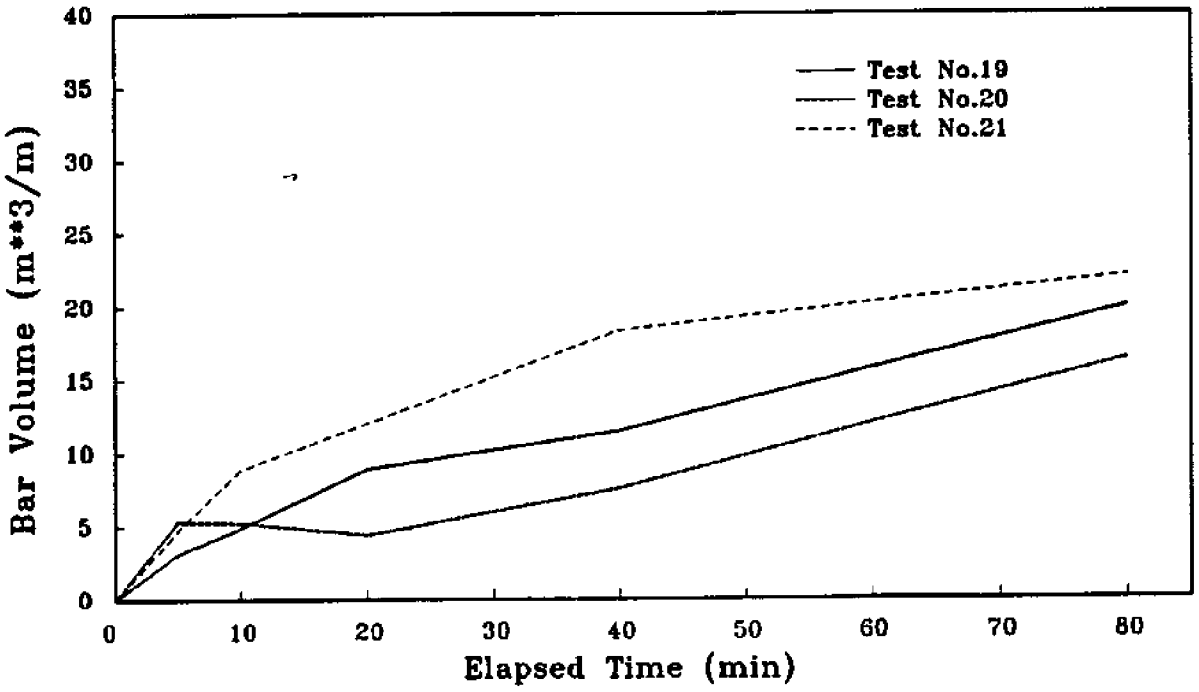

Figure 4.23: Growth Of Bar Volume With Horizontal Scale Equal to 40.

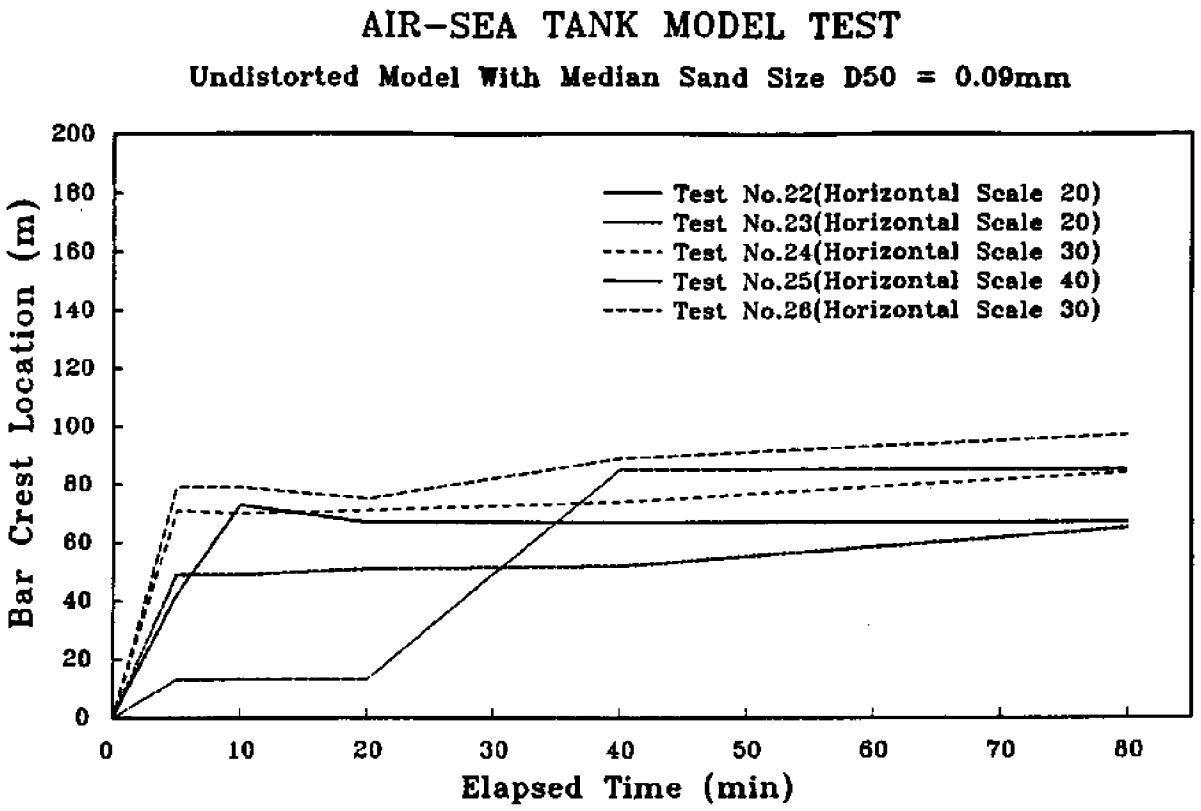

Figure 4.24: Horizontal Movement Of Bar Crest With $D_{50} = 0.09mm$

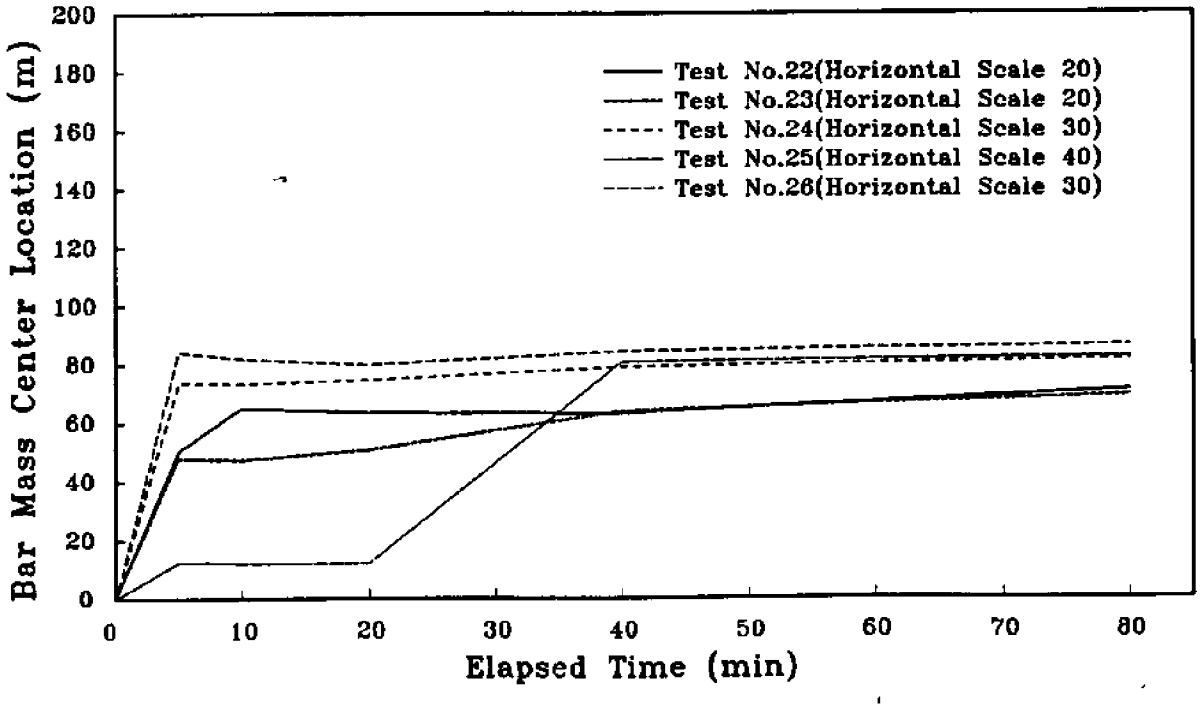

Figure 4.25: Horizontal Movement Of Bar Mass Center With $D_{50} = 0.09mm$

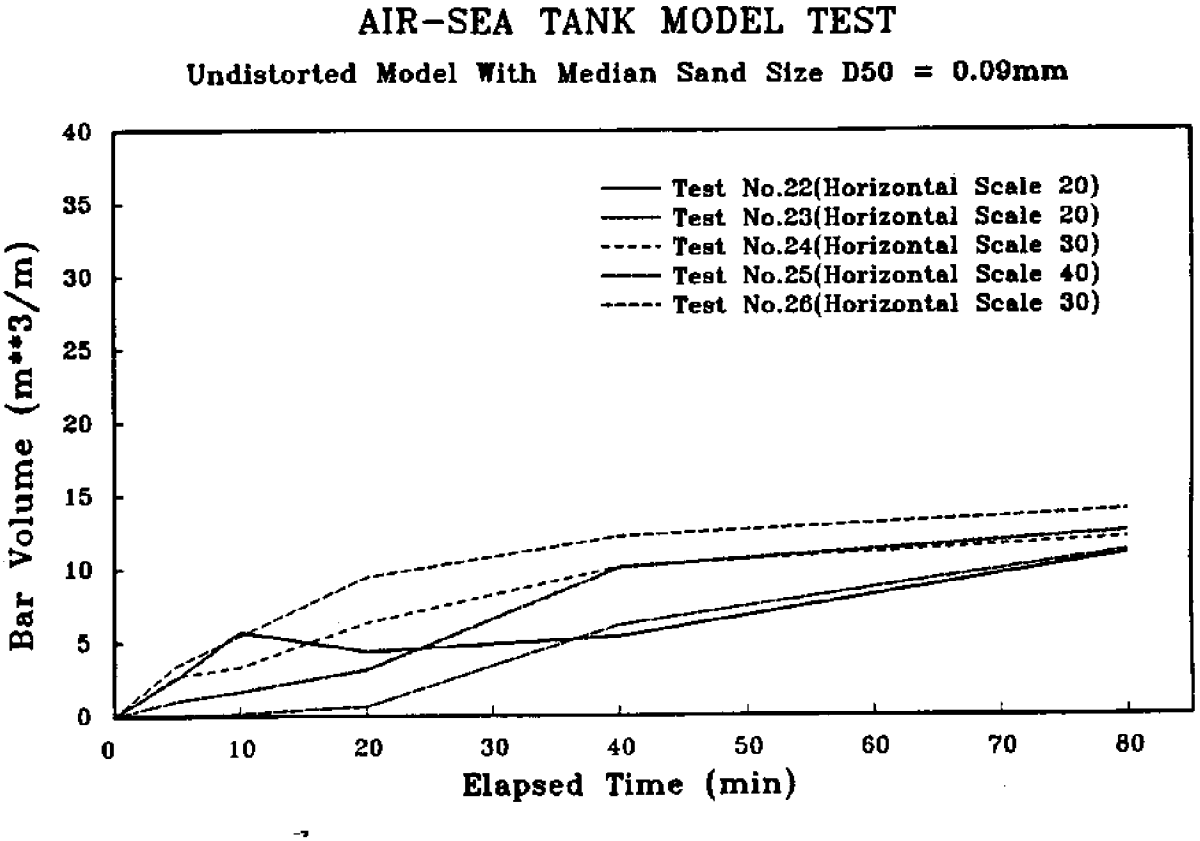

Figure 4.26: Growth Of Bar Volume With $D_{50} = 0.09mm$

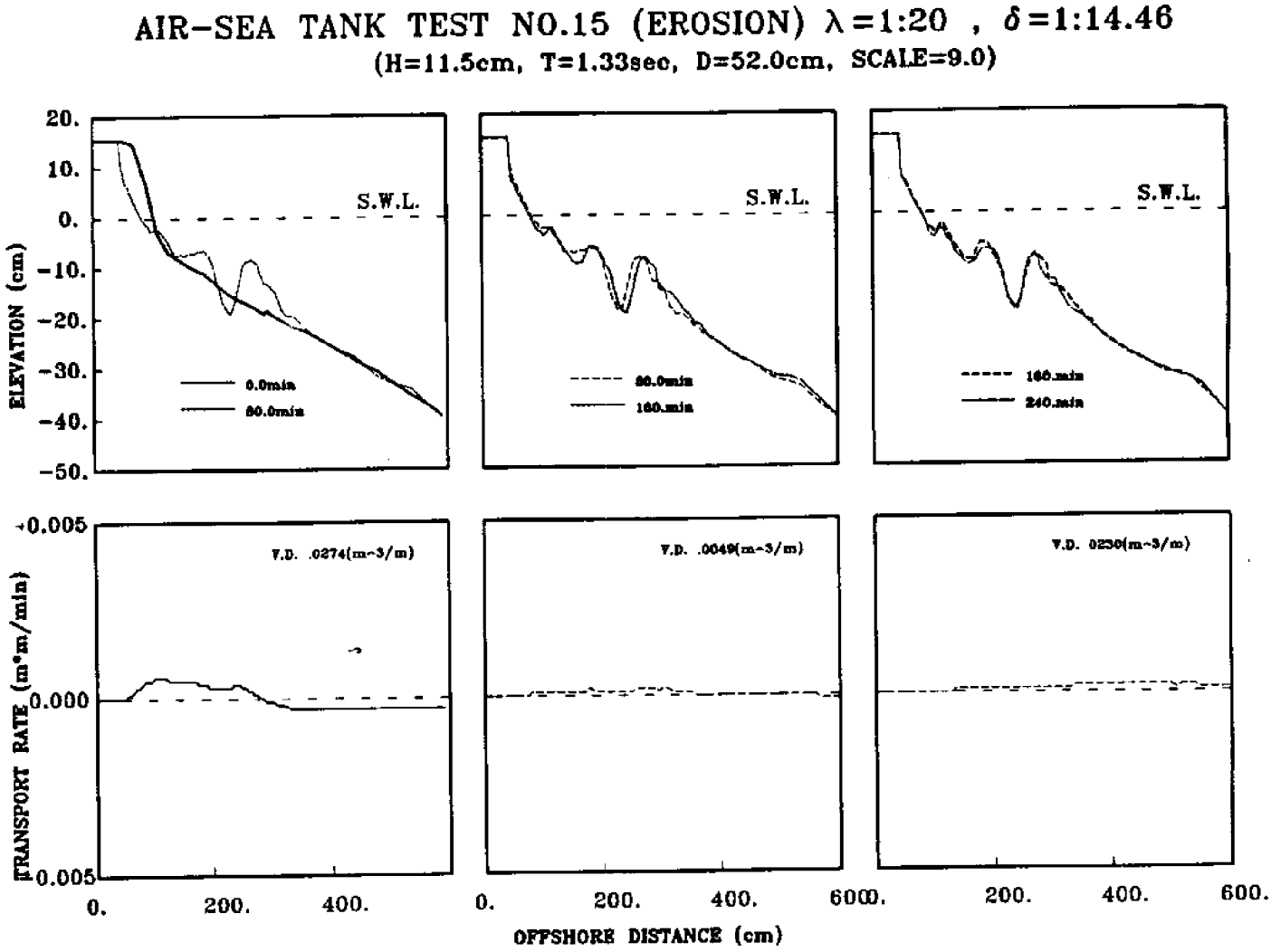

Figure 4.27: Beach Profile Evolution And Sediment Transport Rate

CHAPTER 5
EVALUATION OF SCALING LAWS

5.1 Methodology and Evaluation Criteria

As stated earlier a specific set of test results from GWK is treated here as the prototype conditions. All the test results were compared with the GWK data set as basis for evaluating the scaling laws. Basically , four different scaling laws from Table 3.1 were selected for the purpose; they are, by first author's name, vallinga, Hughes, Wang 1 and Wang 2. They practically cover the existing scope of the profile modeling law. These four scaling laws are repeated here in Table 5.1.

To facilitate quantitative evaluation certain criteria are employed here. The entire beach profile is first divided into two parts: from the shoreline to the end of the first slope of the profile is defined as the dune profile region and from the beginning of the second slope of the profile to the end of the toe is defined as the bar profile region such as given in Figure 5.1. Six different quantities were used for evaluations, two related to the dune region and four related to the bar region; they are:

A. Dune Region:

The RMS value of the dune region profile.

The dune erosion volme.

B. Bar Region:

The RMS value of the bar region profile.

The location of bar center of mass.

The location of bar crest.

The volume of bar.

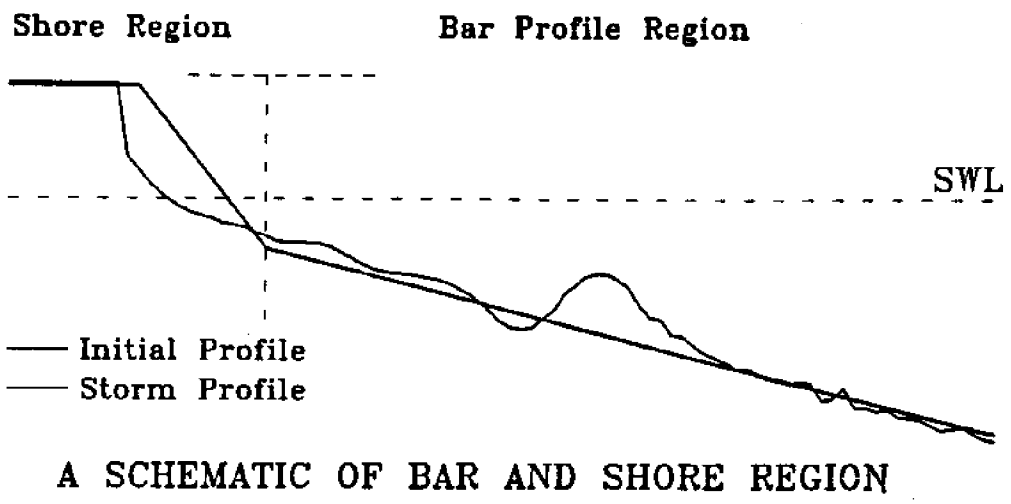

Figure 5.1: Definition of The Dune and Bar Regions

Table 5.1: **Four Fall Speed Distorted Model Laws**

Author	Geometric Distortion	Hydrodynamic Time Scale	Morphological Time Scale
Vellinga (1982)	$\frac{N_\lambda}{N_\delta} = (\frac{N_q N_\delta}{N_W^2})^{0.28}$	$N_T = \sqrt{\frac{N_\delta}{N_g}}$	$N_{t_m} = \sqrt{\frac{N_\delta}{N_g}}$
Hughes (1983))	$\frac{N_\lambda}{N_\delta} = (\frac{N_q N_\delta}{N_W^2})^{1/2}$	$N_T = \frac{N_\lambda}{\sqrt{N_\delta N_g}}$	$N_{t_m} = \frac{N_\lambda}{\sqrt{N_\delta N_g}}$
Wang, et.al (1990))	$\frac{N_\lambda}{N_\delta} = (\frac{N_q N_\delta}{(N_\rho N_W)^2})^{1/4}$	$N_T = \sqrt{\frac{N_\delta}{N_g}}$	$N_{t_m} = \sqrt{\frac{N_\delta}{N_g}}$
Wang,et.al (1994)	$\frac{N_\lambda}{N_\delta} = (\frac{N_q N_\delta}{(N_\rho N_W)^2})^{1/4}$	$N_T = \sqrt{N_\lambda}$	$N_{t_m} = \sqrt{N_\lambda}$

All the above quantities were evaluated relative to the reference prototype quantites in terms of error such that the set with the least error represents the best fit. Detailed formulas for computations will be presented later in the appropriate sections.

Geometrical scaling was evaluated first based on the RMS error of the profiles in the two regions. Wave height and wave period scalings were then evaluated by comparing the scaled final profiles of all the test cases with the prototype final profile. Finally, the best-fit data sets from each horizontal-scale group, i.e., N_λ =20, 30 and 40, were selected to evaluate the morphological time scale.

5.1.1 Geometrical Scaling and Equilibrium Profile

The gerometrical scale was evaluated by comparing the RMS (root mean square) error of the final test profiles with the prototype. The RMS error is defined as

$$c = [\frac{1}{n}\sum_{i=1}^{n}(h_i^P - h_i^M)^2]^{\frac{1}{2}} \tag{5.1}$$

where h^P and h^M are profile elevation of prototype and model, respectively. There are basically only two geometrical scaling laws in the 4 modeling laws listed in Table 5.1 as the Vellinga's and the two Wang's laws are nearly the same. These two geometrical scaling laws are,

$$N_\delta = N_\lambda^{2/3} \tag{5.2}$$

and

$$N_\delta = N_\lambda^{4/5} \tag{5.3}$$

The data were scattered but collective the latter scaling law appeared to perform better. Figure 5.2 shows the comparisions of all the final profiles for the cases of N_λ =20 with the prototype based on the scaling Equation 5.3.

From this figure one may also argue that the gross feature of the final profiles may be expressed by a simple form which could be defined as the equilibrium profile. A number of equilibrium profile forms have been proposed, notably by Bruun (1954), Dean (1977), Vellinga(1982) and Wang (1990). They are all in the following general form:

$$h = \alpha(\frac{SW}{\sqrt{g}})^n x^m \tag{5.4}$$

where h is the water depth, x is distance from shoreline, S is the submerged specific weight, W is the sediment fall velocity and α is non-dimensional coefficient. The value of $\alpha(\frac{SW}{\sqrt{g}})^n$ is also known as the scale parameter. Moore (1982) analyzed 500 or so beach profiles and proposed A to be a function of particle size. Later, Dean, Vellinga and Wang all suggested that particle fall velocity is a more appropriate parameter instead of the partical size. Vellinga (1982) proposed A to be equal to $0.39W^{0.44}$ from analyzing field profile along the Dutch coast. Dean (1985) re-analyzed the values complied by Moore (1982) and gave the best fit as $A = 0.51W^{0.44}$; this formula was also found suitable for GWK data by Wang (1990). As to the value m, Bruun and

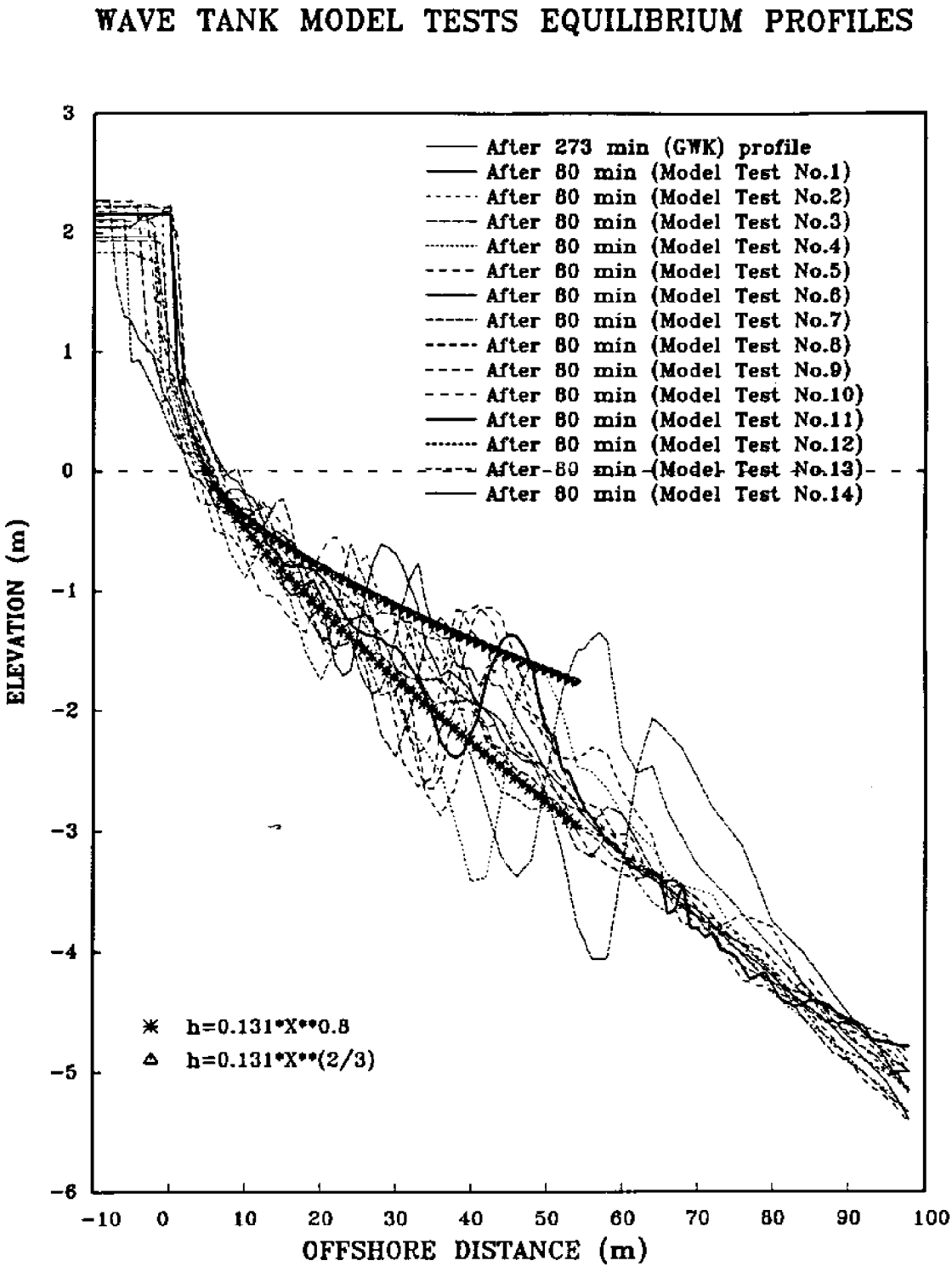

Figure 5.2: Equilibrium Profile Comparison Between Model Test Results and Modeling Laws

Dean suggested to be 2/3, Vellinga used 0.78 and Wang came up with 4/5. Equation 5.4 was also plotted in Figure 5.2 using two different values of n = 2/3 and 4/5. The A parameter is equal to 0.131 for both cases based on the fall velocity equation given above. It appeared that value of m=4/5 gave a better fit for the specific data set in the inshore segment of the profile. It should be noted here that, to a certain degree, irrespective to which value of m one selects, the equilbrium curve can also be adjusted to fit any secific data set by adjusting the value A.

5.1.2 Wave Height and Wave Period Scaling

Based on the analysis given in the previous section, the basic goemetrical scaling by Wang is selected for the subsequent analysis of wave height, wave period and morphological time scalings. In this section, the scalings of the former two are addressed and the latter will be adressed in the next section.

As mentioned ealier the analysis of wave height and wave period is based upon final profiles. Figure 5.3 to figure 5.5 plots the scaled final profile of each test case for the ASW test series against the protype. The results of the 10 WF tests are presented in Figure 5.6

To establish the best scaling relationships from the data, the four of the criteria given earlier were employed. The procedures are the same for analyzing each criterion. It is explained here with the dune volume computation. The dune volume error is defined as

$$\frac{V^m - V^p}{V^p} \tag{5.5}$$

where V^p is the volume deficit (eroded volume) between the final and the initial profile in the prototype and V^m is scaled-up volume deficit in the model. These values are plotted against model wave heights, for different model wave periods, as shown in Figure 5.7. These constitute a series of curves. The zero crossing(s) should represent the best-fit model wave height(s) and wave period(s). From them the best-fit scaling ratios can be obtained. A rather clear trend between the dune volume error and wave height can be detected. This trend is almost linear revealing a expected relationship that increasing wave height resulted in increased erosional volume. The effect of wave period on volumetric erosion is less clear revealing a rather weak relationship between dune volumetric erosion and wave period. From this figure the best fit values of wave height and wave period are determined to be 13.5 cm and 1.33 sec, respectively. The corresponding scaling ratios based on this creterion are 11.1 and 4.5 for wave height and wave period.

The above procedure was also applied to determine the best-fit modeling scales for the other three criteria. Figure 5.8 to 5.10 show the plots of those other three parameters: the RMS error of the bar profile, the bar volume and the bar mass center. From these figures the best-fit scaling ratios based on different creteria are determined. The results are summarized in Table 5.2.

5.1.3 Evaluation of Morphological Time Scale

To evaluate the morphological time scale one requires a comparison of the model data with the prototype at each time step. This would be an unwiedy task if all the

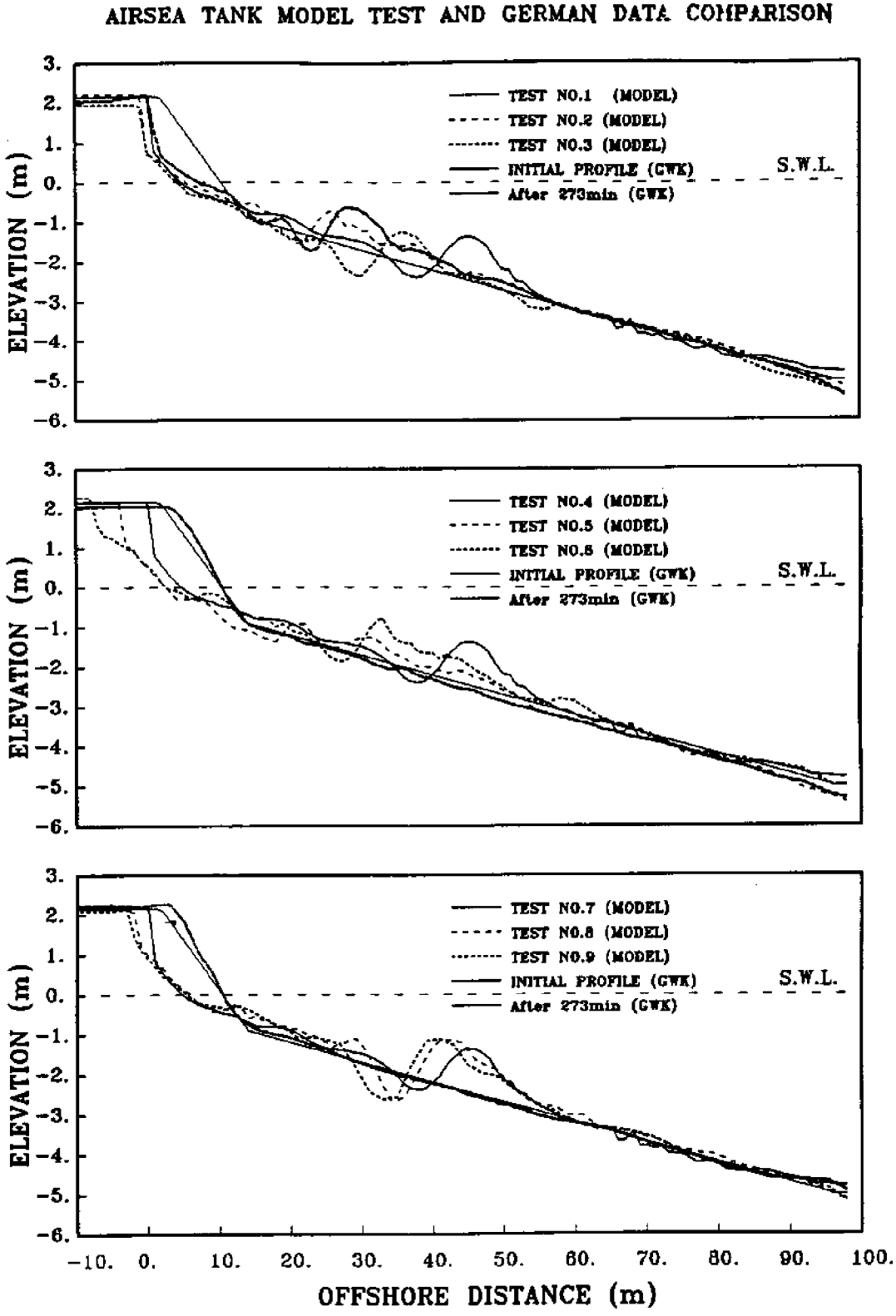

Figure 5.3: ASW Model Tests and Prototype Final Profile Comparison (1)

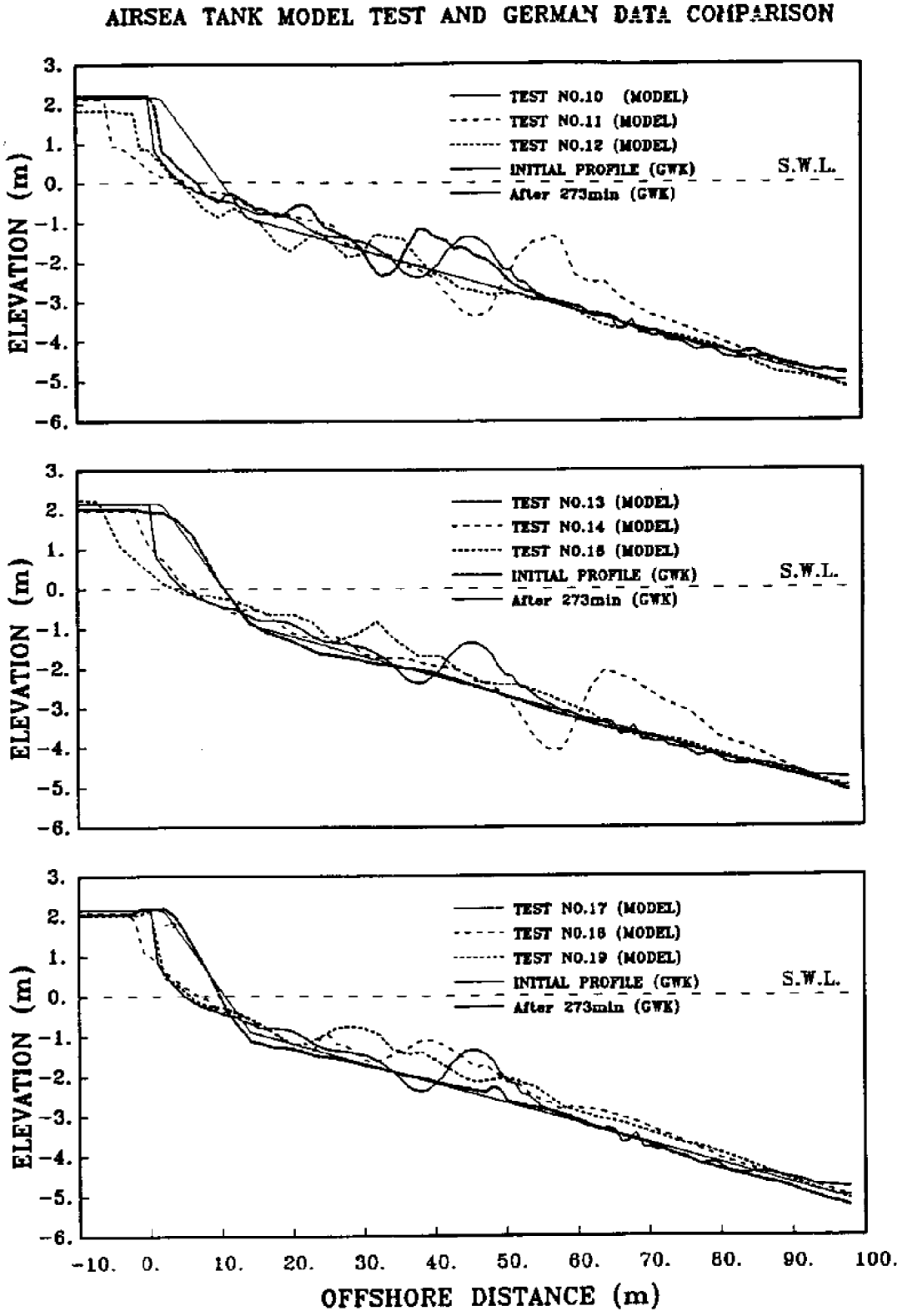

Figure 5.4: ASW Model Tests and Prototype Final Profile Comparison (2)

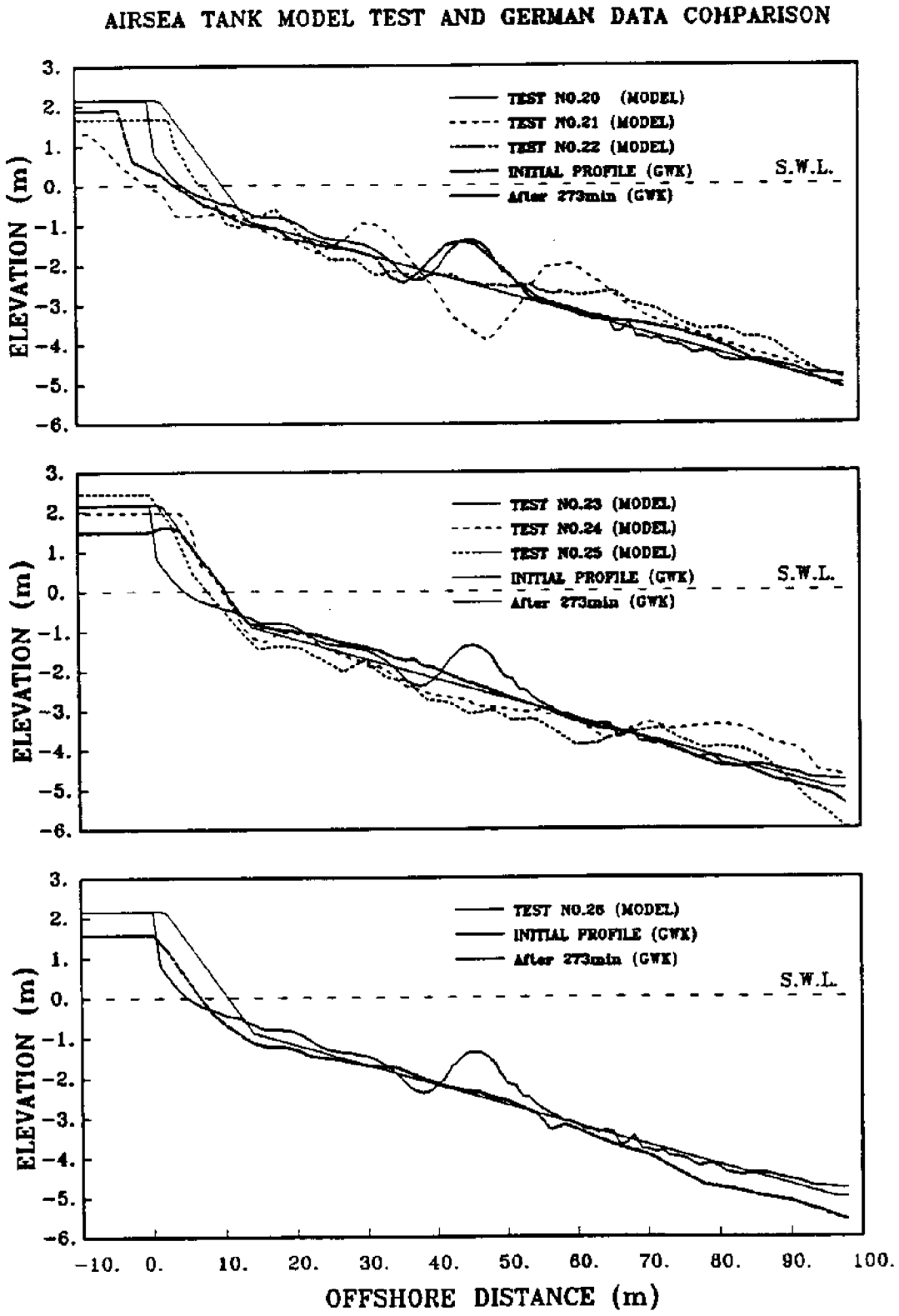

Figure 5.5: ASW Model Tests and Prototype Final Profile Comparison (3)

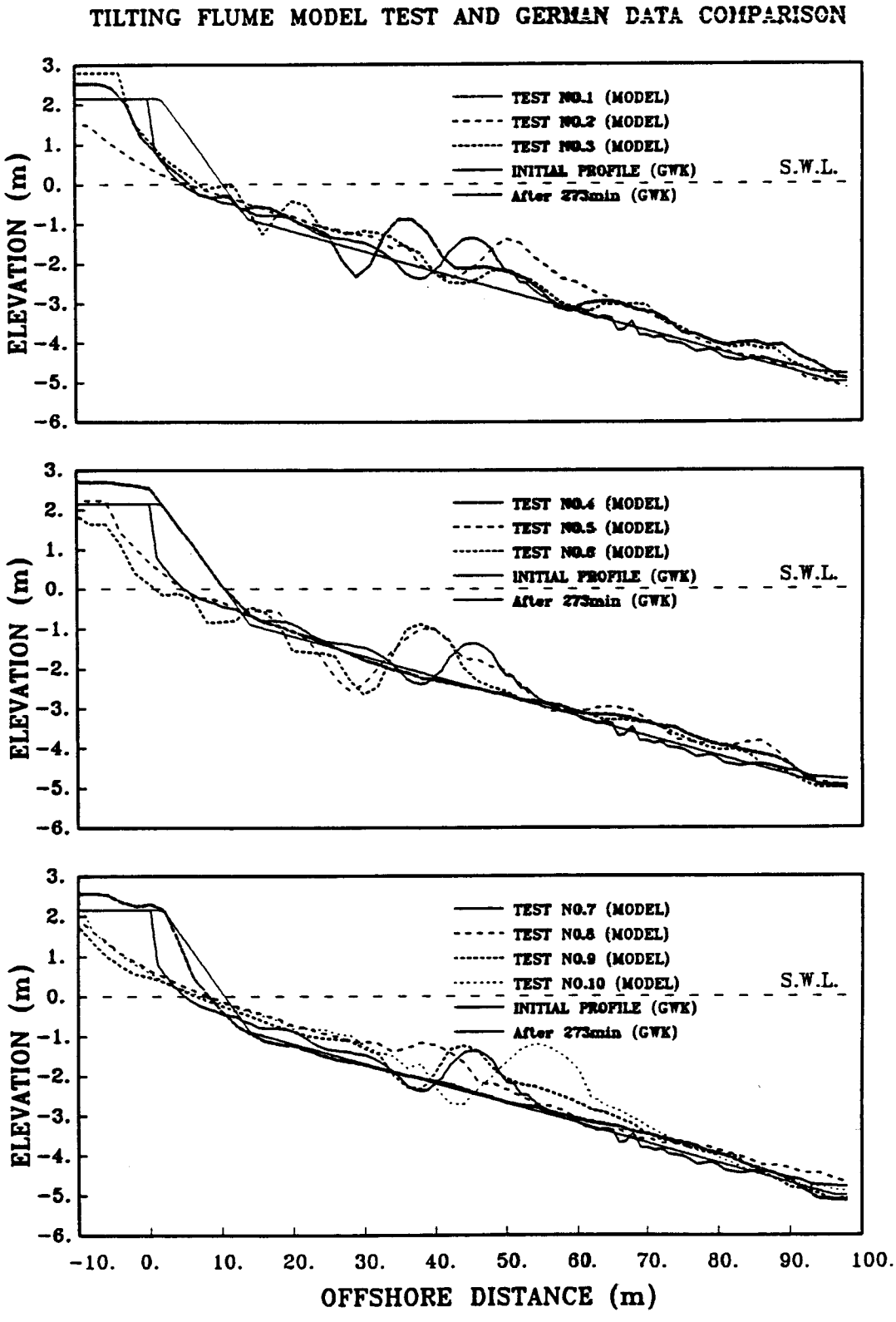

Figure 5.6: WF Model Tests and Prototype Final Profile Comparison

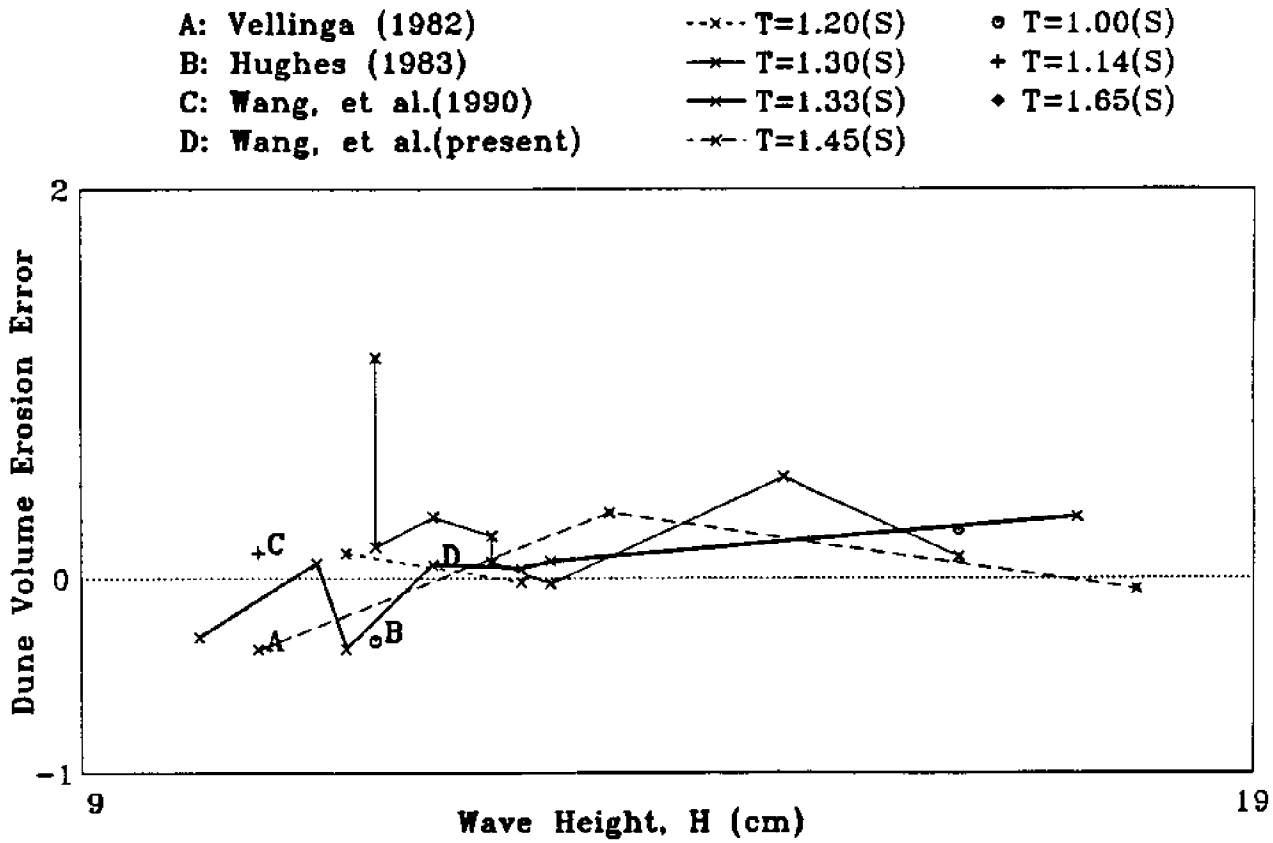

PLOT OF DUNE VOLUME ERROR (N_λ =20, N_δ =14.5)

Figure 5.7: Dune Volume Erosion Error Criterion

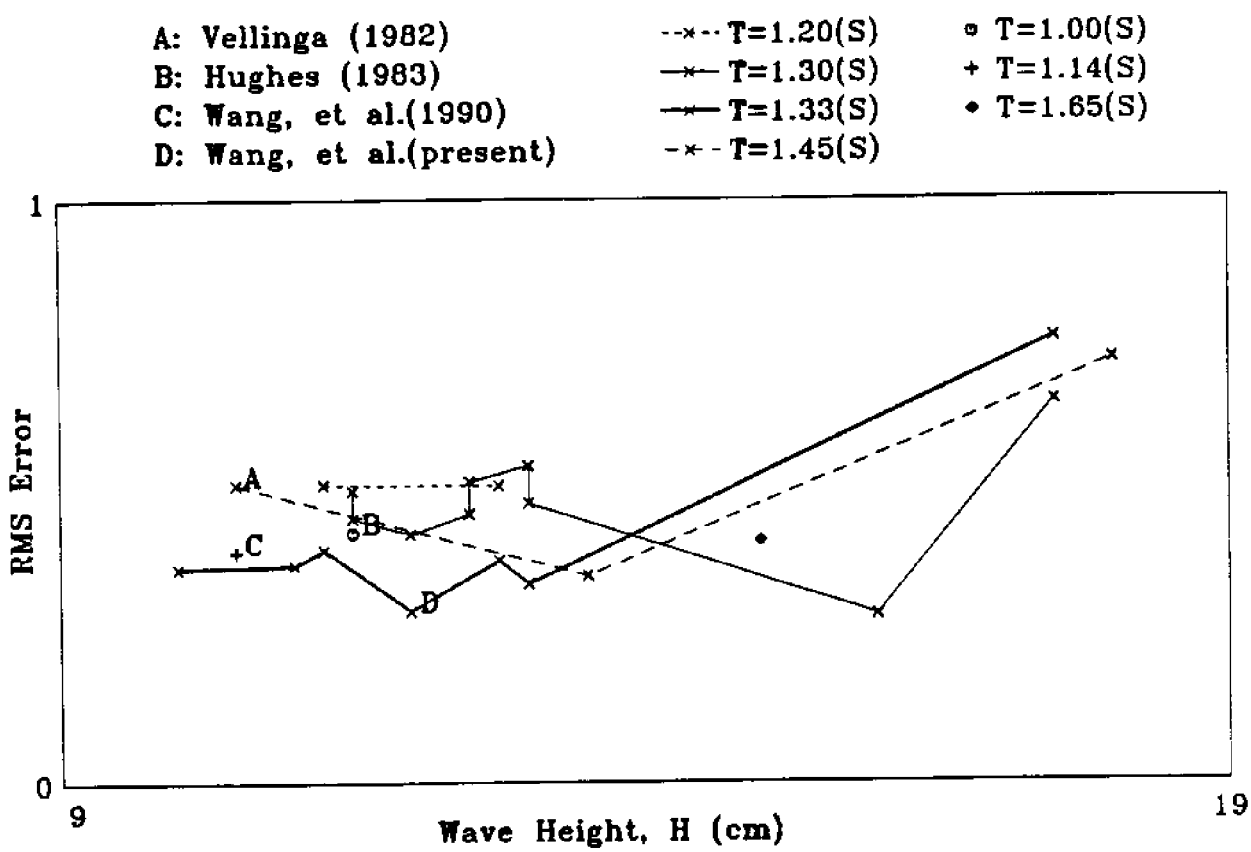

PLOT OF RMS ERROR OF BAR PROFILE (N_λ =20, N_δ =14.5)

Figure 5.8: The RMS Error of The Bar Profile Criterion

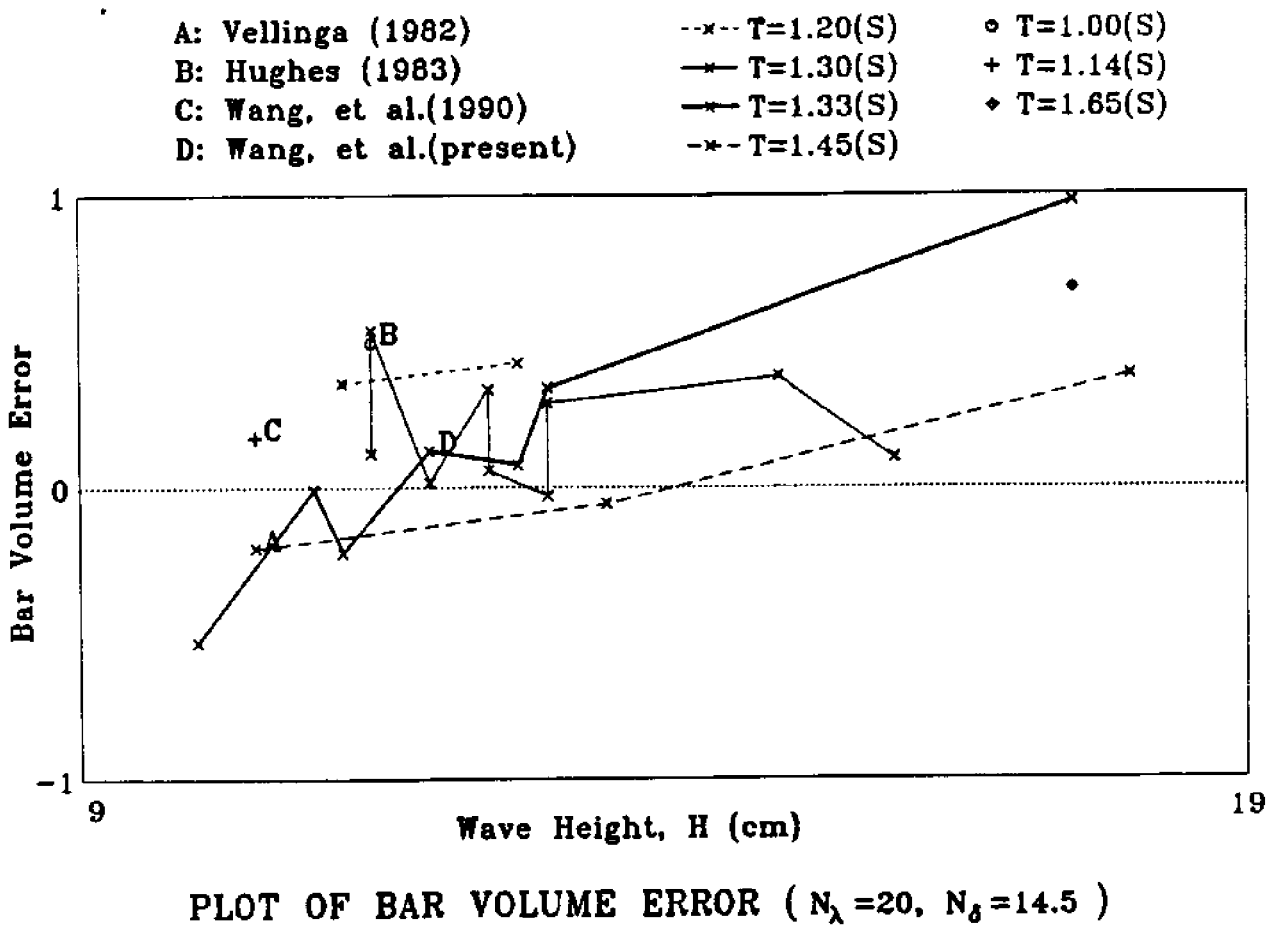

PLOT OF BAR VOLUME ERROR (N_λ =20, N_δ =14.5)

Figure 5.9: Bar Volume Error Criterion

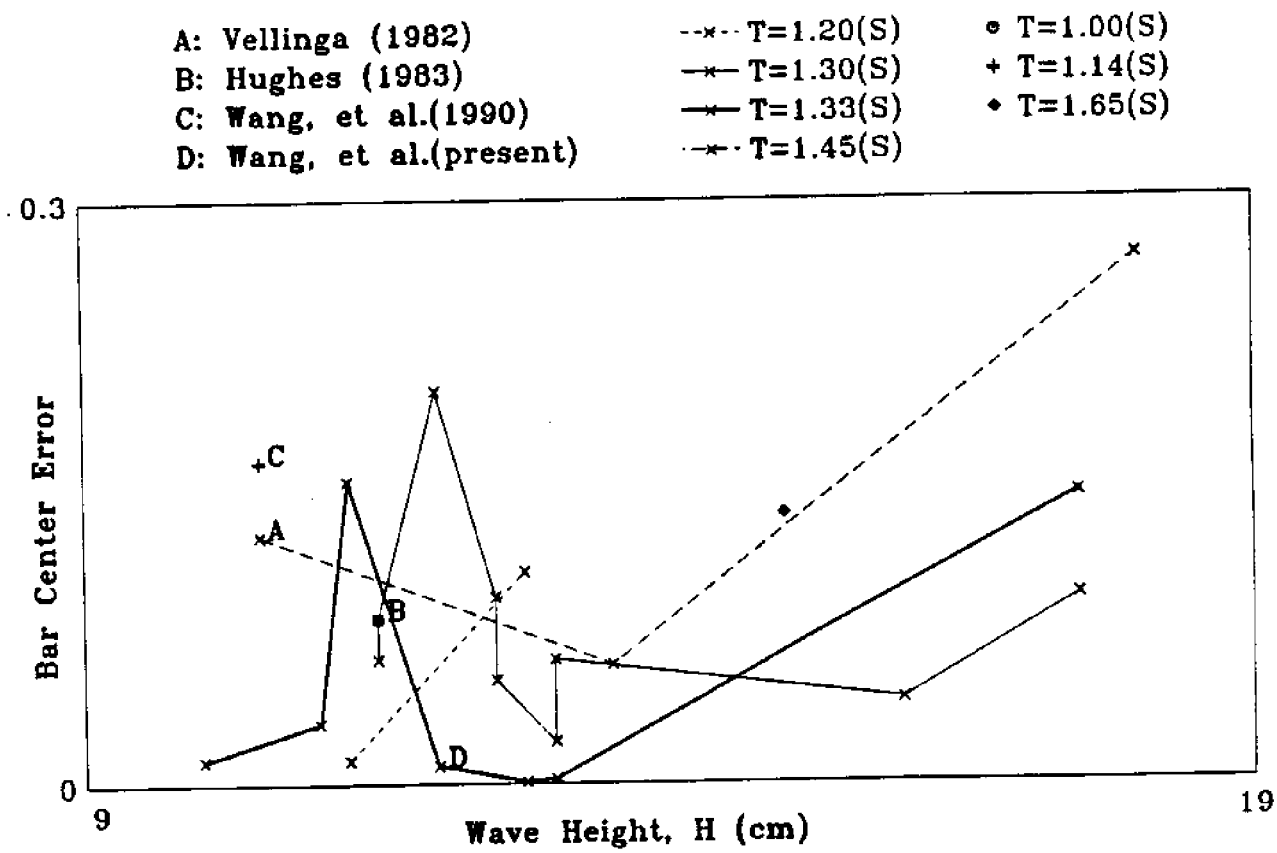

PLOT OF BAR LOCATION CENTER ERROR (N_λ =20, N_δ =14.5)

Figure 5.10: Bar Location Error Criterion

Table 5.2: **Comparison of Model Performances**

Ex.1: Given $N_\lambda = 20$, $N_W = 2$.

Author	N_δ	N_H	N_T	N_t
Vellinga (1982)	14.5	14.5	3.8	3.8
Hughes (1983)	14.5	14.5	5.3	5.3
Wang, *et al.*(1990)	14.5	14.5	5.3	3.8
Wang(present)	14.5	10.5	4.5	4.5
Experimental data	N_δ	N_H	N_T	N_t
Bar location	14.5	11.5	4.5	4.5
Bar volume change	14.5	11.3	4.5	4.5
Dune volume change	14.5	11.1	4.5	4.5

Ex.2: Given $N_\lambda = 40$, $N_W = 2$.

Author	N_δ	N_H	N_T	N_t
Vellinga (1982)	25.2	25.2	5.0	5.0
Hughes (1983)	25.2	25.2	7.8	7.8
Wang, *et al.*(1990)	25.2	25.2	7.8	5.0
Wang(present)	25.2	15.9	6.3	6.3
Experimental data	N_δ	N_H	N_T	N_t
Bar location	25.2	16.7	6.0	6.3
Bar volume change	25.2	16.7	6.0	6.3
Dune volume change	25.2	16.7	6.0	6.3

data sets were used. In here, the best-fit data set from the three differnt horizontal scale groups ($N_\lambda = 20$, 30, and 40) were selected from the ASW and WF tests results.

The morphorlogical scale was then examined from this data set. The selection of the best-fit data set was guided by the results of the previous sections. The error quantities established above are now plotted for each test case.

Figure 5.11 shows the results of dune region error parameters (dune erosion volume and dune profile RMS) for the cases in the ASW test.

Figure 5.12 gives the results of bar region error parameters for the ASW tests. From these two figures, the best-fit data sets selected (judged to have the smallest overall error) are No.8 for $N_\lambda = 20$, No.18 for $N_\lambda = 30$ and No.20 for $N_\lambda = 40$. Similarly, Figures 5.13 and 5.12 give the dune and bar parameters results for the WF tests. From here, No.9 is selected as a compromise for the best overall fit. These data sets are then used to establish the best-fit morphorlogical scale. In theory, this can be accomplished by the same procedure as described in the previous section except that the comparisions are to be made at each time step for the three selected cases. In practice, this is rather tidious and there is not sufficent data points at each time step. An alternative procedure is employed.

There are three different morphological time scaling laws guided by the morphological time scales given in Table 5.1. Wang(1990) suggested that the particle trajectory should be preserved which leads to $N_t = \sqrt{N_\delta}$. Both Vellinga (1982) and Hughes (1986) modeling laws give $N_t = N_\lambda/\sqrt{N_\delta}$. The study referred to as Wang 2 suggests that both motion time scale and morphological time scale are governed by the scaling law, or, $N_t = \sqrt{N_\lambda}$.

Now, the time elaspsed changes of the 6 quanities, i.e., the dune erosion volume, bar volume the RMS values of profiles, etc., are plotted in accordance with the three morphological scaling laws and are compared with the GWK results. The GWK data contained 21 different elapsed time at 5, 13, 20, 27, 34, 48, 62, 76, 90, 111, 132, 162,

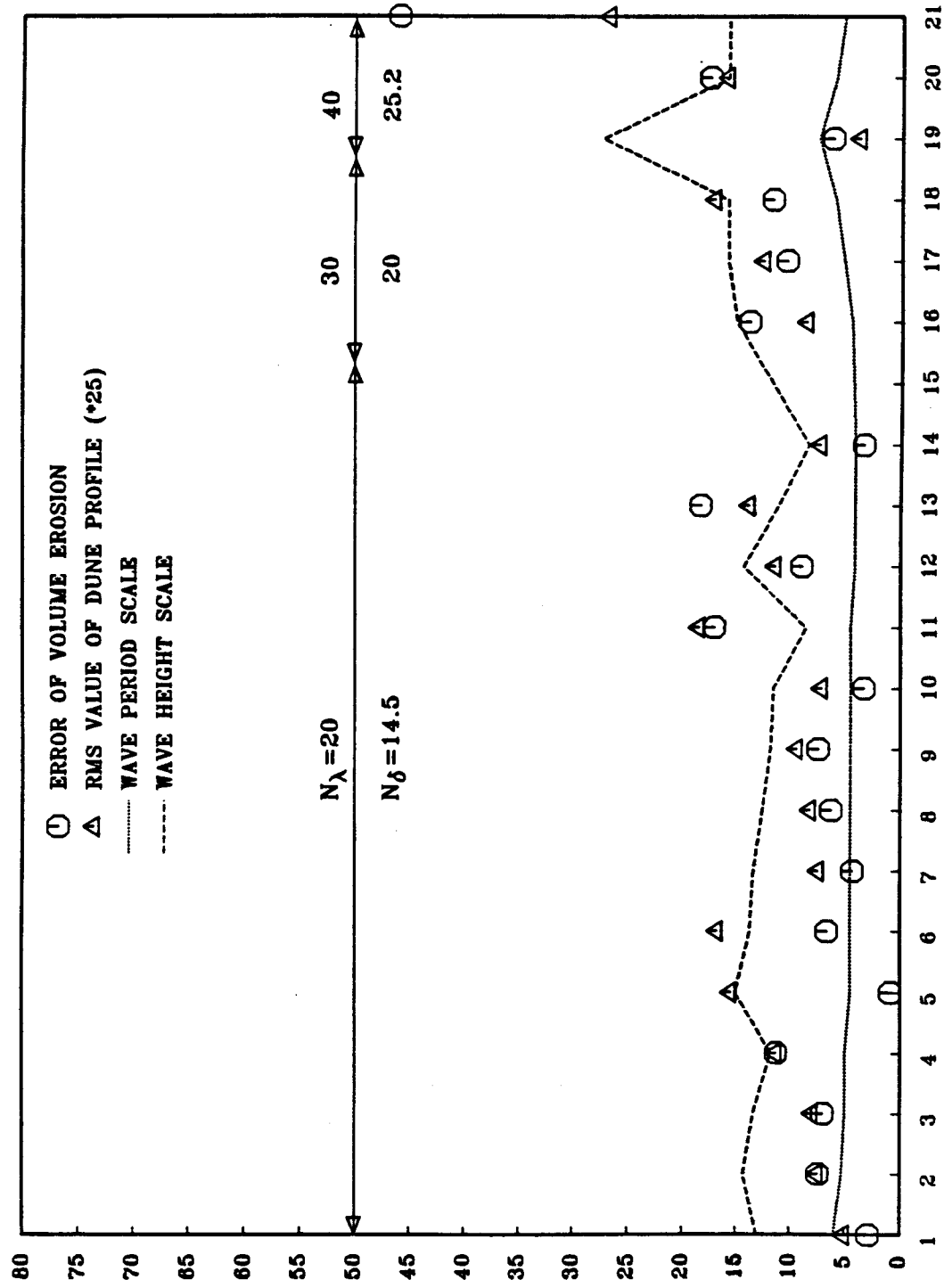

Figure 5.11: Summary of ASW Test Results Based On Dune Profile Parameter

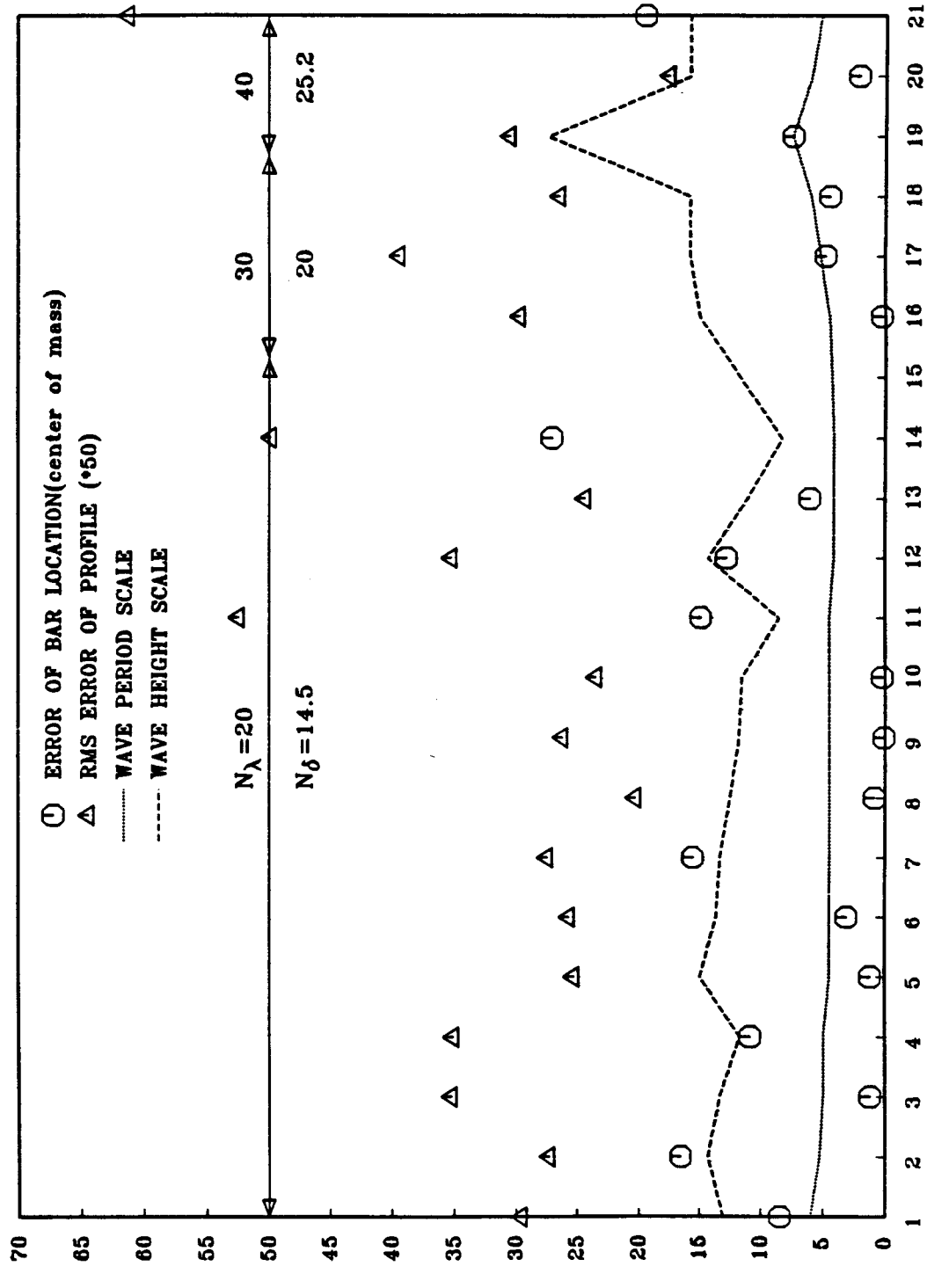

Figure 5.12: Summary of ASW Test Results Based On Bar Profile Parameter

176, 190, 204, 217, 231, 245, 259, 273 minute, respectively. From these comparisions, the best-fit morphorlogical time scale is obtained.

Dune Region

There are two criteria in the dune region, the dune volume erosion and the profile RMS value.

For dune erosion, a number of observations can be made. From the ASW results (Figure 5.15) all three scaling laws over predict the total erosional volume and the larger the scale ratio, or the smaller the model, the larger the over-prediction. The over prediction largely occurred in the initial stage (0 to 100 minutes prototype time). Also, it appears that none of the tests including the prototype has reached equilibrium at the end of the runs.

The results from WF test are shown in Figure 5.16. All modeling laws also over predict the total erosional volume.

Therefore, these results suggest that the best-fit morphological time scale ratio has to be smaller than any of the 3 modeling laws.

The comparisions of profile RMS error are given in Figure 5.17 for ASW cases and in Figure 5.18 for the WF case. For this criterion all 3 modeling laws appeared to perform reasonably well as the scaled values all custered in a narrow range around the prototype results. Overall the Wang 2 model may be slightly better.

Bar Profile Region

Four different criteria have been developed for this region, the profile RMS value, the bar volume, the bar mass center and the bar crest location. The results of these four criteria are plotted in Figure 5.19 to 5.22 for the ASW tests and Figure 5.23 for the WF tests.

From these figures a number of observations are made. The bar mass center is the most stable and consistant criterion. All three modeling laws appeared to give reasonable results for all three data sets. The bar crest location is next consistant

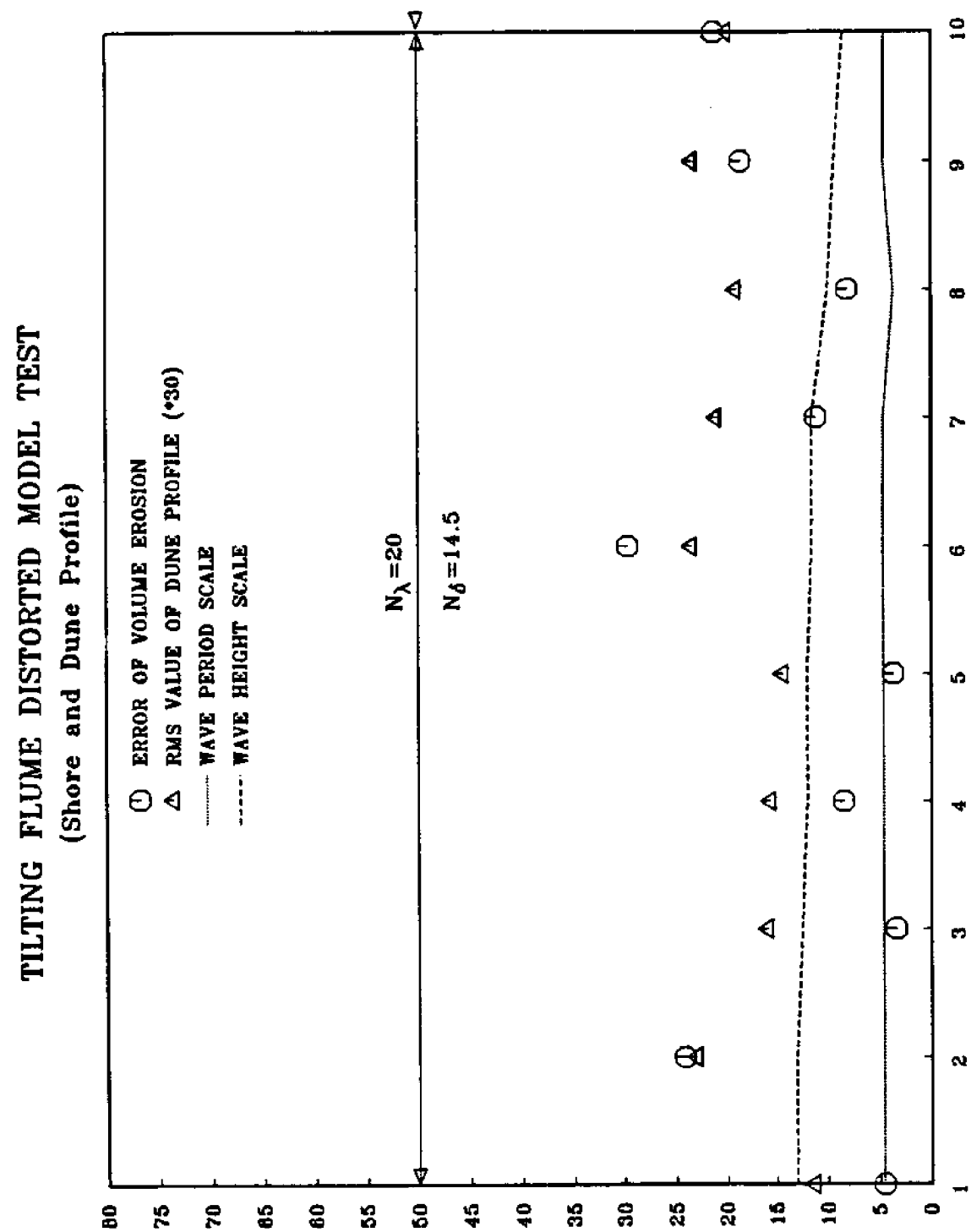

Figure 5.13: Summary of WF Test Results Based On Dune Profile Parameter

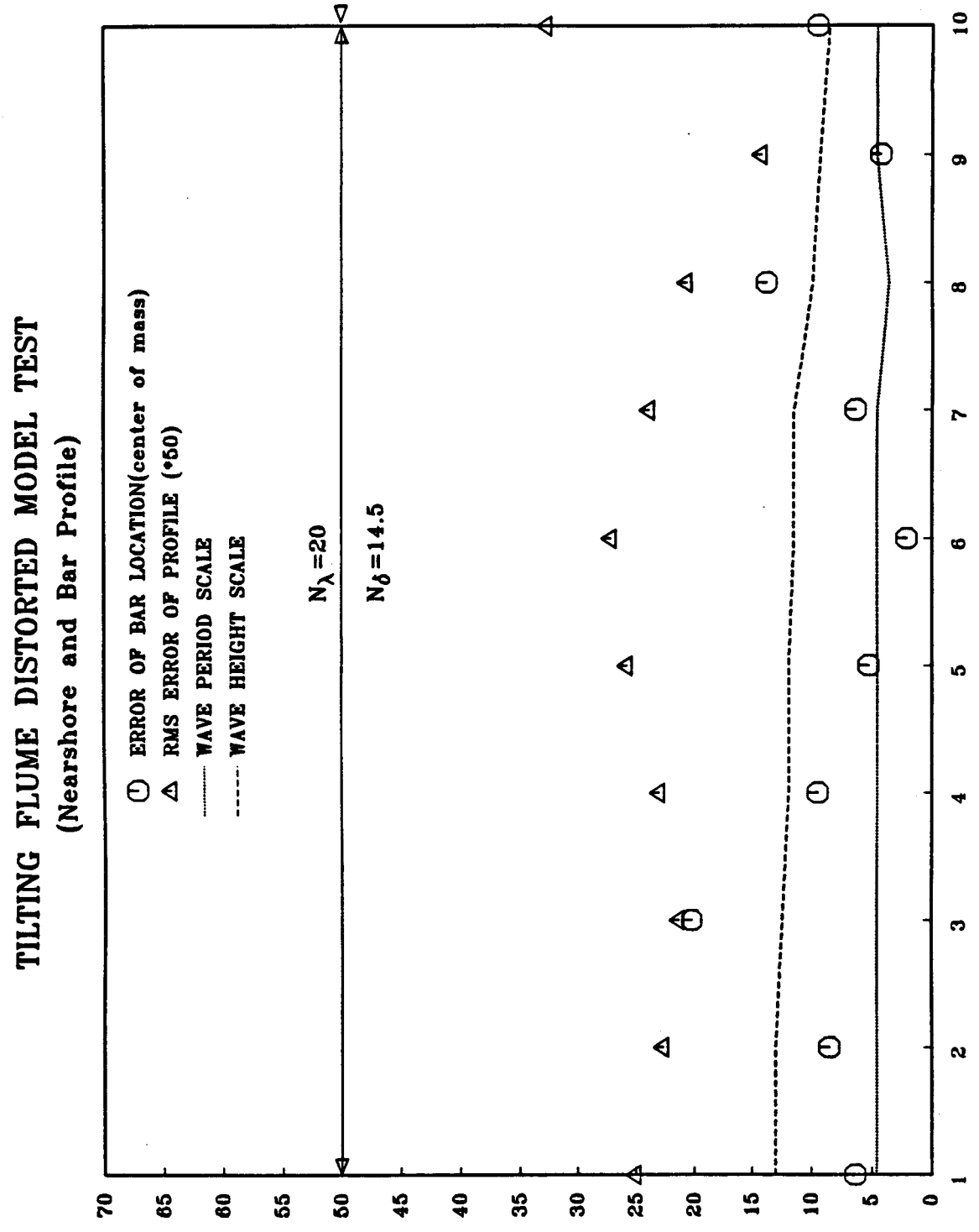

Figure 5.14: Summary of WF Test Results Based On Bar Profile Parameter

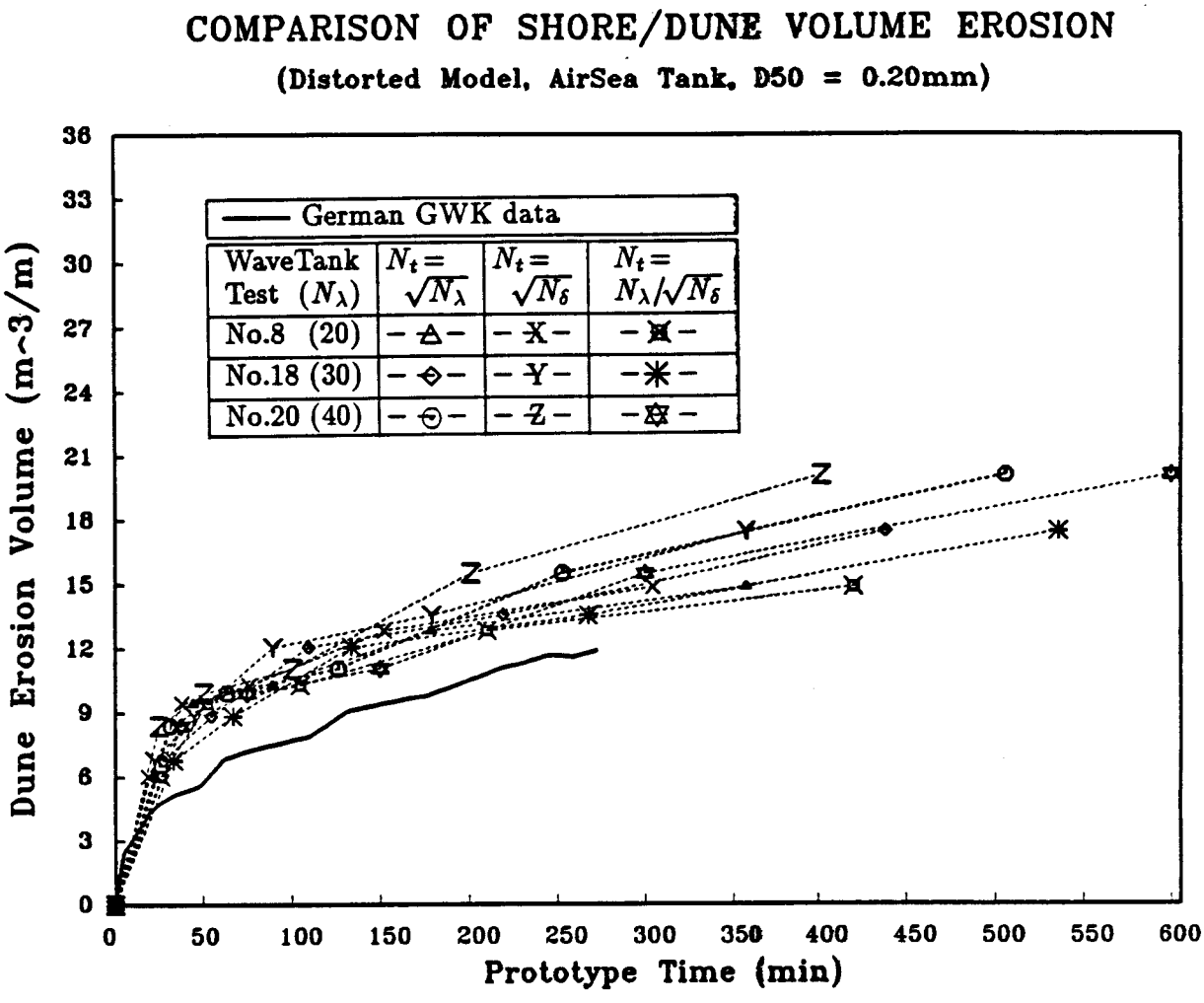

Figure 5.15: Dune Profile Evolution Scaling from ASW results

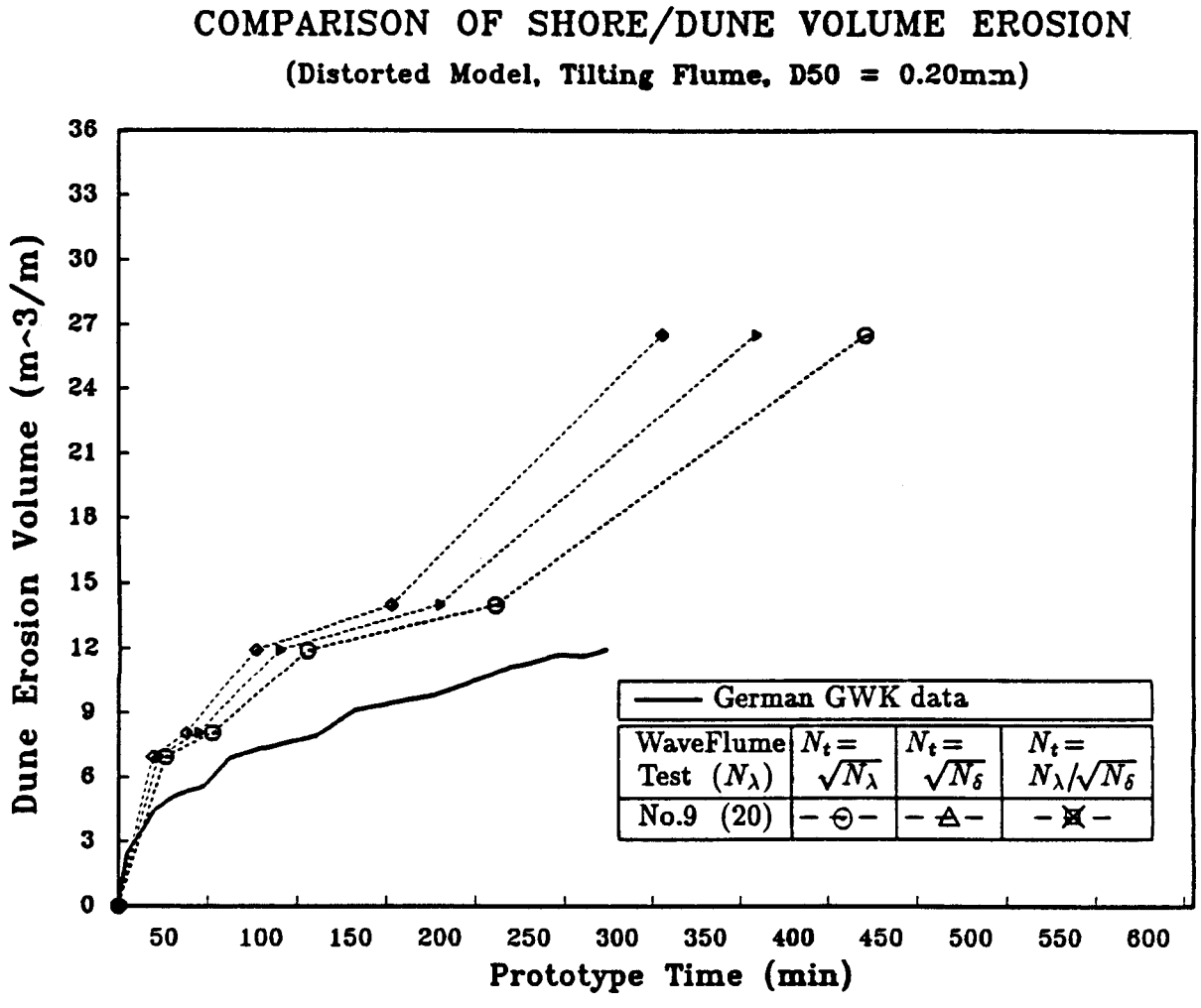

Figure 5.16: Dune Profile Evolution Scaling From WF results

criterion. All modeling laws give reasonable scaled results for three data sets with the exception of No.18 ($N_\lambda = 30$). The bar volume criterion is less stable than bar mass center and bar crest as the scaled results scattered over a wider range after the initial stage (about 50 minutes prototype time).The scaled bar volumes, however, are reasonable when compared with prototype data. Finally, the profile RMS did not serve as a consistant criterion. The modeling laws performed poorly in two data sets (No.18 in ASW and No.9 in WF) and marginally adquate in the other two (No.8 and No.20).

5.1.4 Summary of Two-Dimensional Test Results

From the above analysis, one may draw the tentative conclusion that the modeling law proposed in this study has the best overall performance compared with other existing modeling laws as summarized in Table 5.2.

5.1.5 Test Results from Three-Dimensional Basin

Four tests were conducted in the three-dimensional basin all at the same horizontal scale of 20. Three of tests were carried out under normal incident wave angle and one under oblique wave angle (see Table 4.7). Only the cases with normal incident wave angle (cases 1, 2 and 3) are discussed here.

It is nortoriously difficult to maintain two-dimensional beach features in a three-dimensional basin, particularily if the input wave is regular. Every case must be exercised to eliminate factors that could induce three-dimensional effects. Some investigators even concluded that in a finite-size basin two-dimensional features are inherently unstable. In the present experiment, three-dimensional features did appear at smaller scales but the overall two-dimensional features were largely maintained through careful and painstaking profile molding and the elimination of wave reflection from side walls. Figure 5.24 shows the initial three-dimensional beach prfiles measured at 5 different cross-sections and Figure 5.25 plots the final profiles at the 5 locations after 80 minutes model test time. As one can see the two-dimensional

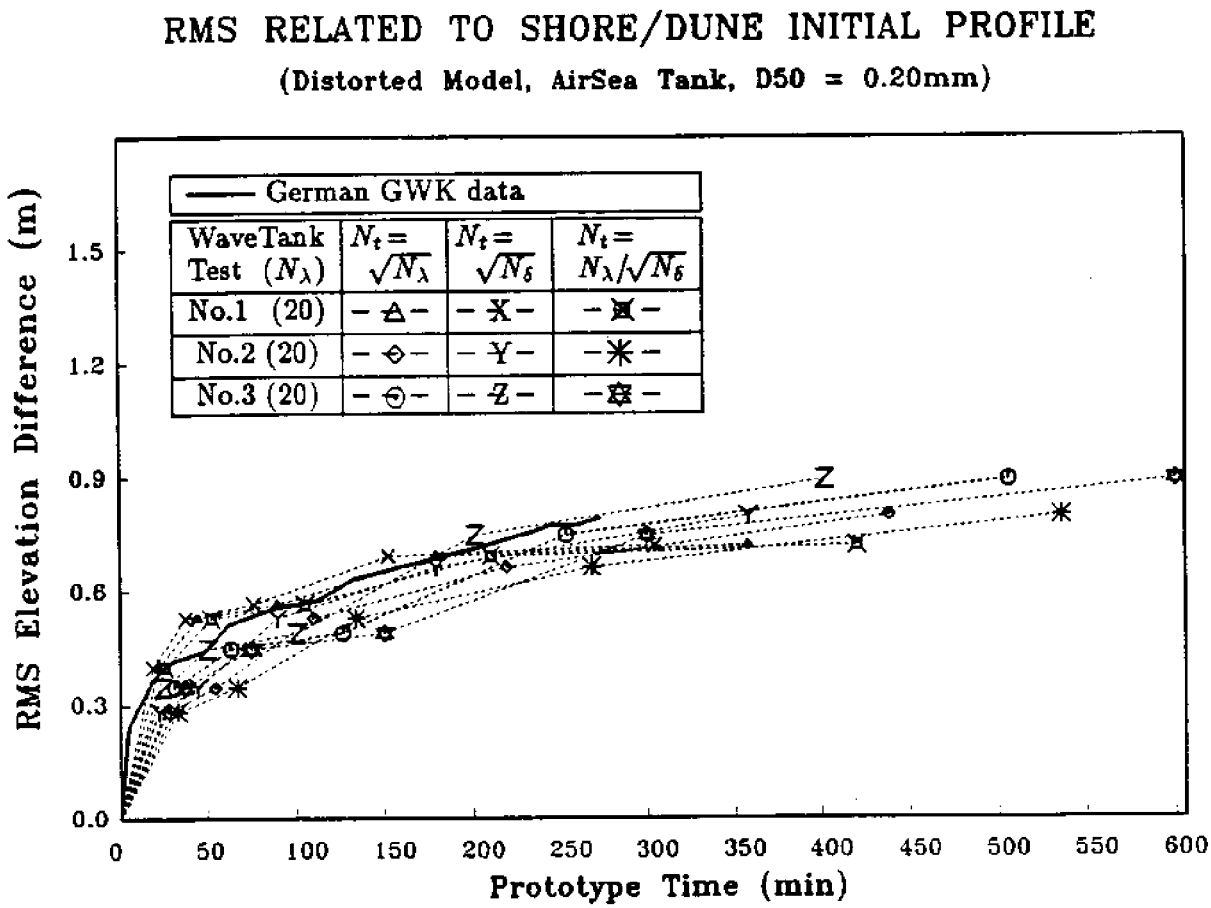

Figure 5.17: Morphological time scaling of Dune Profile RMS Value from ASW Tests

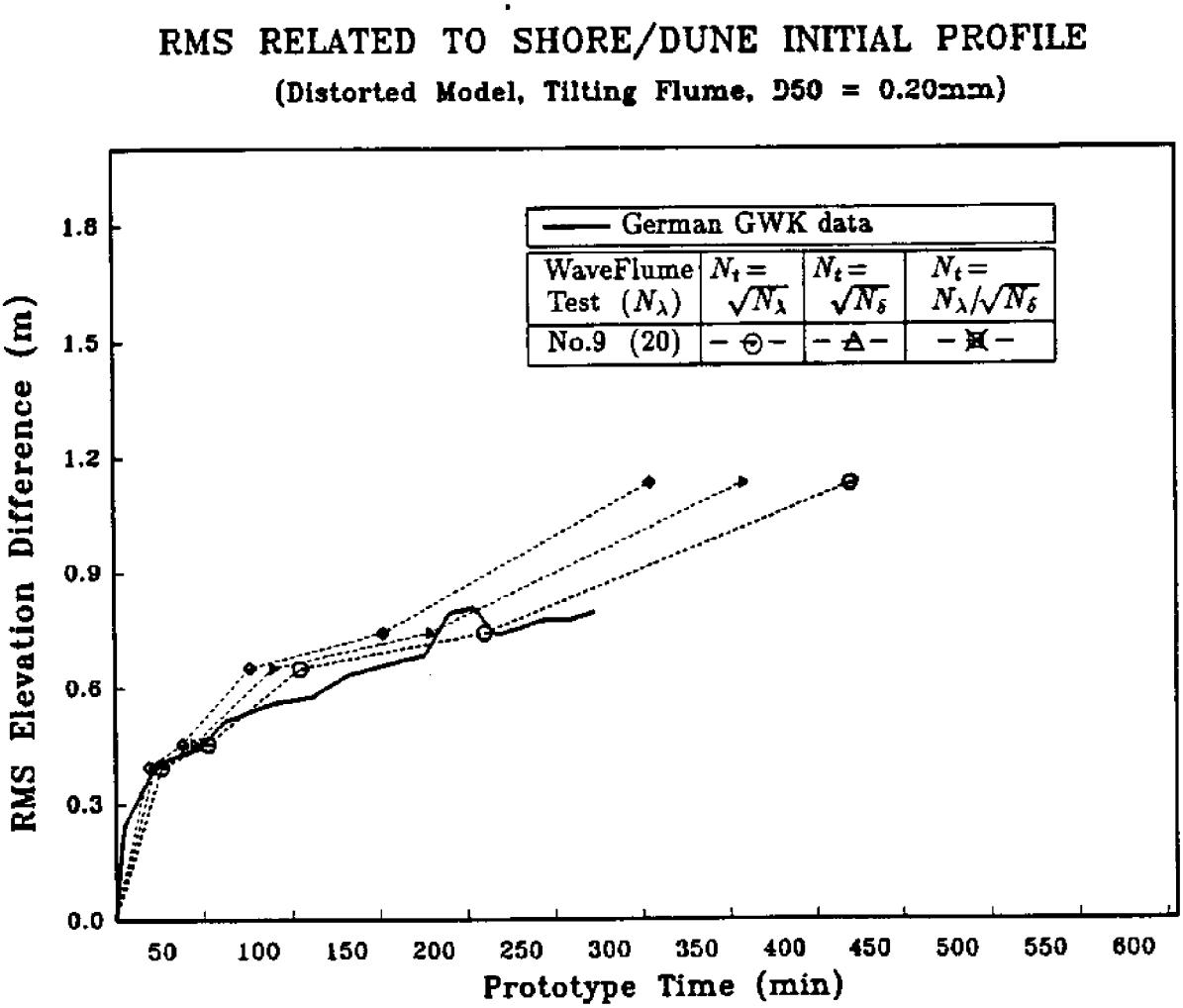

Figure 5.18: Morphological time scaling of Dune Profile RMS Value from WF Tests

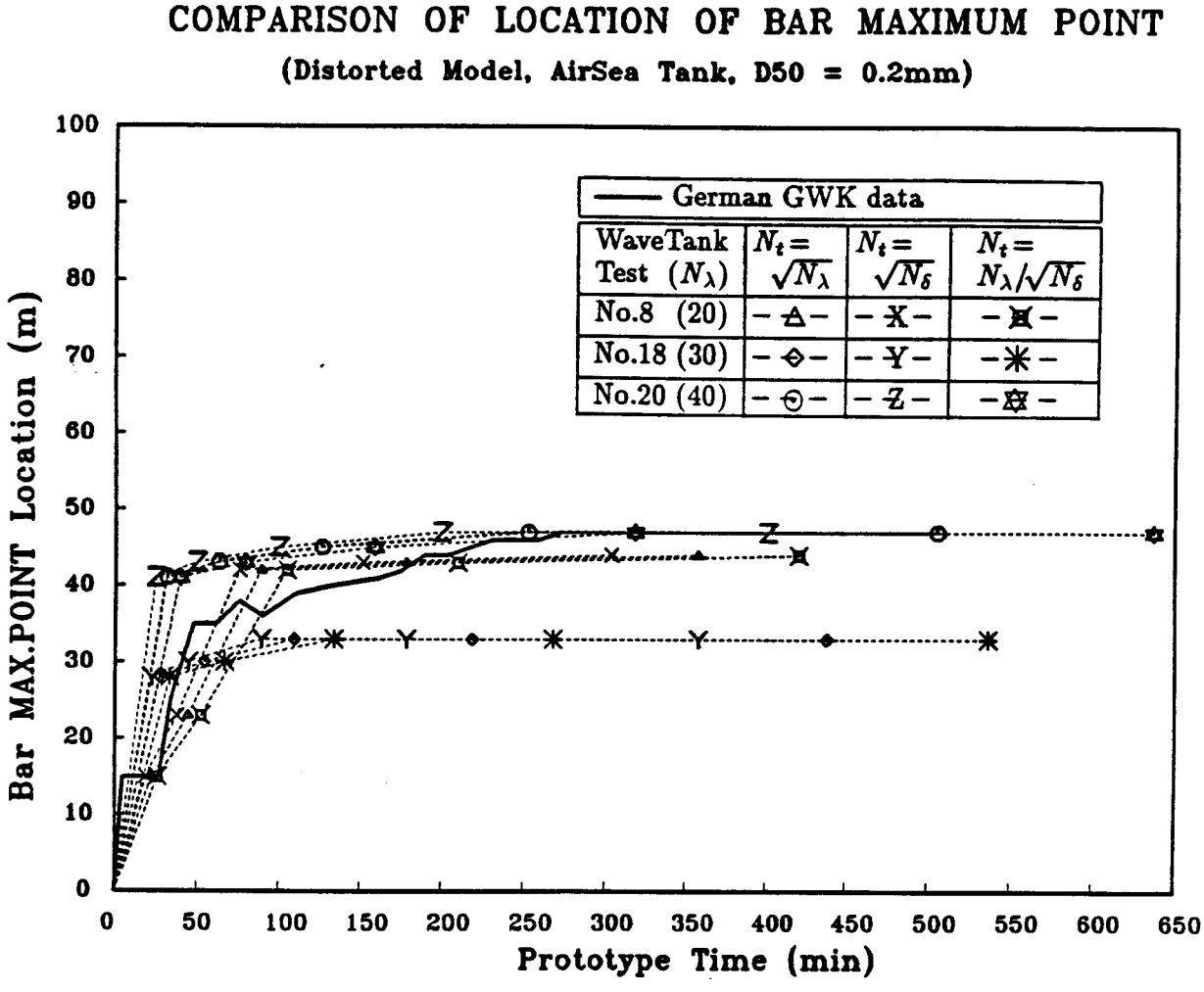

Figure 5.19: Morphological time scaling of Bar Crest Location from ASW Tests

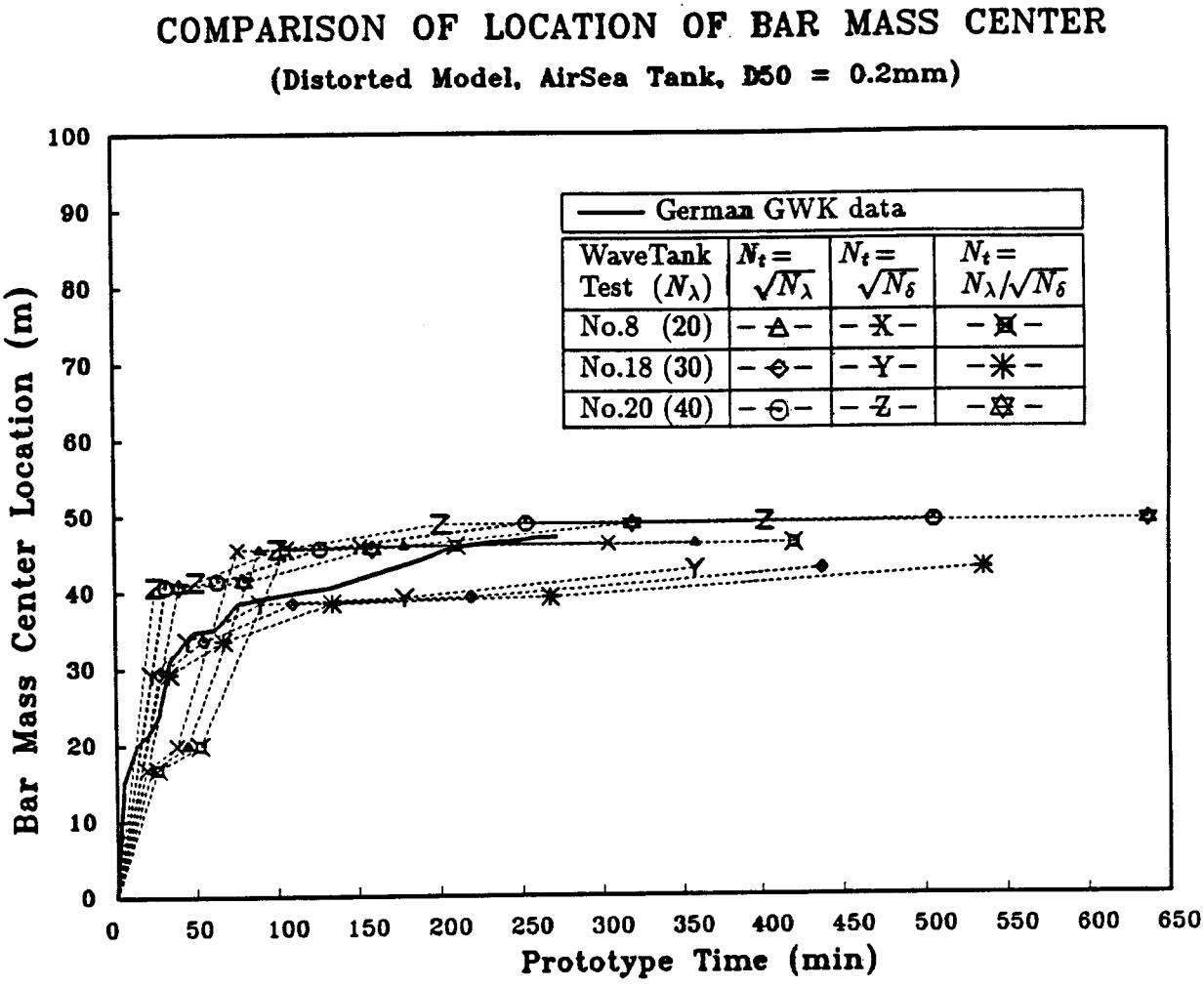

Figure 5.20: Morphological time scaling of Bar Mass Center Location from ASW Tests

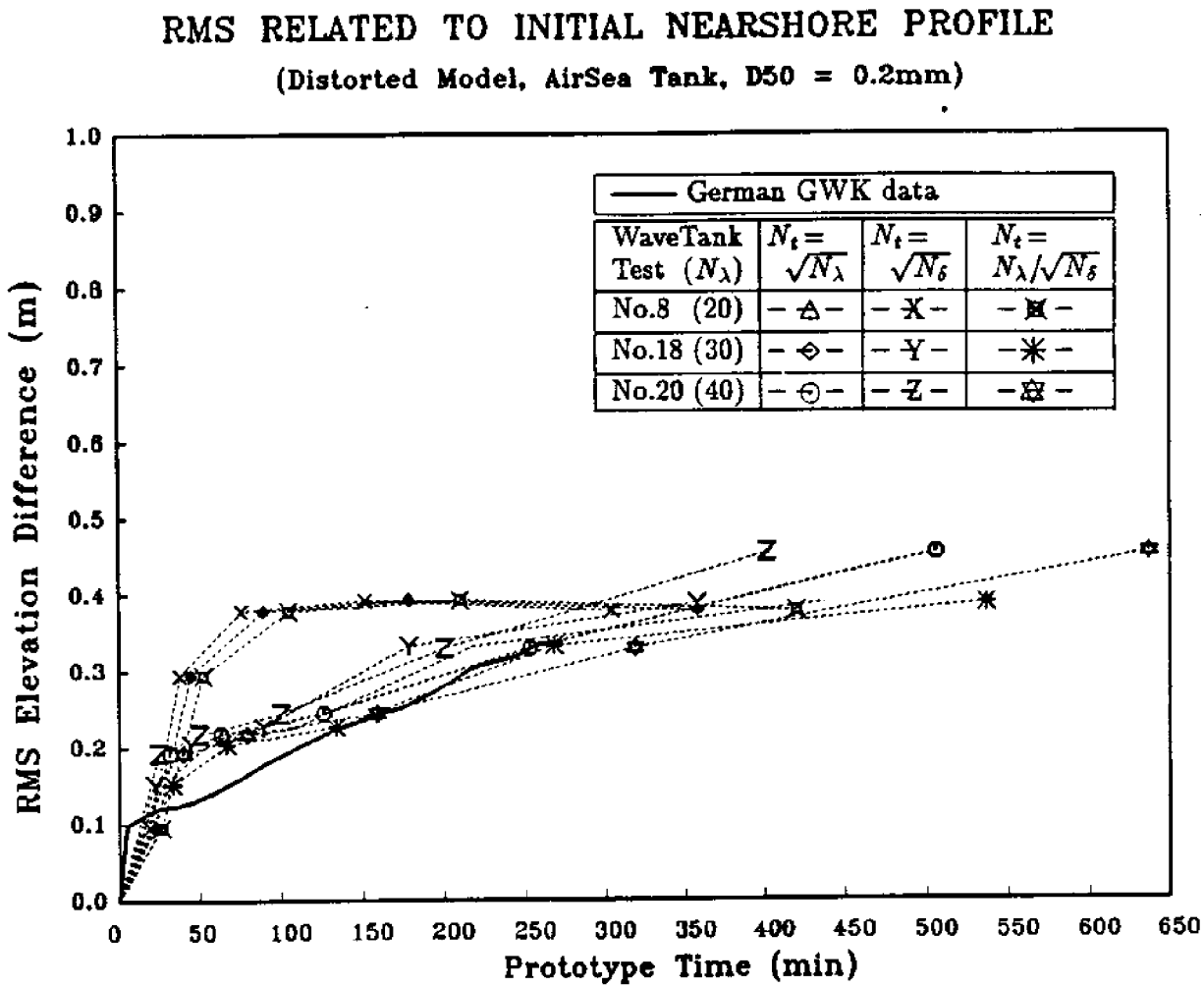

Figure 5.21: Morpholigical Time Scaling of Bar Profile RMS Value from ASW Tests

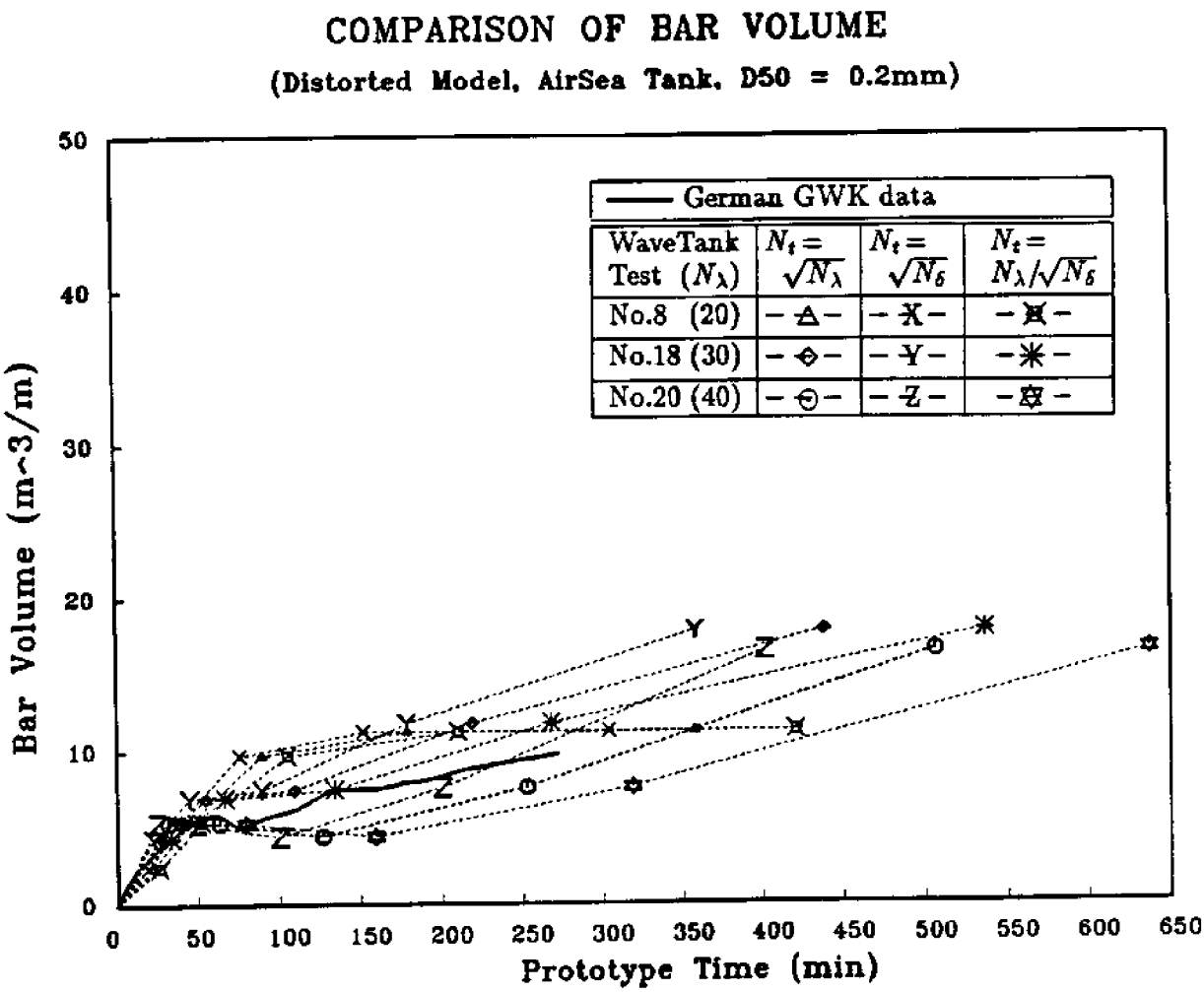

Figure 5.22: Morphological time scaling of Bar Volume from ASW Tests

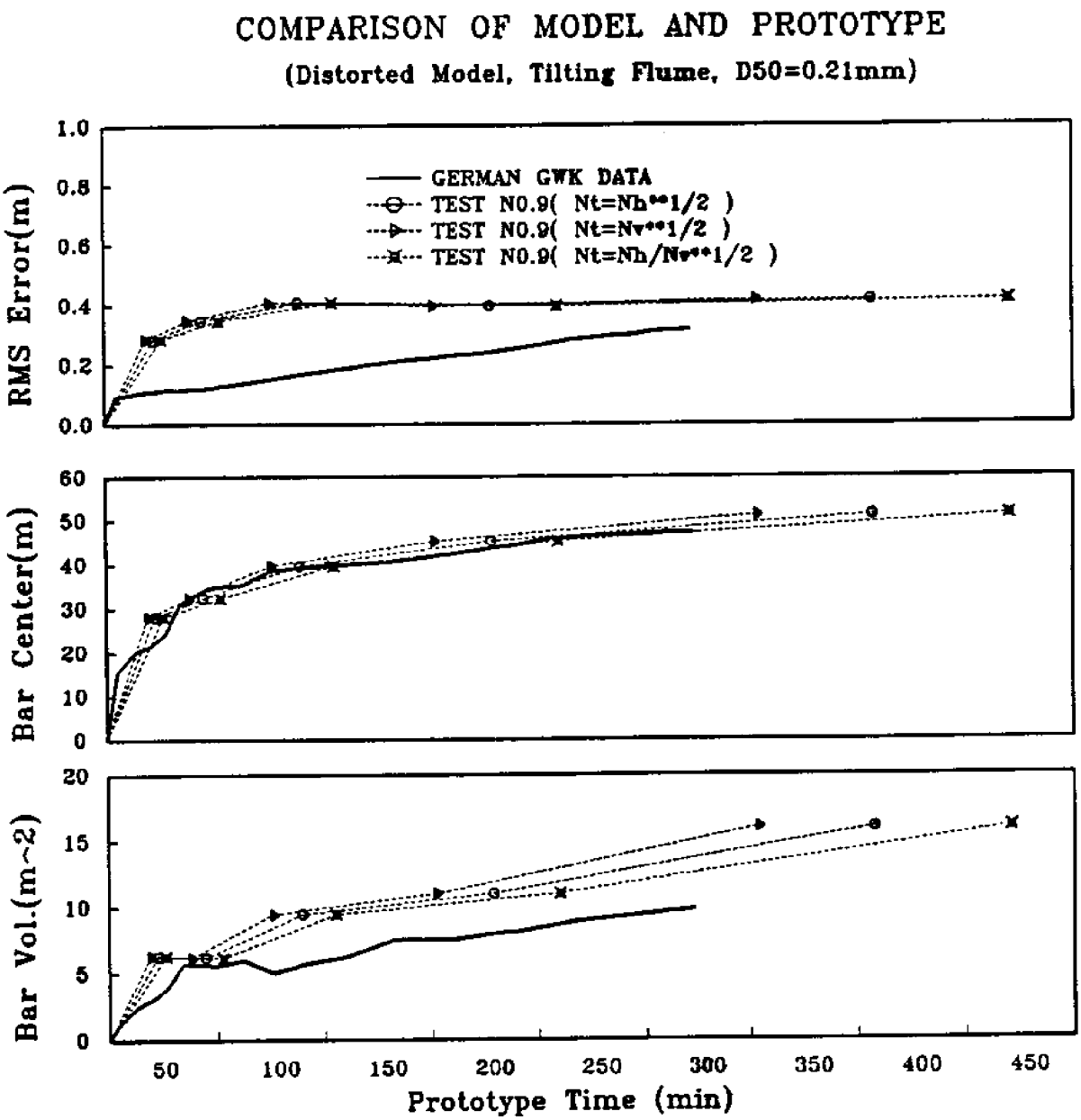

Figure 5.23: Morpholigical Time Scalings from WF Tests

feature was largely maintained. First of all, it is observed here that both transport and profile response are very close to that in the two-dimensional tests. Details on dune erosion and bar features are further examined.

The test conditions were so selected that cases 1 and 2 were based on Wang1's criteria of wave height and wave period scalings whereas cases 3 were based on Wang2's criteria. Again, the 6 criteria used in the two-dimensional tank tests are employed here.

Figure 5.26 to 5.28 show the results of bar region criteria for the three cases, seperately. One can easily see that case 3 represents the best fit which supports the Wang2 modeling law as that from the two-dimensional test results. Figure 5.29 gives the initial and final profiles of each section against prototype data.

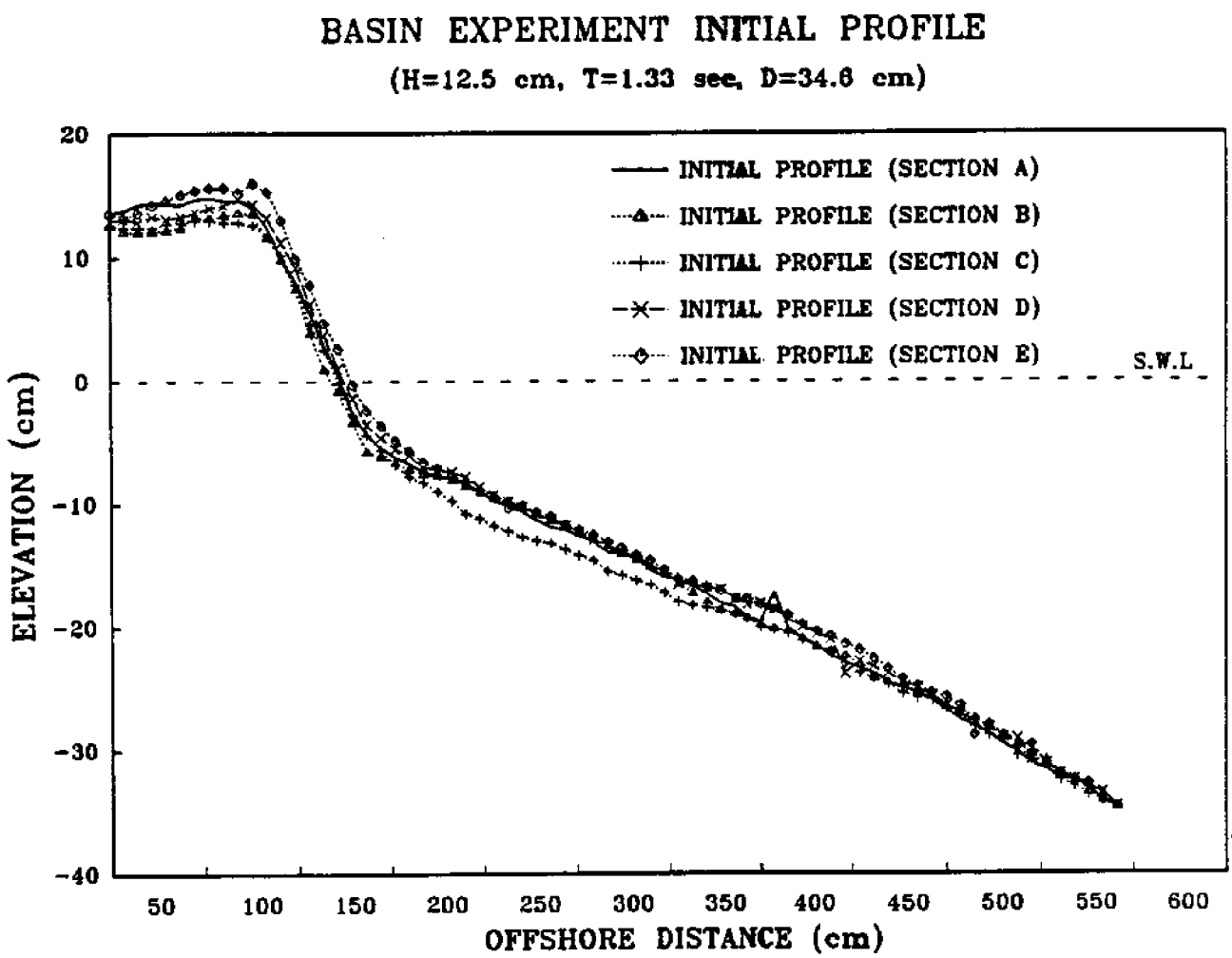

Figure 5.24: Initial Profiles Comparison Between 5 Sections for Case 3

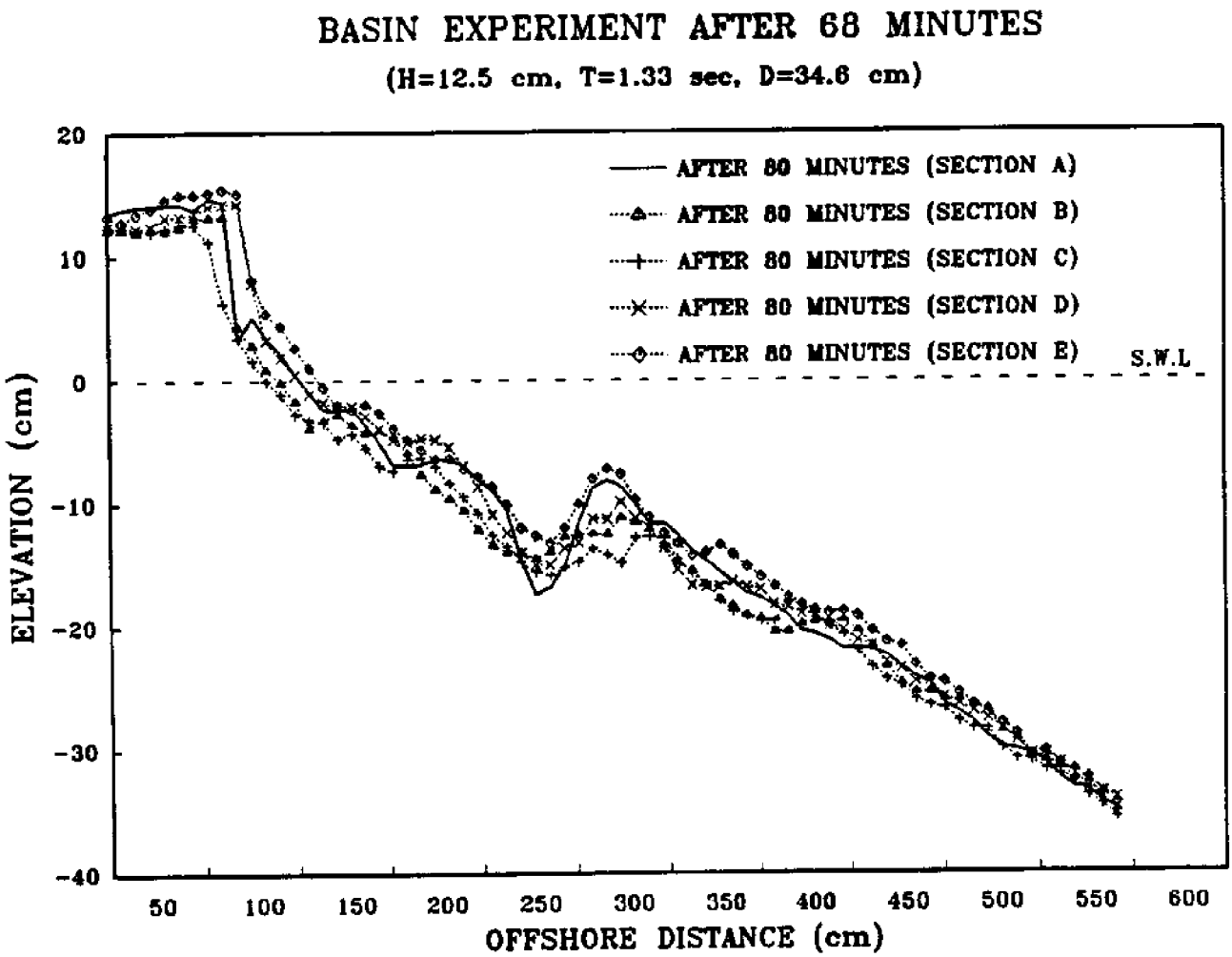

Figure 5.25: Final Profile Comparison Between 5 Sections for Case 3

The two criteria in the dune region, dune erosion volume and dune profile RMS values, are plotted in Figure 5.30 and 5.31. Based on profile RMS criterion all three morphological scales appeared to given reasonable results. In terms of dune erosional volume both Hughes and Wang2 over predict but Wang1 yields a good fit.

5.2 Test Results from Undistorted Model

As previously mentioned in chapter 4, when the median sediment size reduced to 0.09 mm, the model is nearly undistorted according to the modeling law. However, the undistorted model test results seemed not so encouraging, especially when the model becomes smaller, i.e., the horizontal geometric scale becomes greater. Maybe the sand is too fine, there is strong scale effect such as cohesive effect involved, which still remains unclear so far.

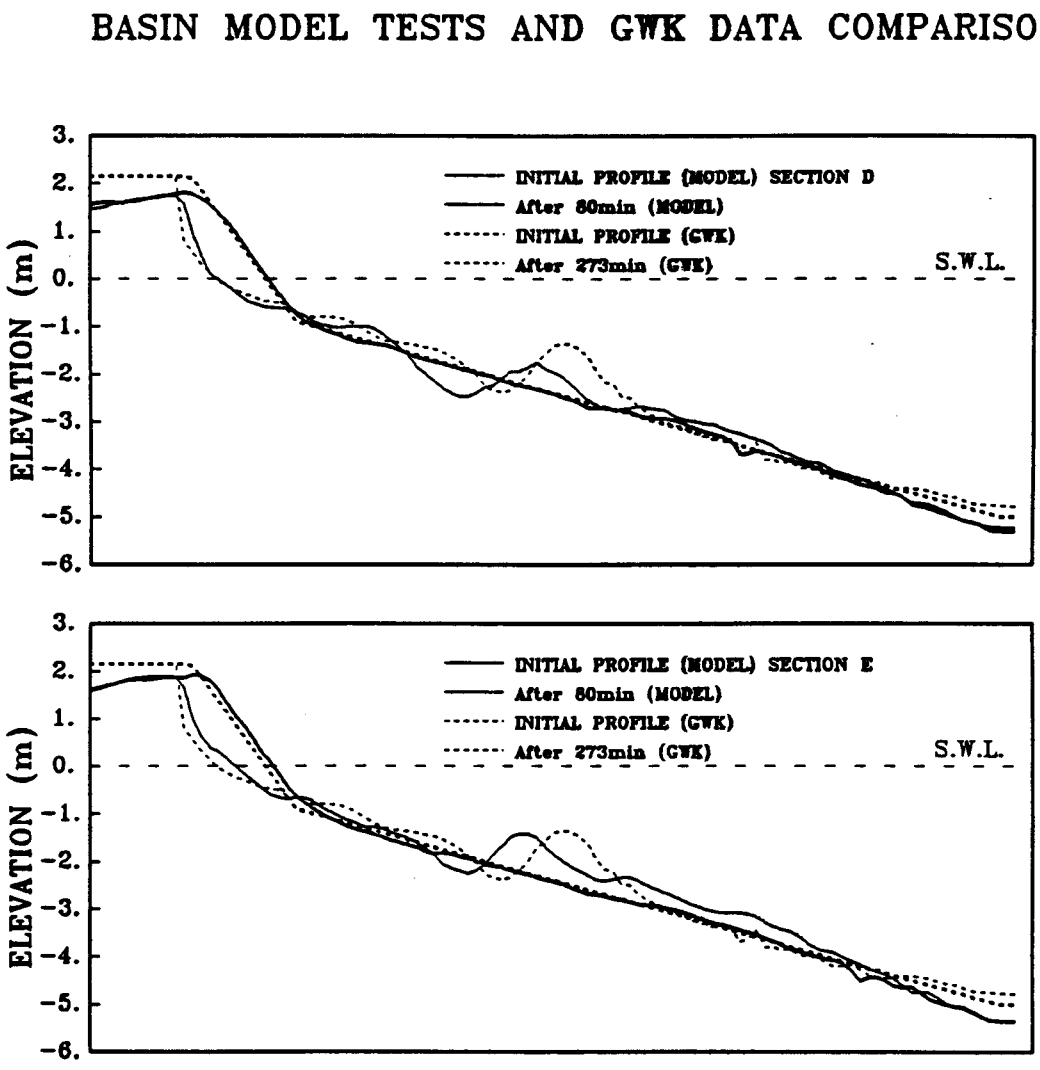

Figure 5.26: Comparison of Wave Basin Model Test No.3 with Prototype

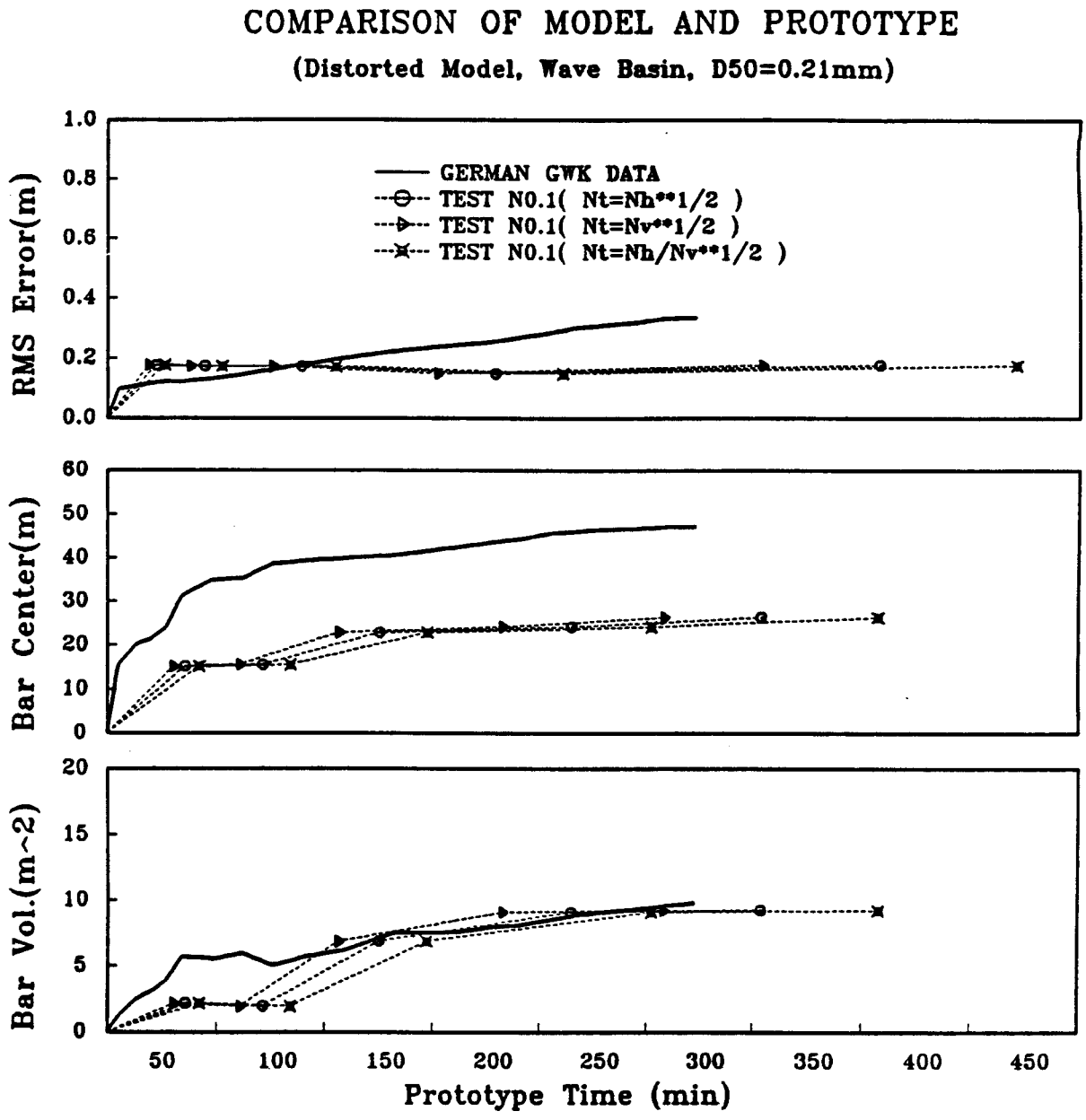

Figure 5.27: Morphological Time Scaling from Wave Basin Test No.1 against Prototype

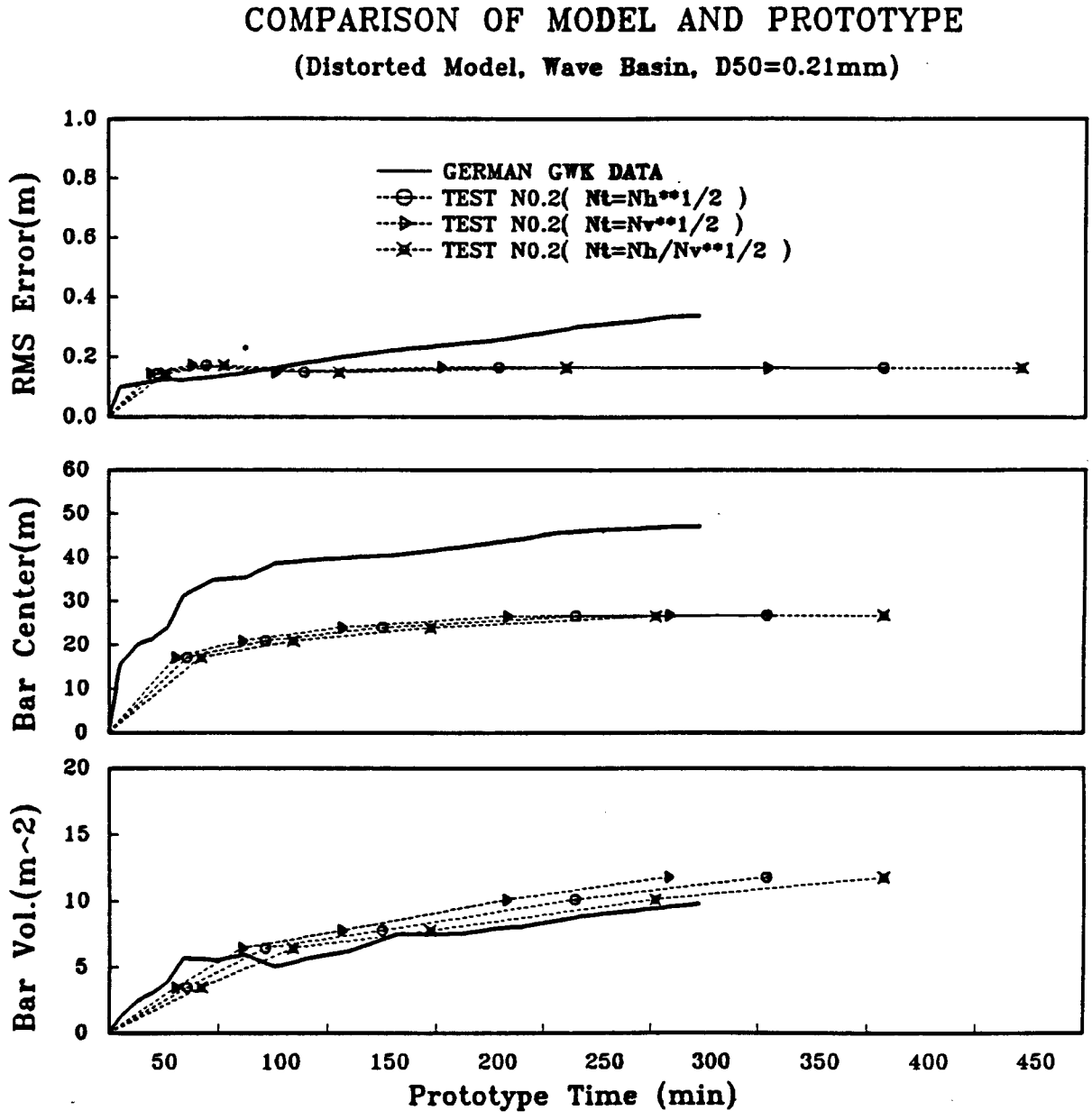

Figure 5.28: Morphological Time Scaling from Wave Basin Test No.2 against Prototype

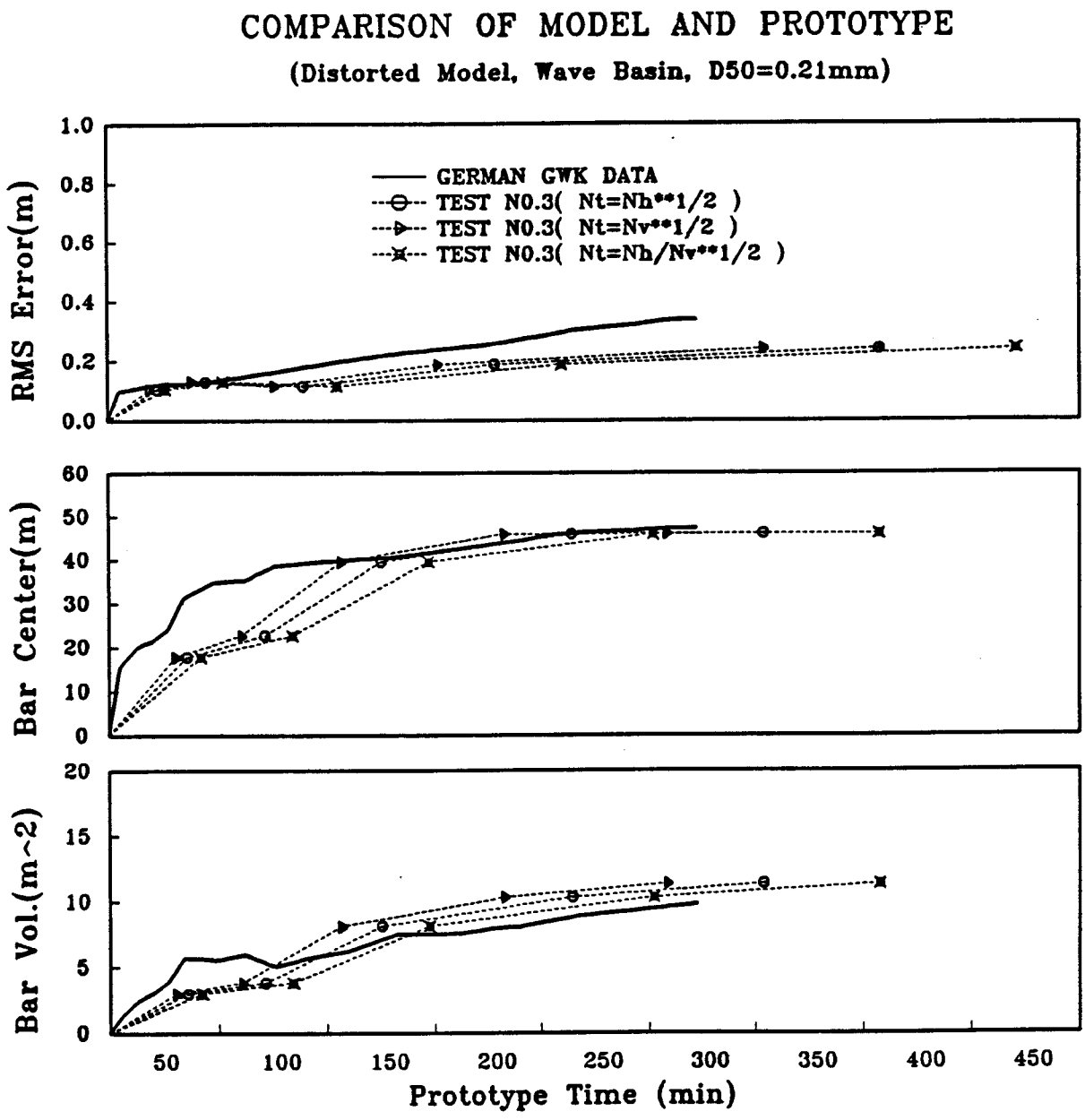

Figure 5.29: Morphological Time Scaling from Wave Basin Test No.3 against Prototype

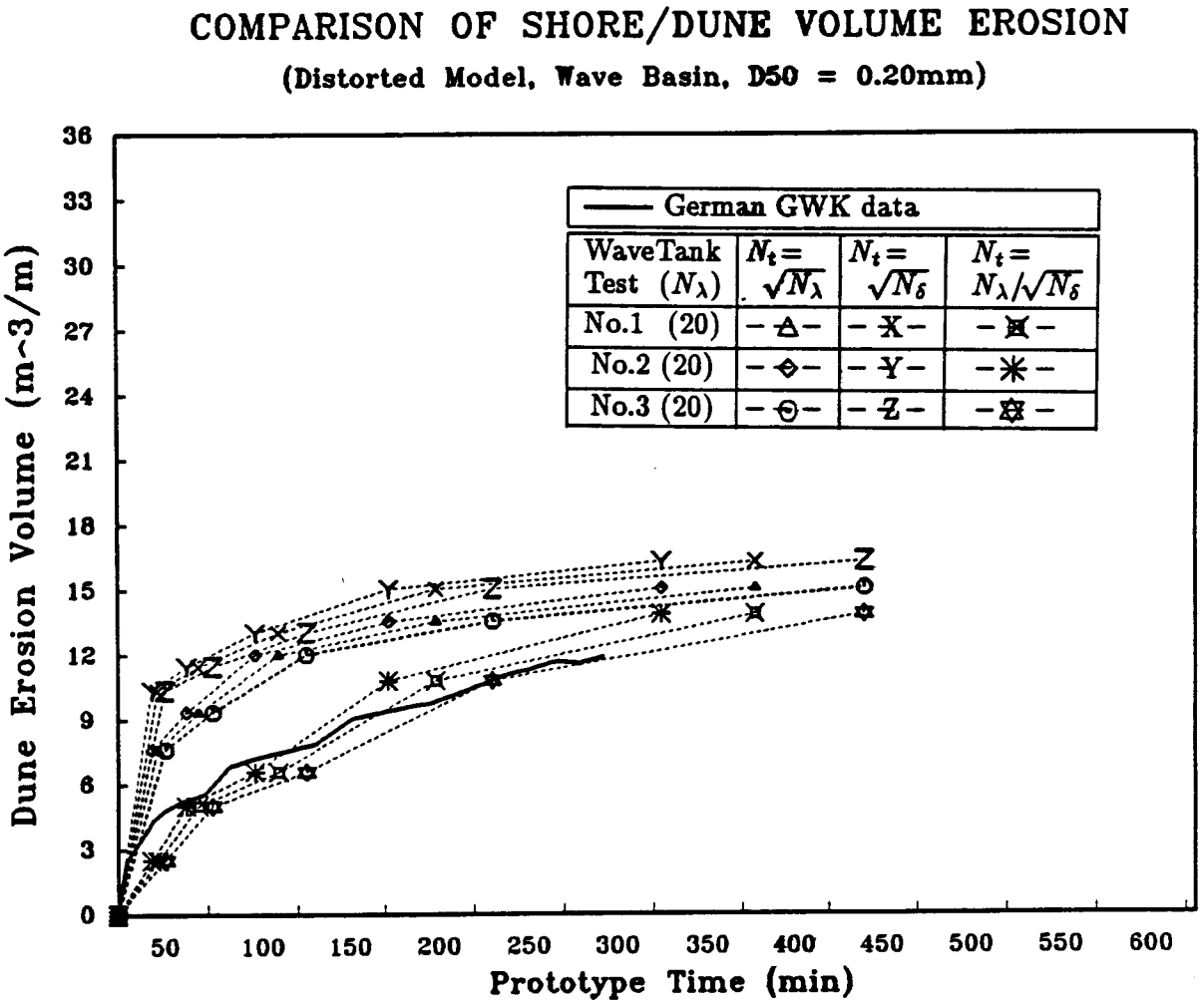

Figure 5.30: Dune Erosion Volume Comparison With Prototype

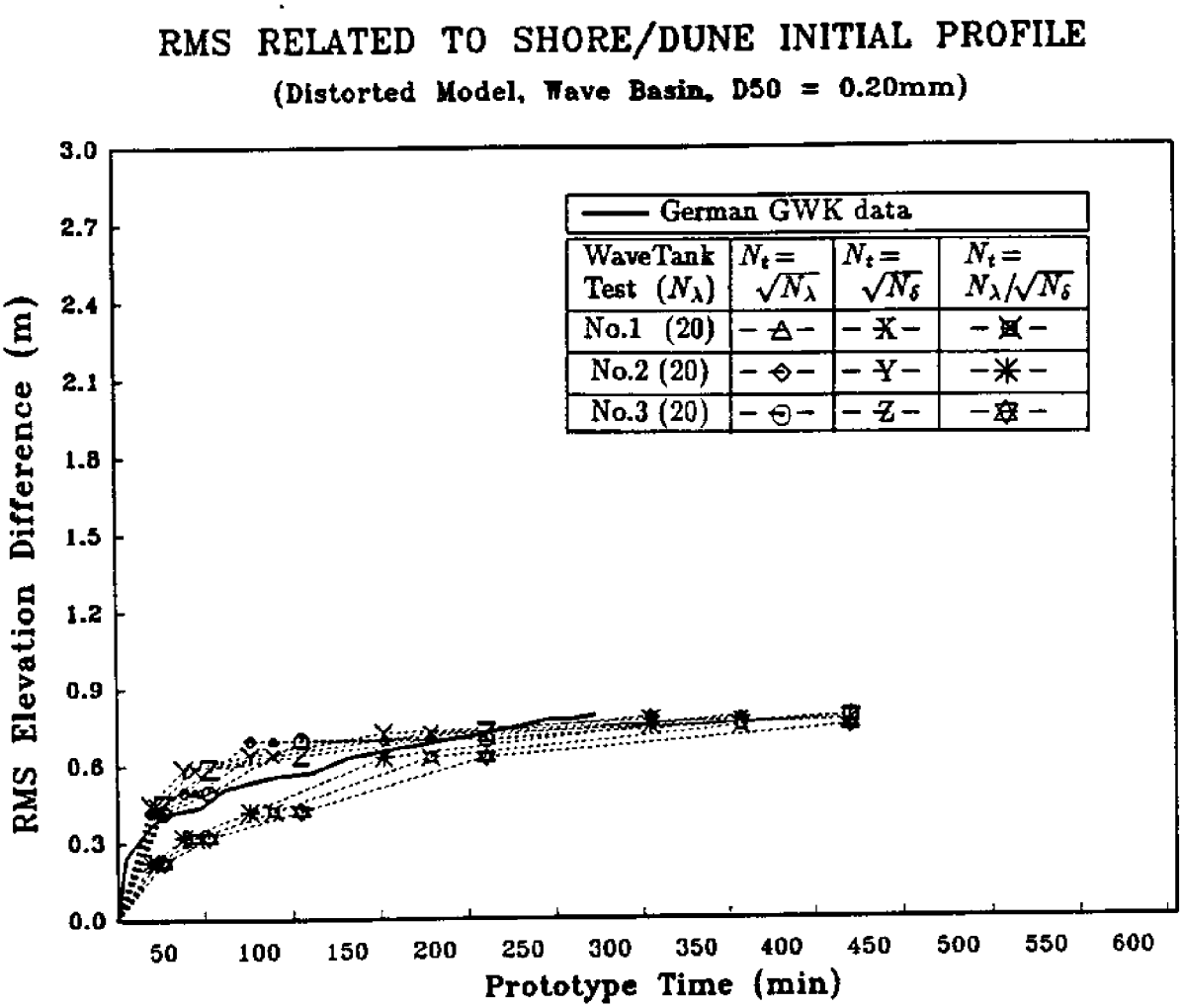

Figure 5.31: Dune Profile RMS Comparison With Prototype

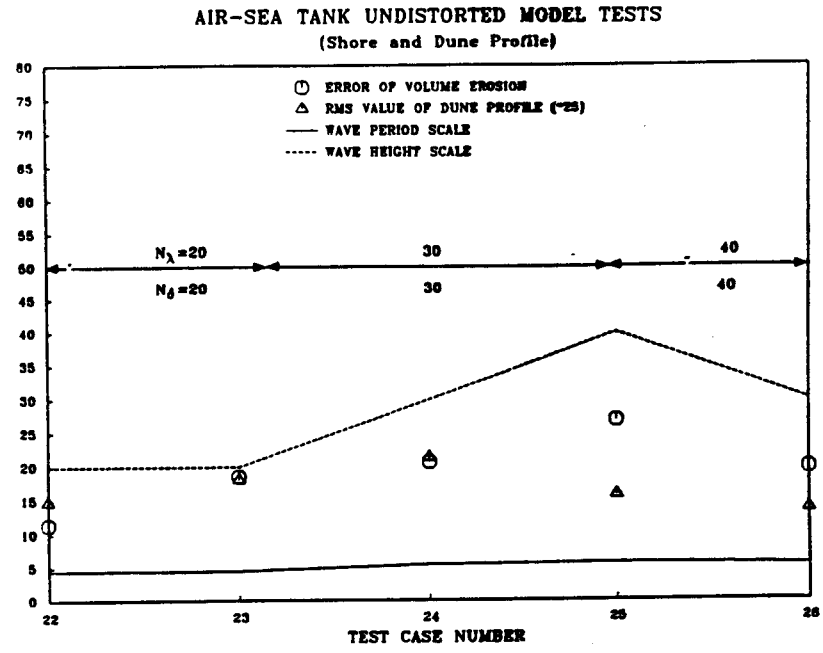

Figure 5.32: Summary of The Undistorted Model Test Results (shore profile)

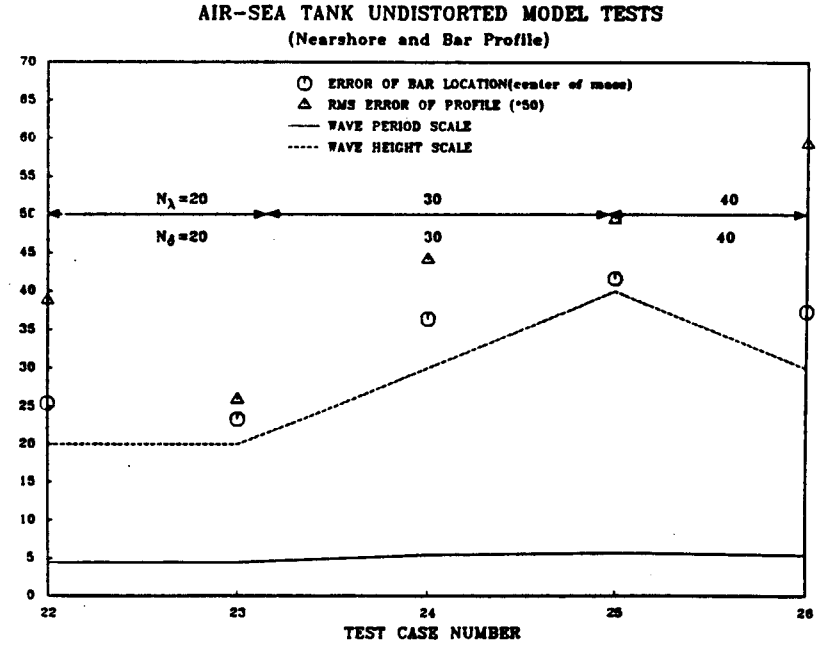

Figure 5.33: Summary of The Undistorted Model Test Results (bar profile)

CHAPTER 6
SUMMARY AND CONCLUSION

Proper movable bed modelling in general coastal engineering problems requires that both suspended load and bed load transport be properly modeled. In practicality this is very difficult at reduced scale; compromise has to be made to model only the dominant mode of transport. The region of interest here is limited to the beach profile inside or near the breaking zone. For this case the assumption is made that the suspended sediment transport is the dominant mode under storm wave condition. Under such limited condition existing distorted scale modeling laws were evaluated in the laboratory. Modified criteria were proposed .

A distorted profile modeling law originally proposed by Wang, et.al.(1990) was modified. The original version requires that the sediment fall velocity parameter and surf zone parameter be preserved. The modified version requires, in addition, that the breaking index be preserved. This, in essence, adds to the constraint that wave height be properly modeled in accordance to the preservation breaking index instead of as simple vertical geometrical scale. It is further proposed that the breaking index scale be a function of beach slope such that $N_\gamma = (N_\delta/N_\lambda)^k N_\delta$. Based on past experience k should be between 0.0 and 1.0 with k equal to 0 reduced to Wang's modeling law. For k=1.0 which represents the other extreme, a modified modeling law is derived here referred to as the Wang2.

Four existing scaling laws including the new one were tested in the laboratory using 2-D tanks and 3-D basin. German large wave tank expeiment results were taken as the prototype data. The beach profile was divided into two regions, the dune region and the bar-profile region. Separate criteria were developed to evaluate

the modeling laws. The major conclusions are listed here:

1. A comprehensive laboratory experiment was carried out to evaluate beach profile modeling laws of distorted geometrical scales.

2. The experiments supported the validity of applying distorted model for the prediction of beach and dune erosion in the nearshore zone.

3. Using overall underwater profile and bar formation as criteria, the newly proposed modeling law appears to have better overall agreement compared with other existing modeling laws.

4. Based on 2-D tank results, all four laws over predict dune erosion volume which is an important quantity of engineering concern. It also appeared that the larger the scale ratio, i.e., the smaller the model, the larger the over prediction. It is suspected that the over prediction may be caused by the inadequate compaction in the 2-D tank experiments. In the 3-D basin the initial profile compaction was more carefully done and the results appeared to agree better with the prototype. Since most of the over prediction occurred in the early stage of the tests, the modeling laws still could be viewed as leading to reasonable approximation of volumetric erosion if one is mainly concerned with the dune erosion at final later times.

5. The test results supported the general opinion that beach erosion is more sensitive to wave height than to wave period.

6. Test results suggested that beach profile including the breaking bar portion could attain a quasi- equilibrium form in the laboratory within the tested duration. Dune erosion equilibrium, however, appeared to have not been attained, at least not for the tested duration. Also the inner portion of equilibrium profile appeared to agree with the power law shape given by $h = Ax^m$. The value of m is closer to 4/5 as proposed by Wang (1990) and Vellinga as oppose to 2/3.

7. One of the main objectives of this study is to evaulate the morphological time scale. This objective was only partially achieved. Within the test range, all four

modeling laws yielded scaled values within a narrow range that agreed reasonably well with the prototype. The proposed new scaling law may have a slight advantage over the others. A definitive conclusion can not be made owing to the data scatter. The results seemed to indicate that morphological time scale is not too sensitive to the variables, or the range of variables, tested which included mainly wave height and wave period. As indicated in item 5, the test results was also not sensitive to wave period.

Since the proposed new modeling law and the original one proposed by Wang represent two extremes of wave-height scaling dependency on beach slope as explained earlier it would be intructional to evaluate the sensitivity of this dependency. In other words, if k=1.0, wave height should be scaled in accordance with $N_H = N_\delta^2/N_\lambda$ whereas for k=0.0 wave height should be scaled as vertical geometrical scale. Figure 6.1 plots the required wave height (in non-dimensional value of H_0/H with H_0 being the required wave height at k=0.0) for different values of k under the present distorted geometrical scales. The results indicated the scale ratio of wave height is not a sensitive one which helps to explain that sometimes it is difficult to decide from the experimental results which modeling law is superior.

8. Finally, it is remarked here that the undistorted experiments using fine sand $D_{50} = 0.09mm$ were not successful. An expected bar profile could not be obtained.

For further studies, it is recommanded here that,

1.The model construction initially placed in the test facility needs to be very carefully carried out to insure proper saturation and compaction. This maybe better achieved by hand compaction and longer shake down test using small waves. The profile may require remolding with additional sand, if necessary, to re-establish the initial profile.

2. There is certainly a need for additional verification. It is hoped that further study will add more confidence to the presented modeling law, or to define more

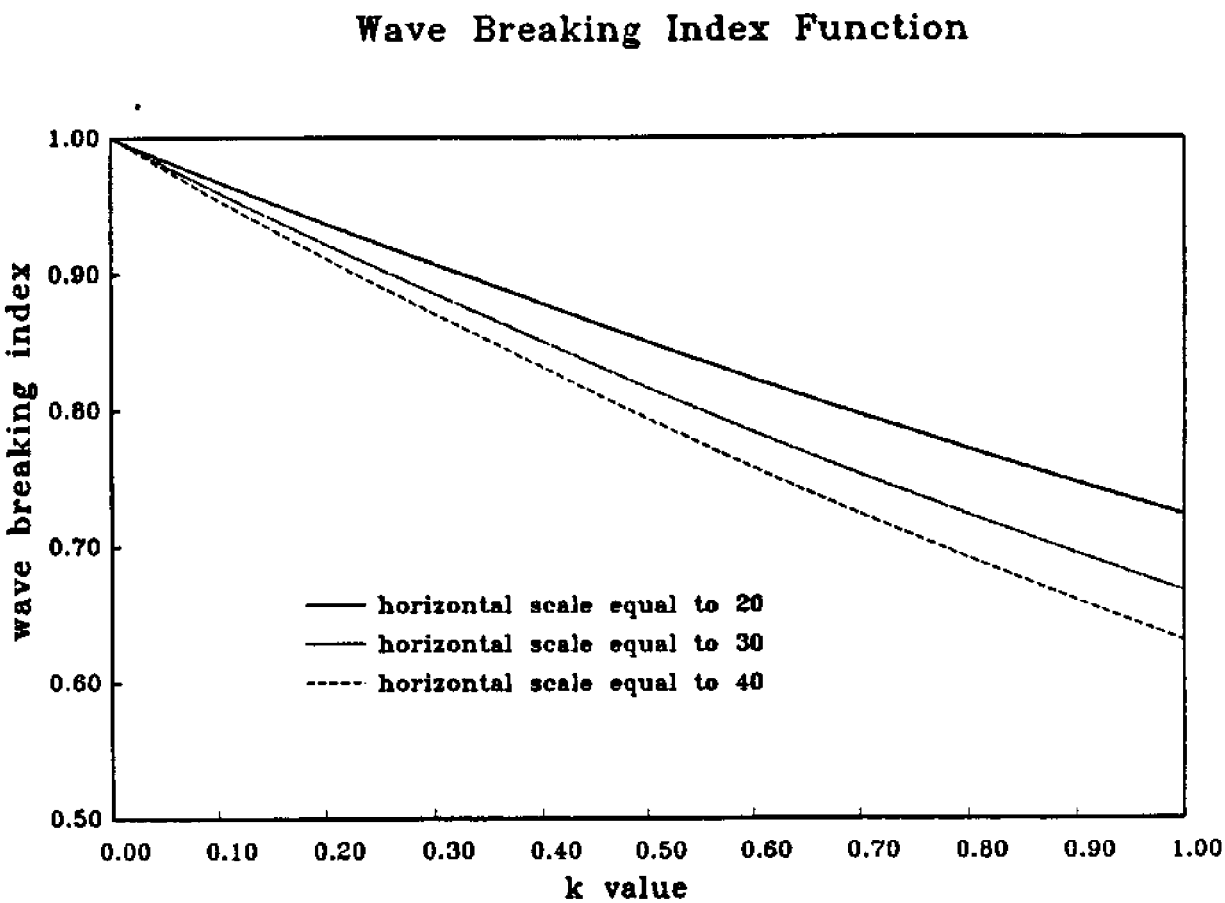

Figure 6.1: Wave Height Scale as A function of k Value

precisely the breaking index modeling law, or to prove modeling of dune and beach surf zone by employing different modeling laws.

3. The test should be extended to random wave conditions for more realistically representing the natural conditins.

4. Anothor problem needs immediate attention is the modeling law of beach accretion.

APPENDIX A
BEACH PROFILE EVOLUTION AND SEDIMENT TRANSPORT RATE

Appendix A shows the total 26 figures of the sediment transport rate pattern and the beach profile evolution with time of the experiments in the airsea wave tank under different wave conditions.

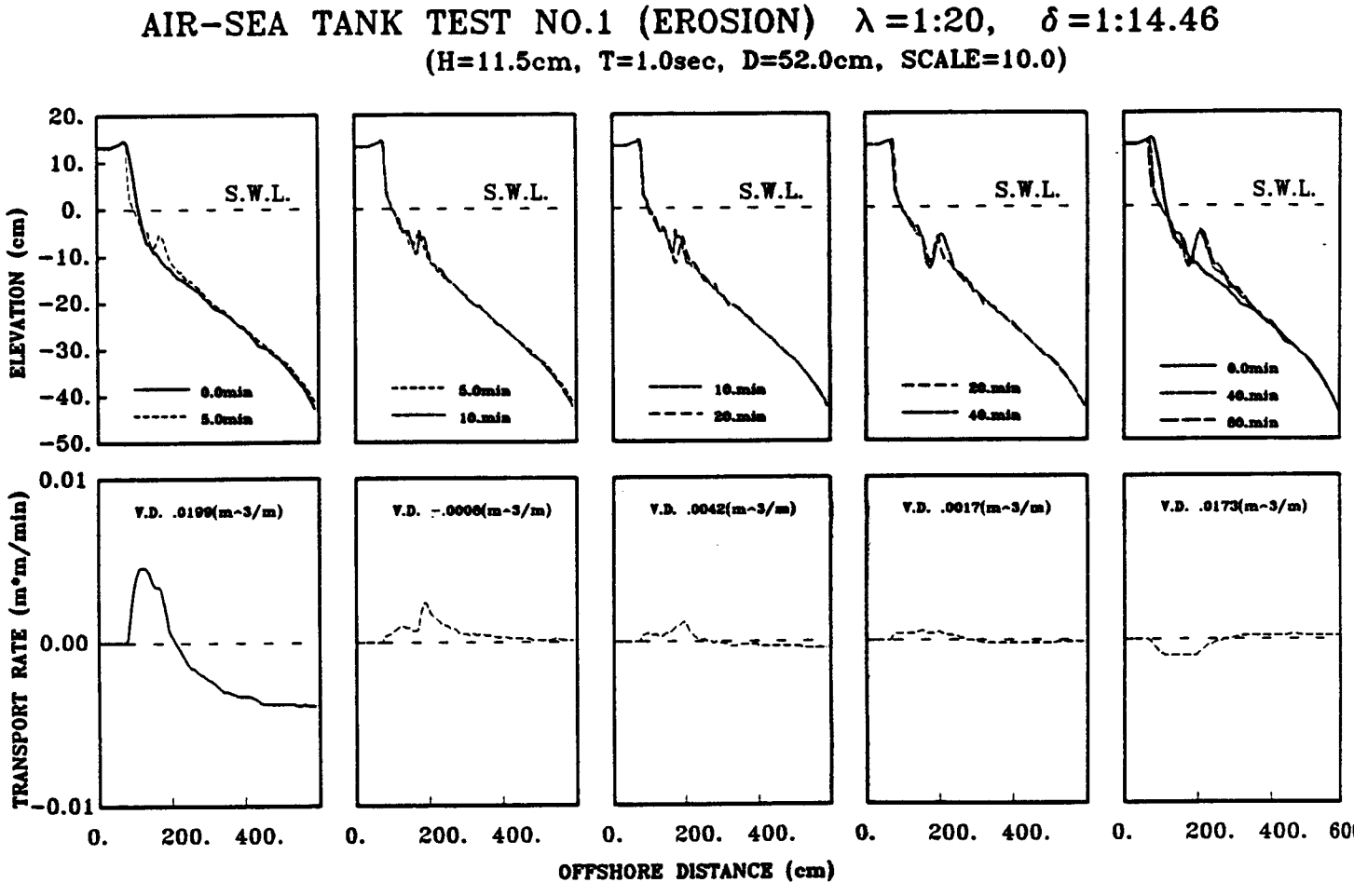

Figure A.1: Beach Profile Evolution and Sediment Transport Pattern of Test No.1

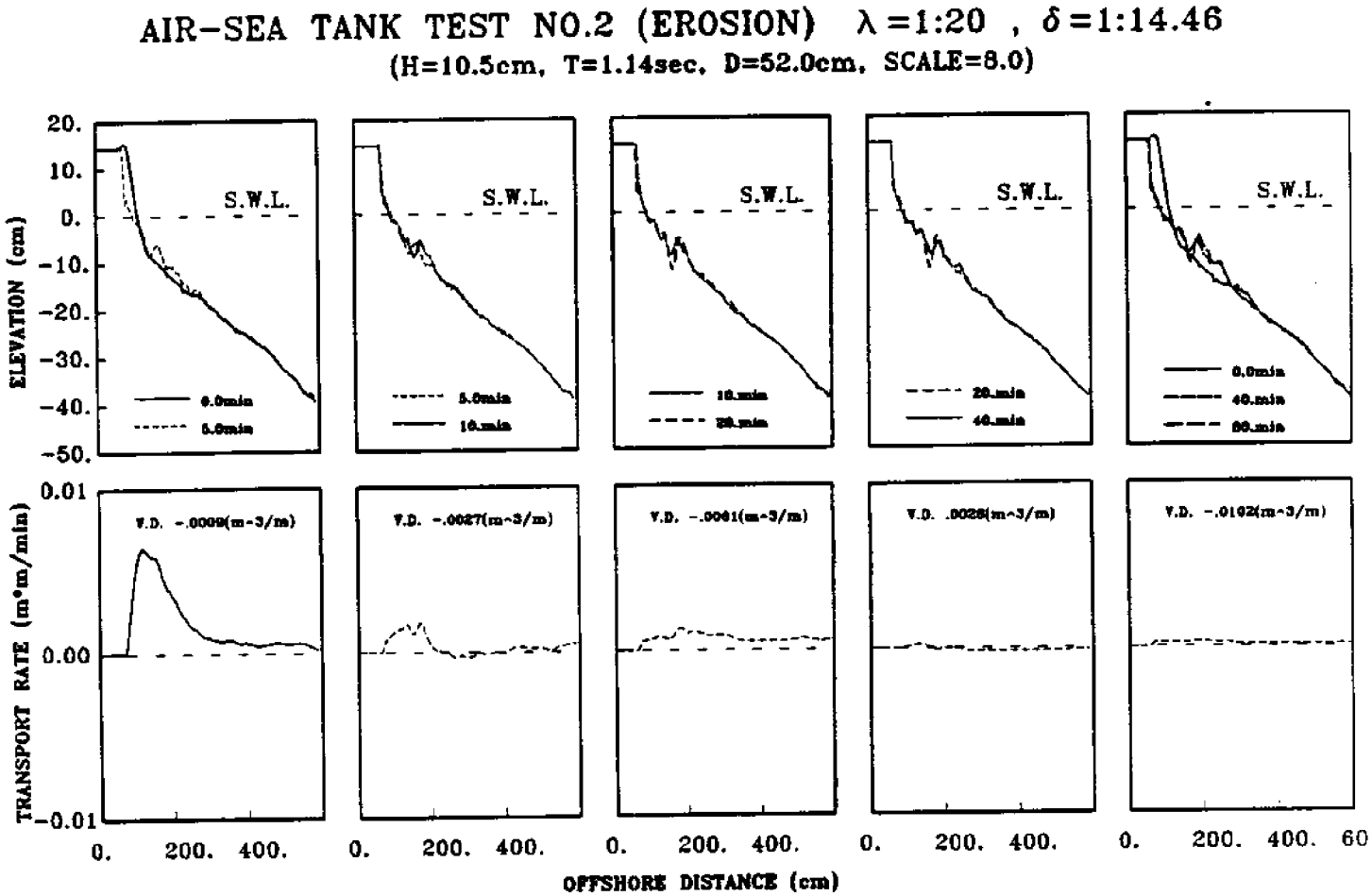

Figure A.2: Beach Profile Evolution and Sediment Transport Pattern of Test No.2

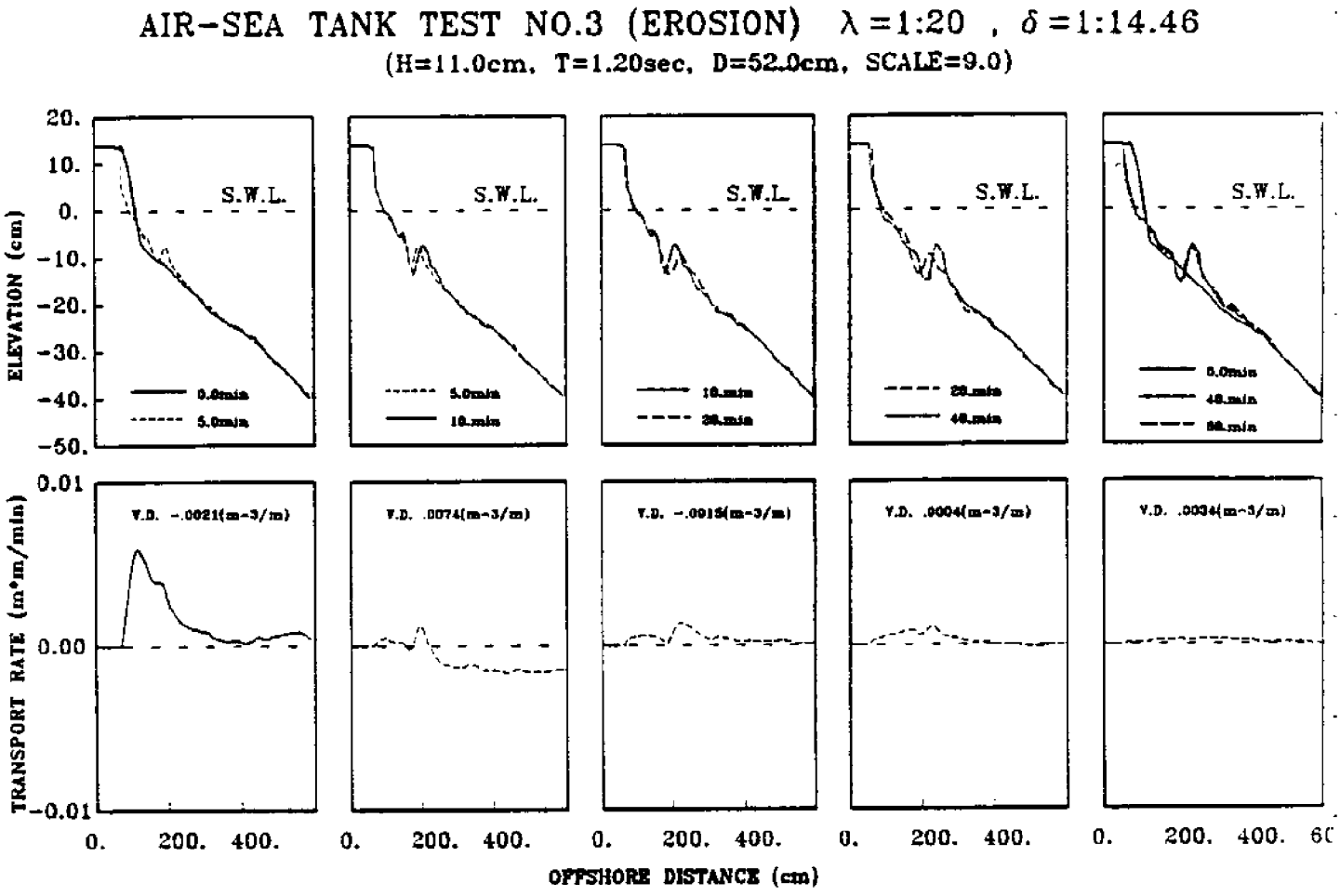

Figure A.3: Beach Profile Evolution and Sediment Transport Pattern of Test No.3

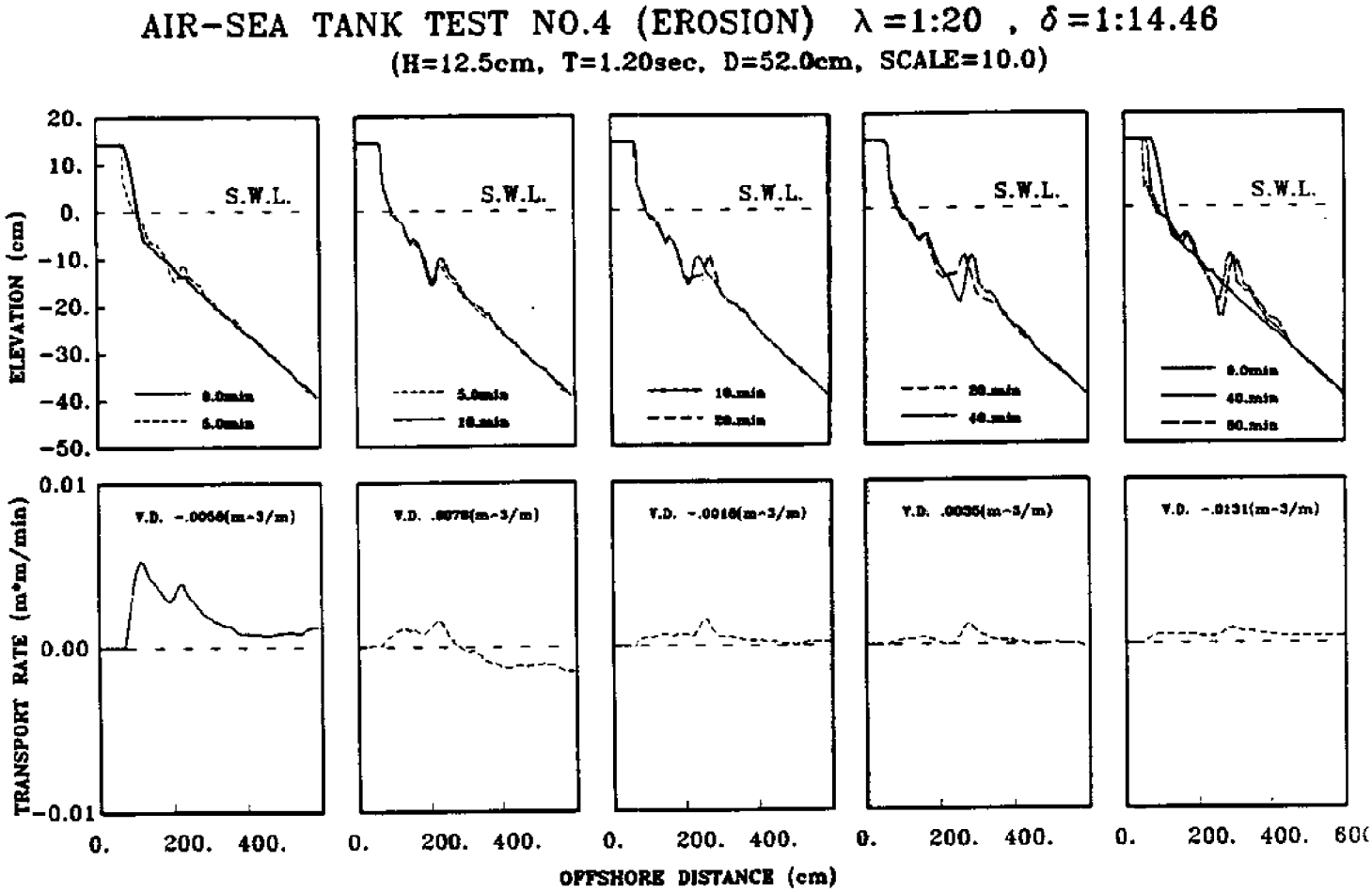

Figure A.4: Beach Profile Evolution and Sediment Transport Pattern of Test No.4

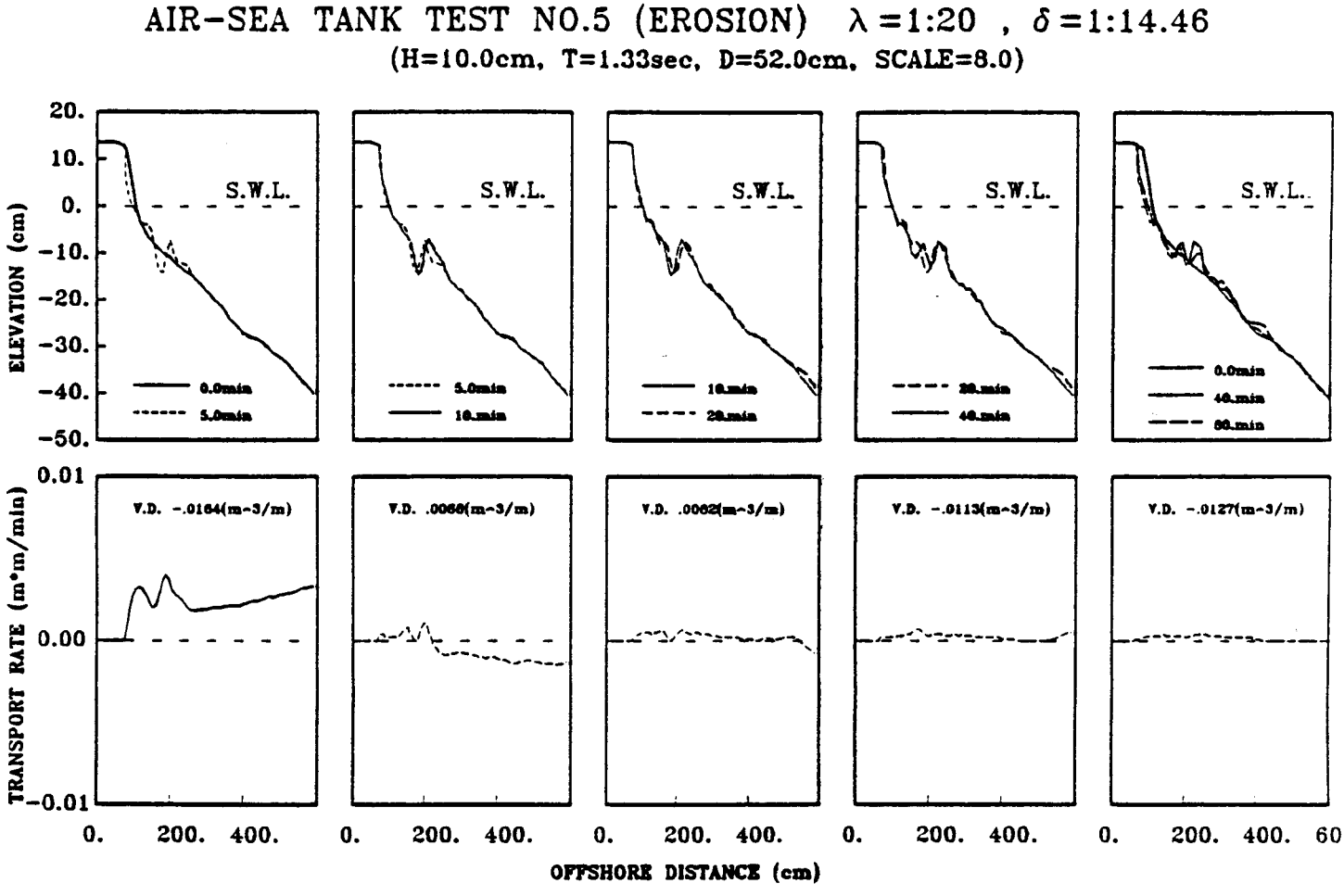

Figure A.5: Beach Profile Evolution and Sediment Transport Pattern of Test No.5

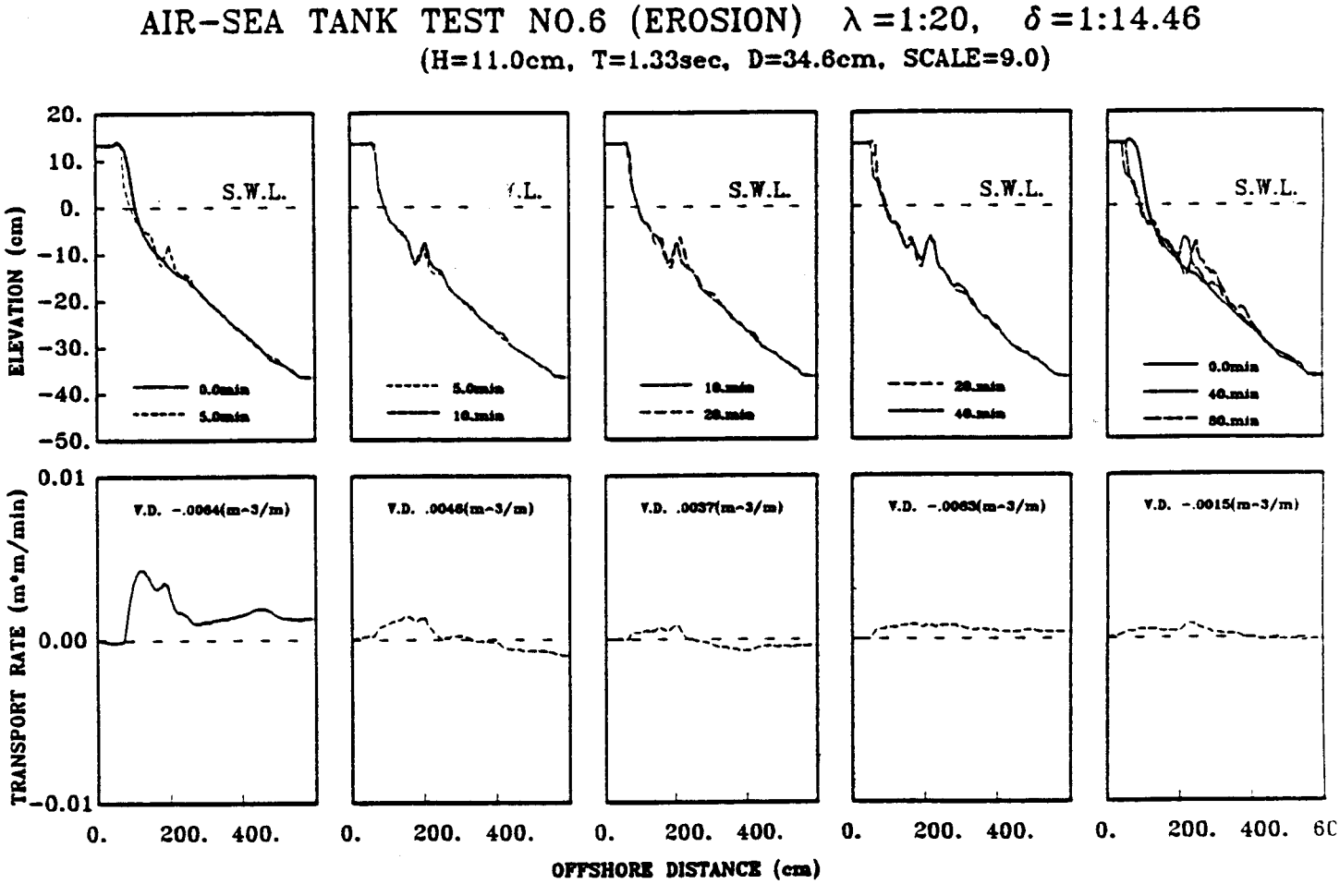

Figure A.6: Beach Profile Evolution and Sediment Transport Pattern of Test No.6

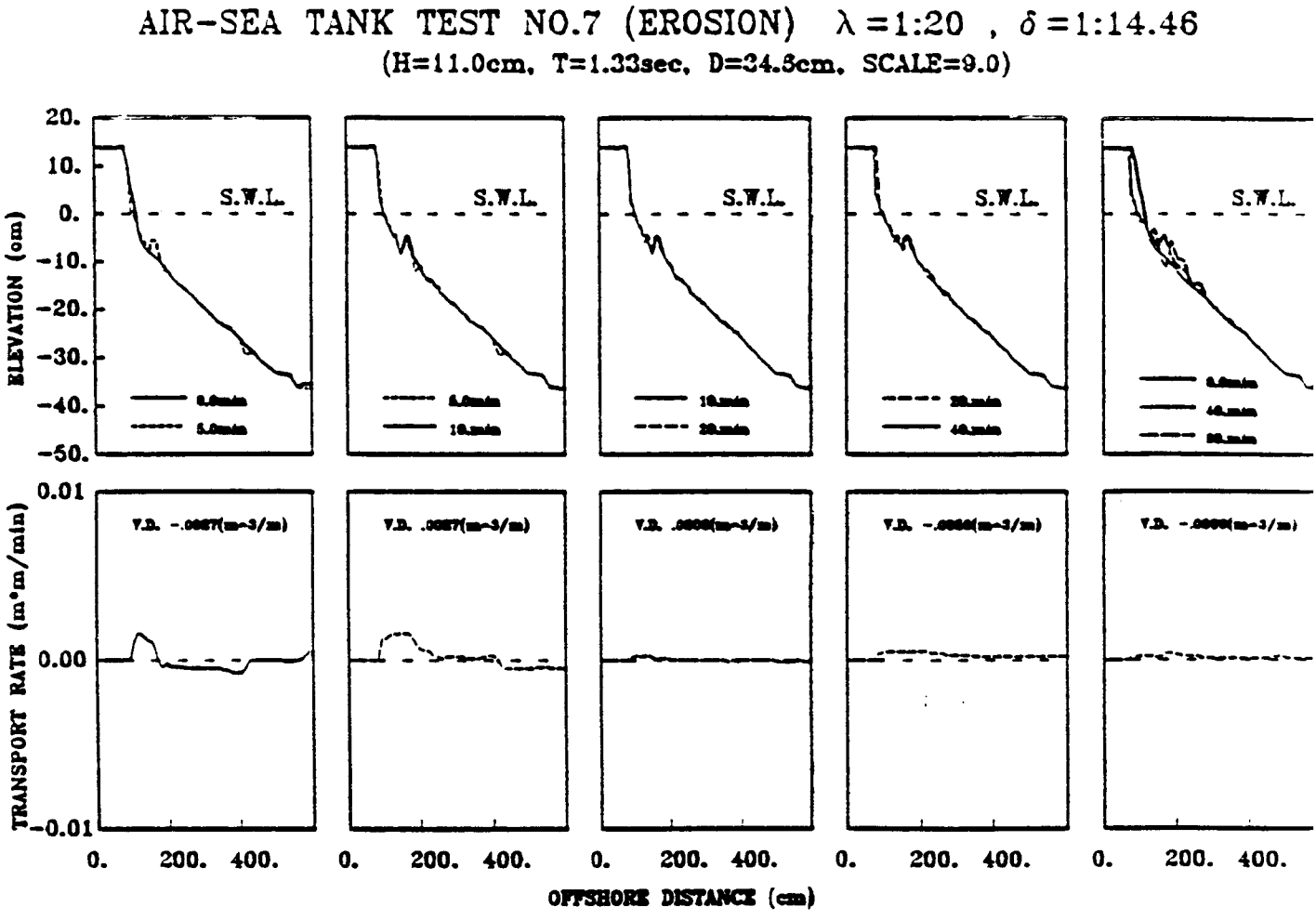

Figure A.7: Beach Profile Evolution and Sediment Transport Pattern of Test No.7

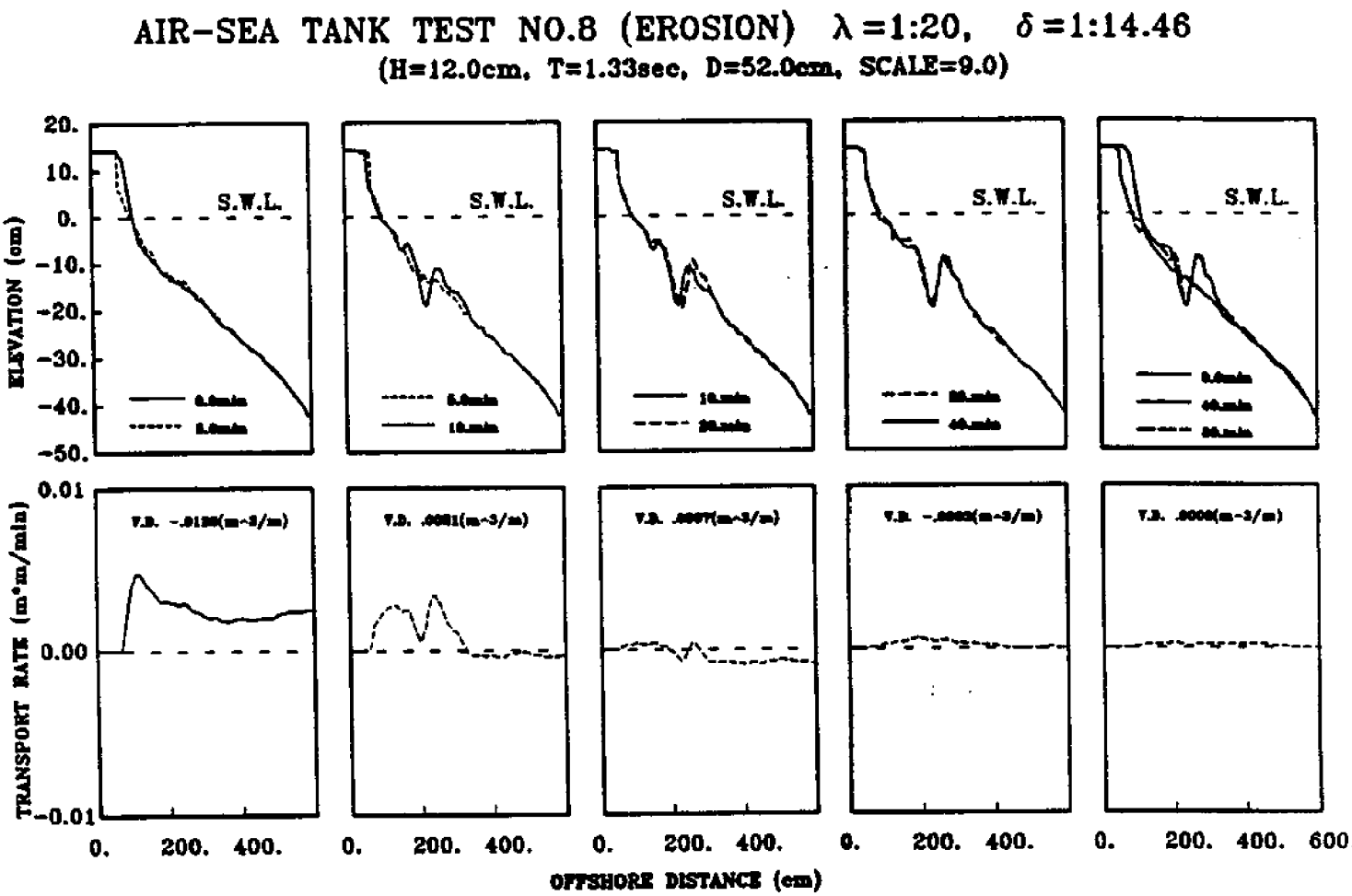

Figure A.8: Beach Profile Evolution and Sediment Transport Pattern of Test No.8

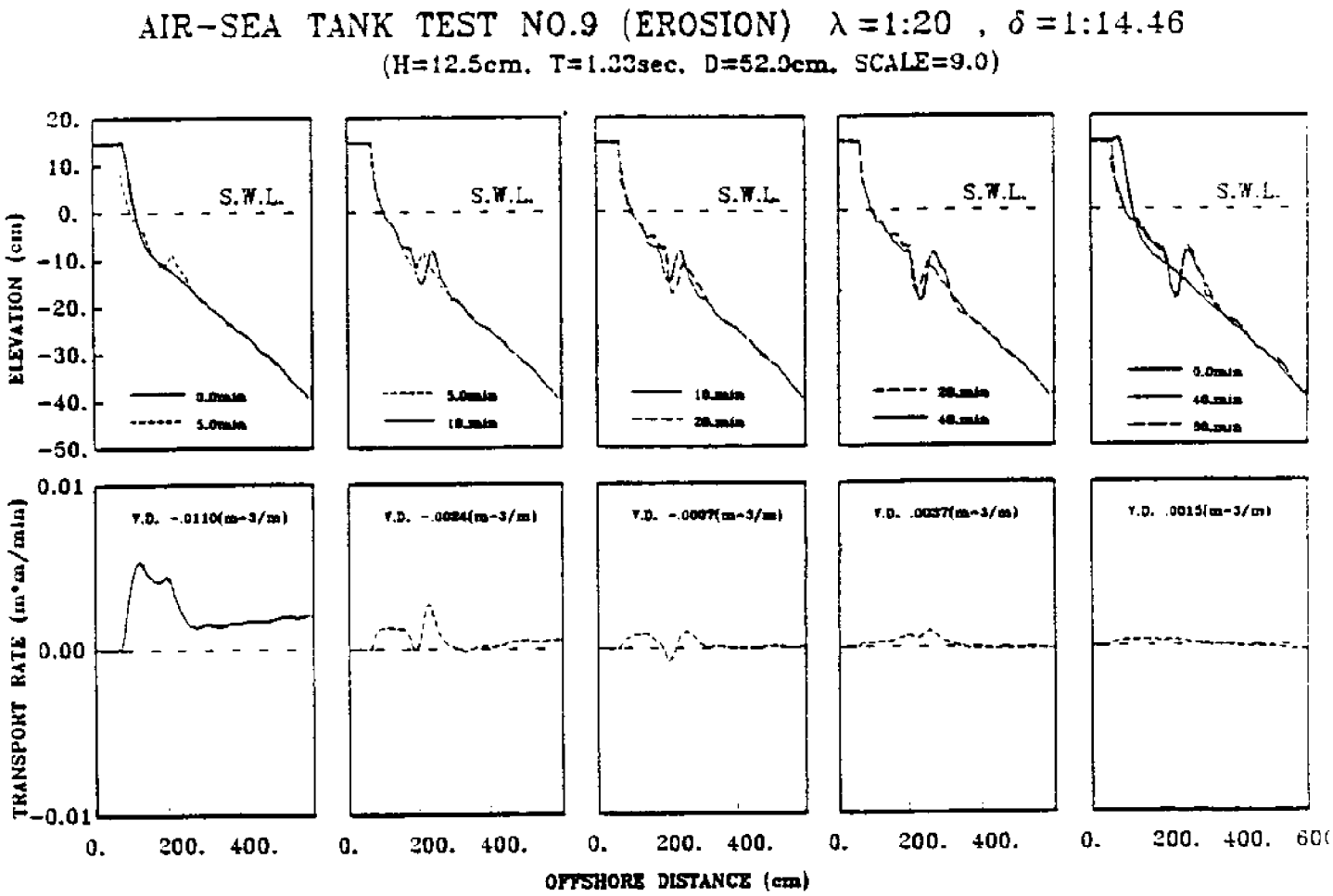

Figure A.9: Beach Profile Evolution and Sediment Transport Pattern of Test No.9

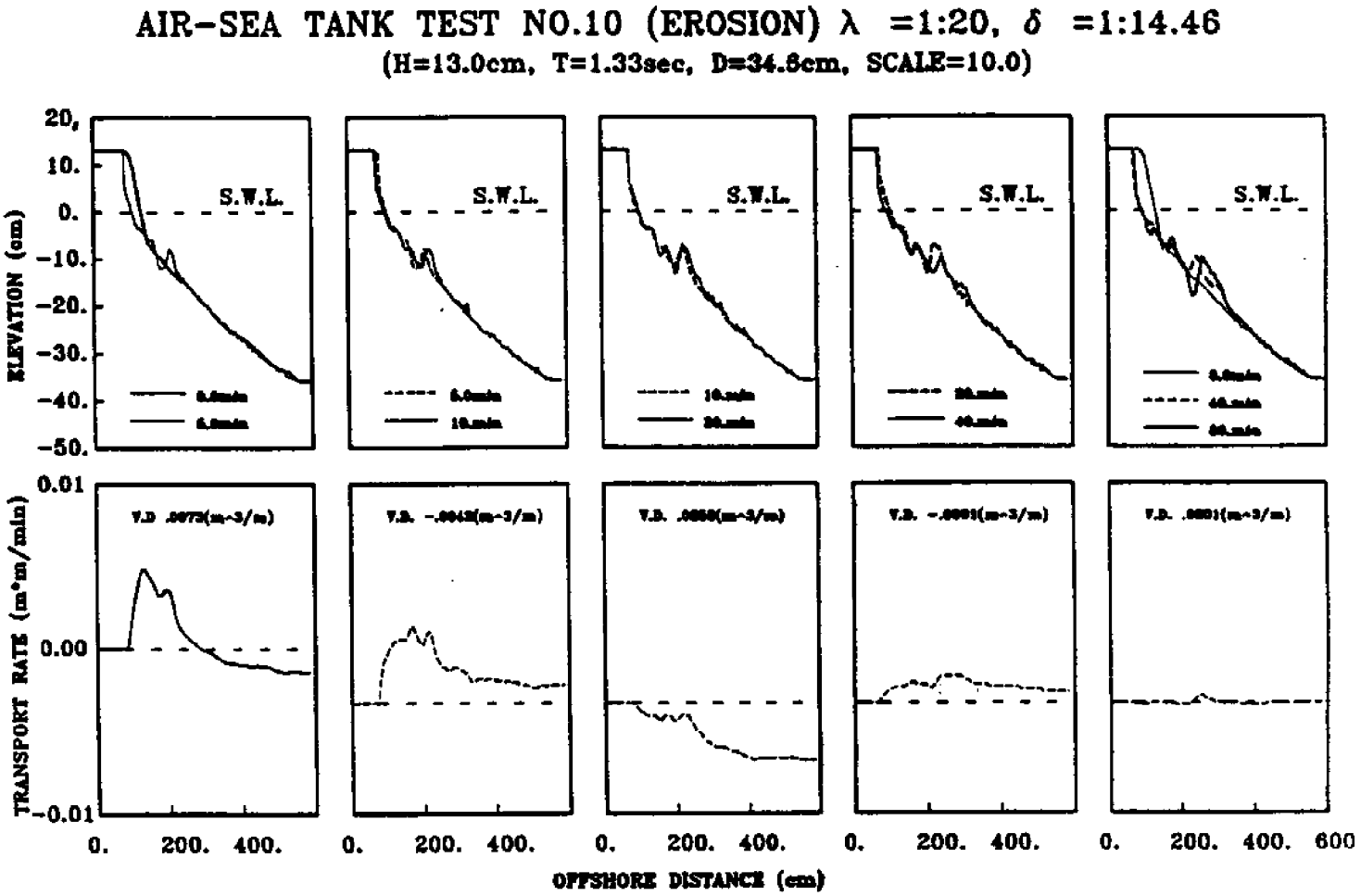

Figure A.10: Beach Profile Evolution and Sediment Transport Pattern of Test No.10

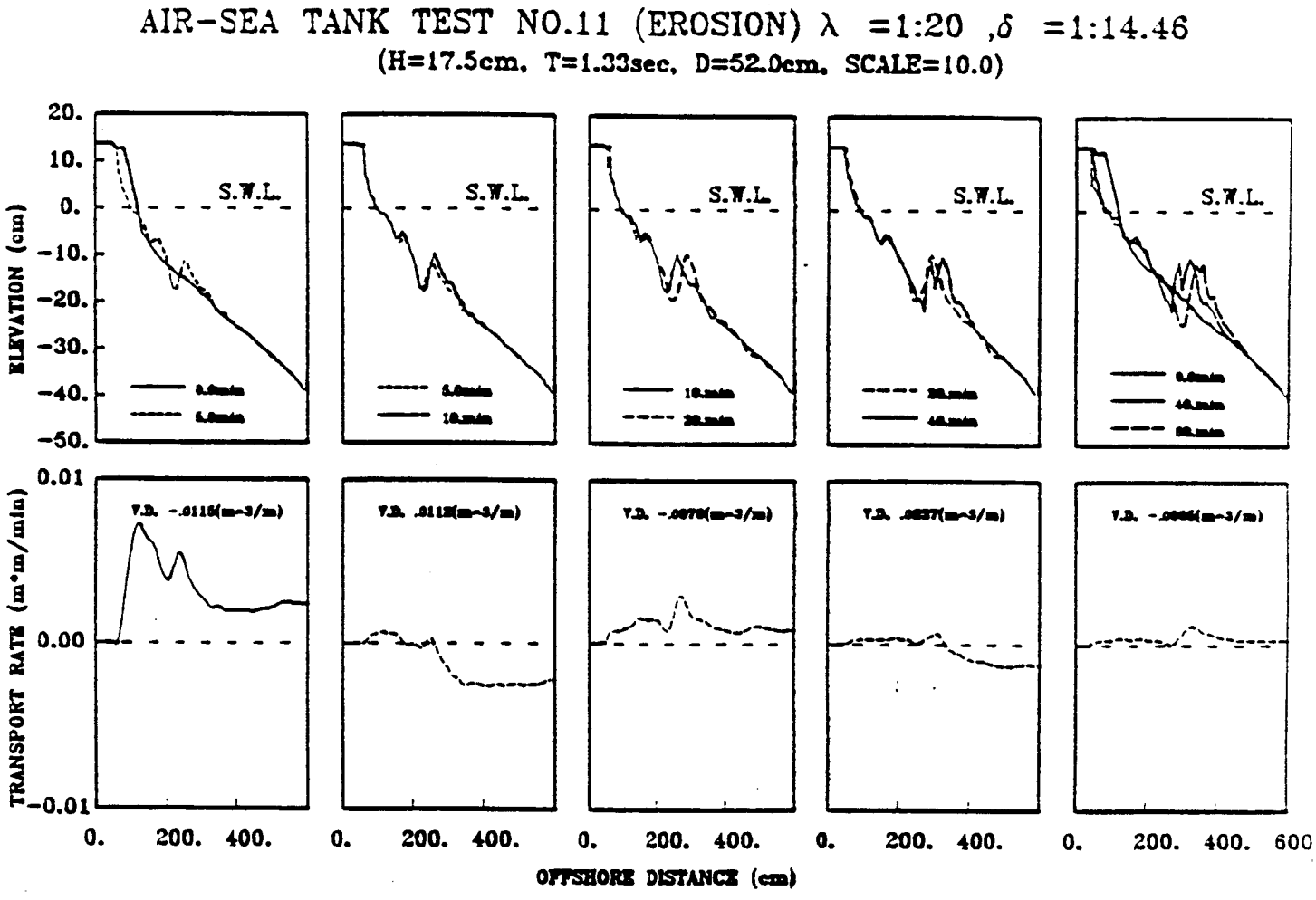

Figure A.11: Beach Profile Evolution and Sediment Transport Pattern of Test No.11

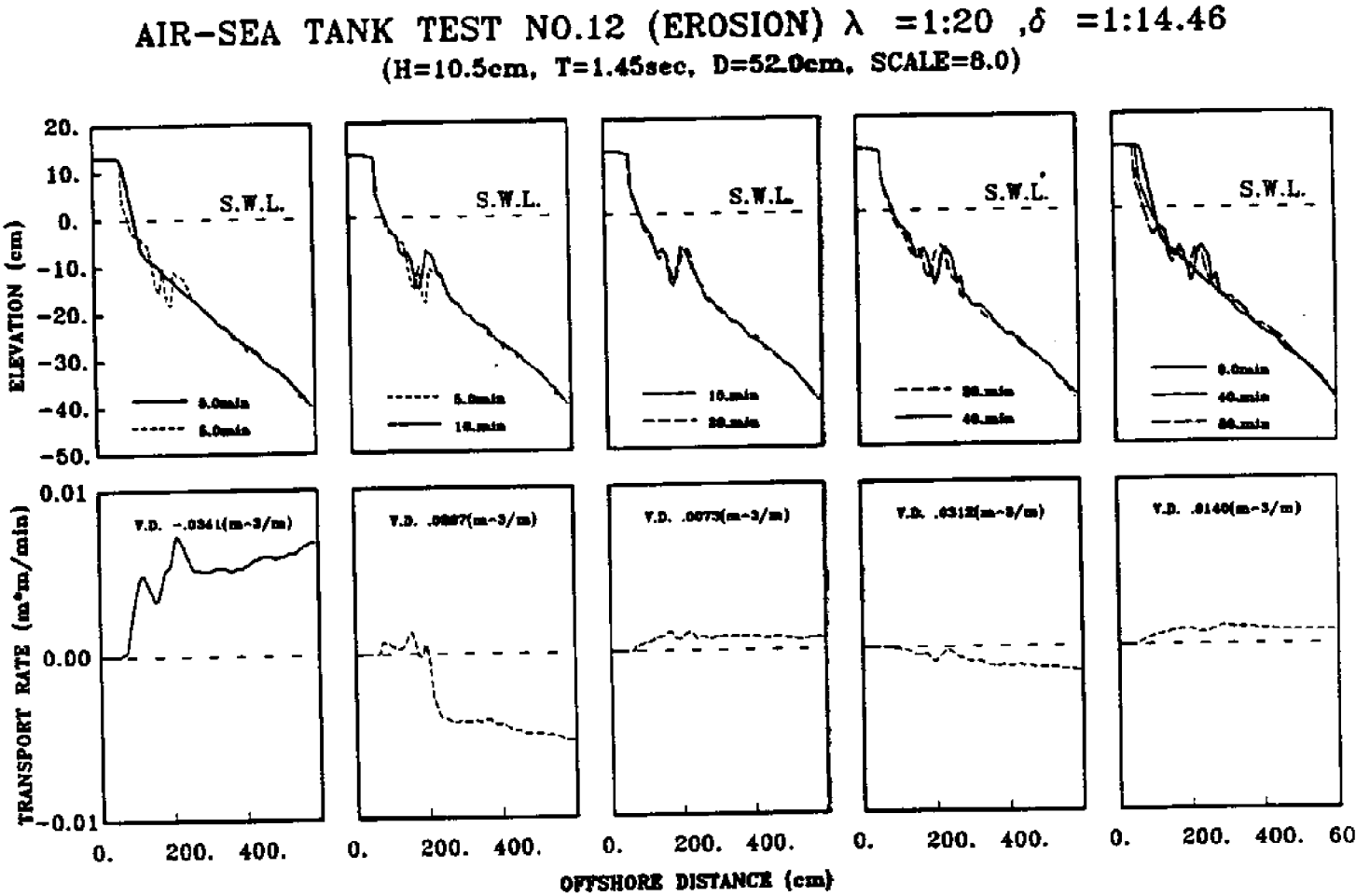

Figure A.12: Beach Profile Evolution and Sediment Transport Pattern of Test No.12

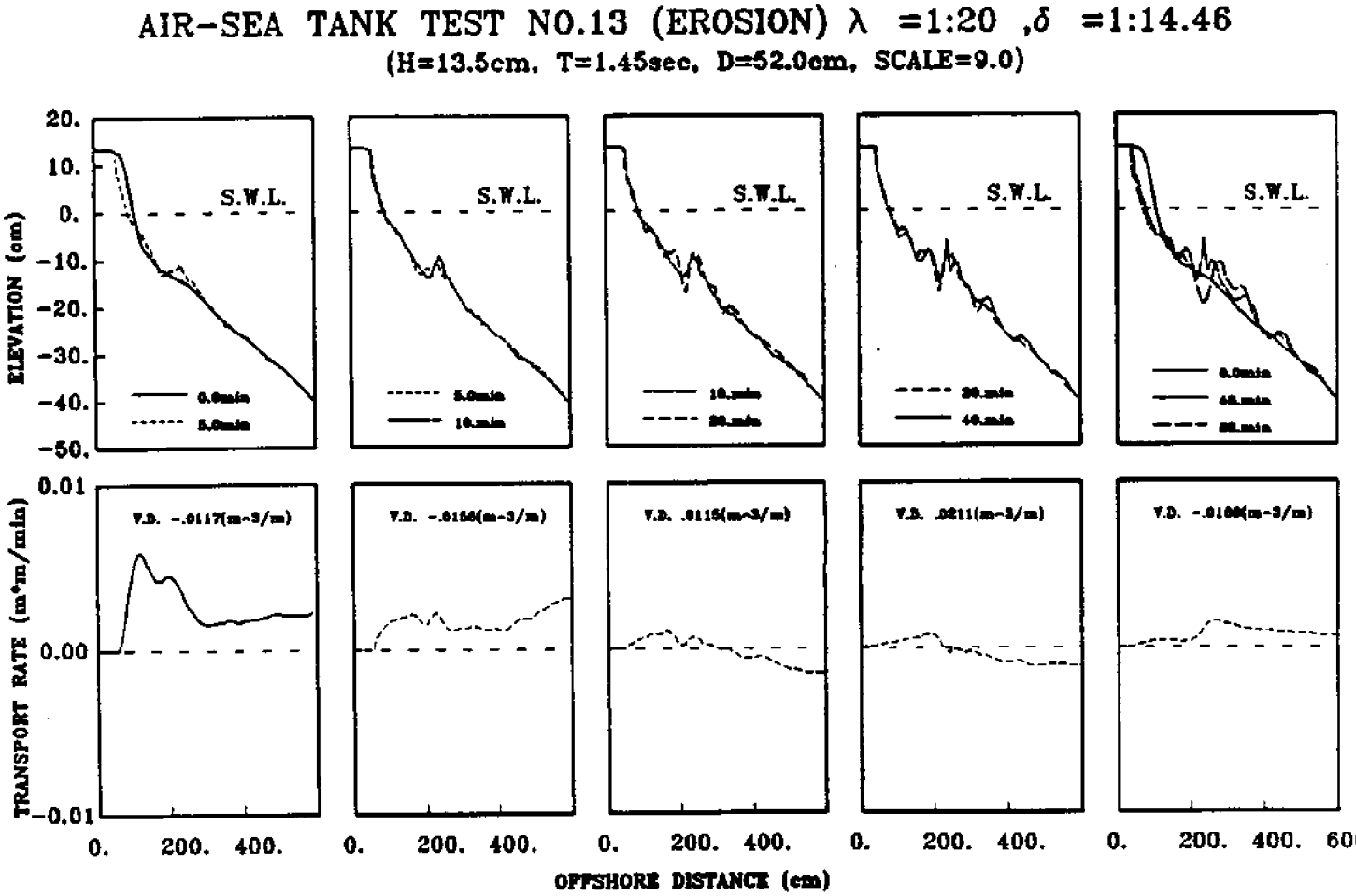

Figure A.13: Beach Profile Evolution and Sediment Transport Pattern of Test No.13

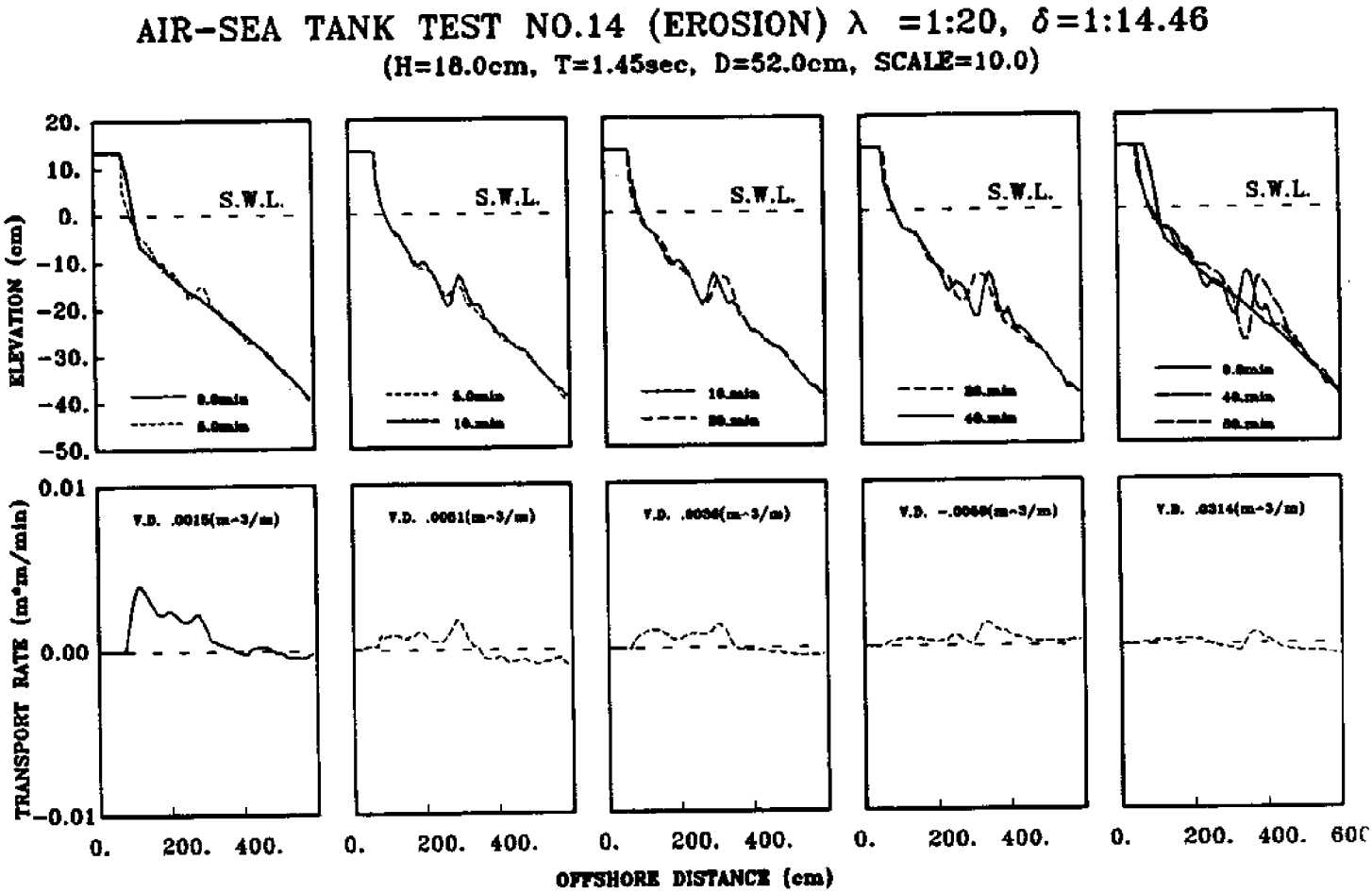

Figure A.14: Beach Profile Evolution and Sediment Transport Pattern of Test No.14

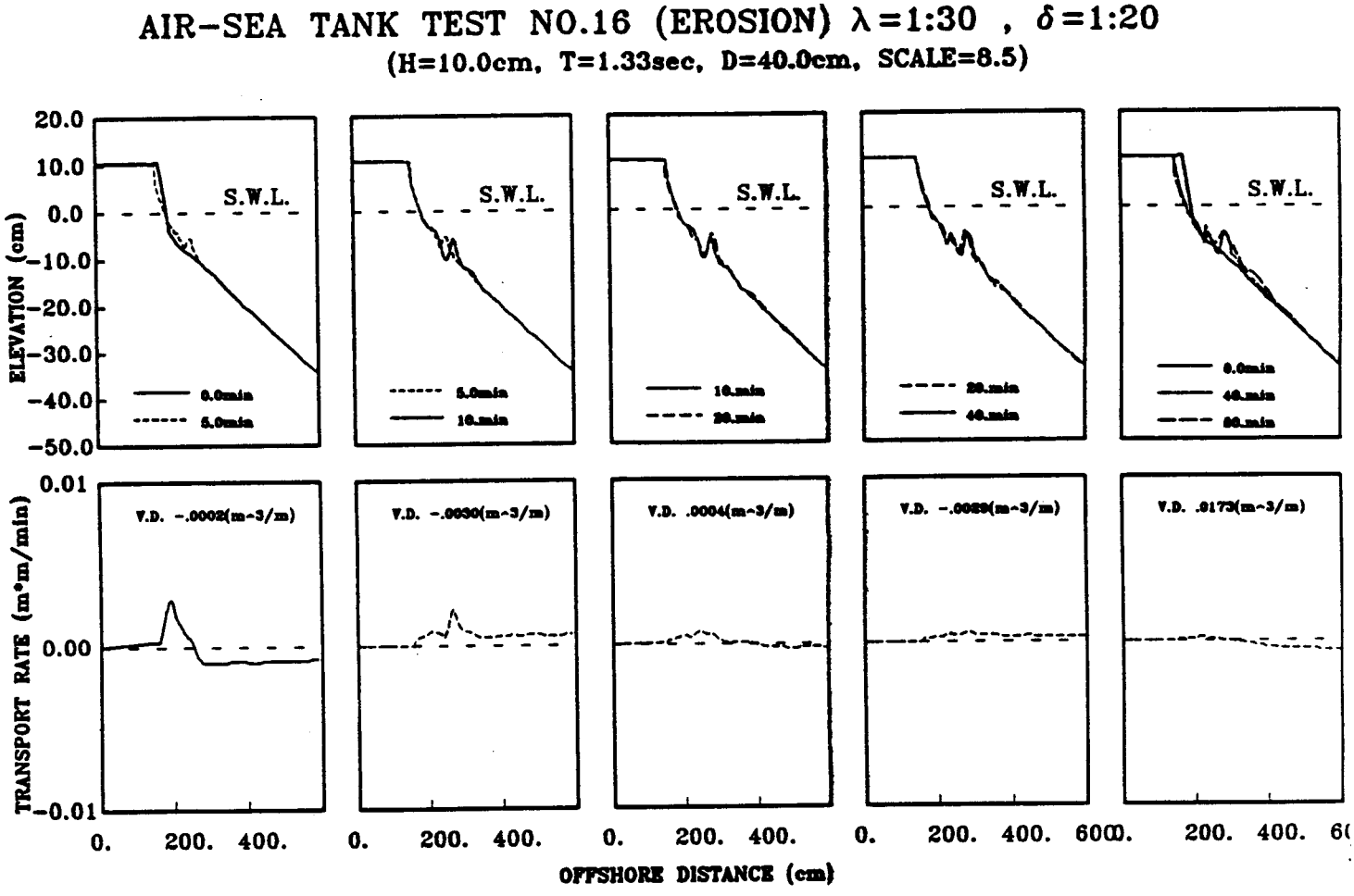

Figure A.15: Beach Profile Evolution and Sediment Transport Pattern of Test No.16

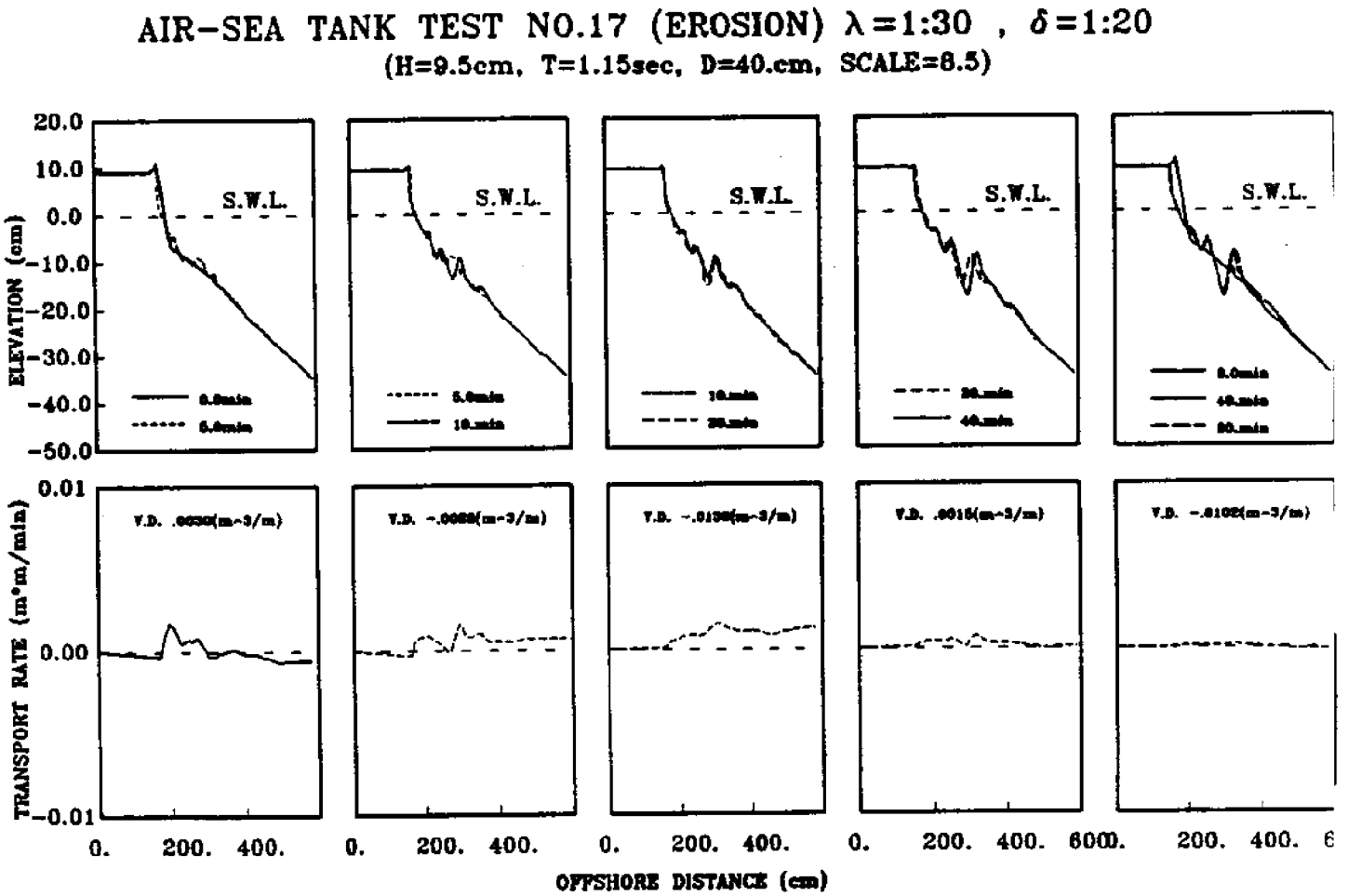

Figure A.16: Beach Profile Evolution and Sediment Transport Pattern of Test No.17

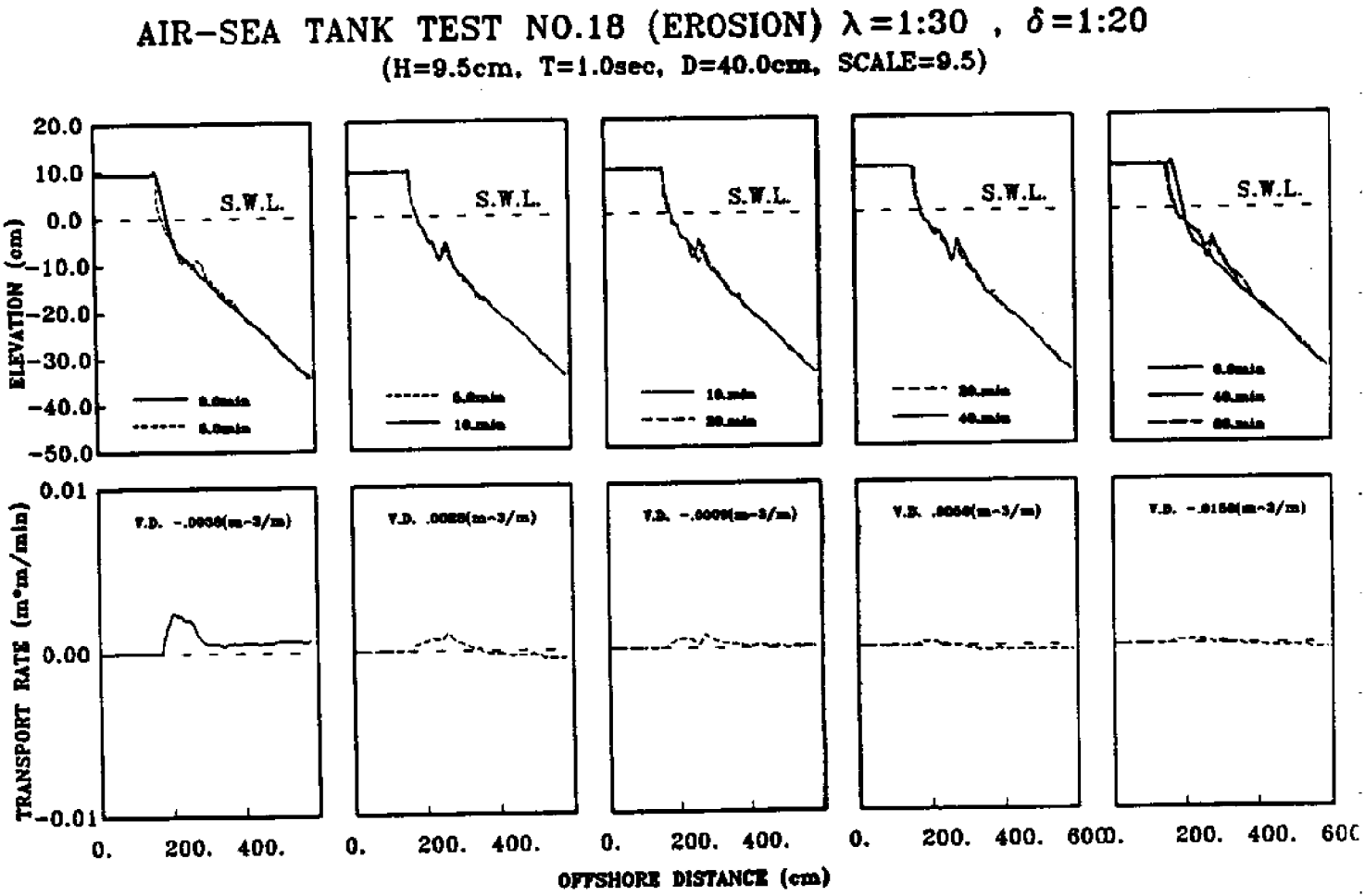

Figure A.17: Beach Profile Evolution and Sediment Transport Pattern of Test No.18

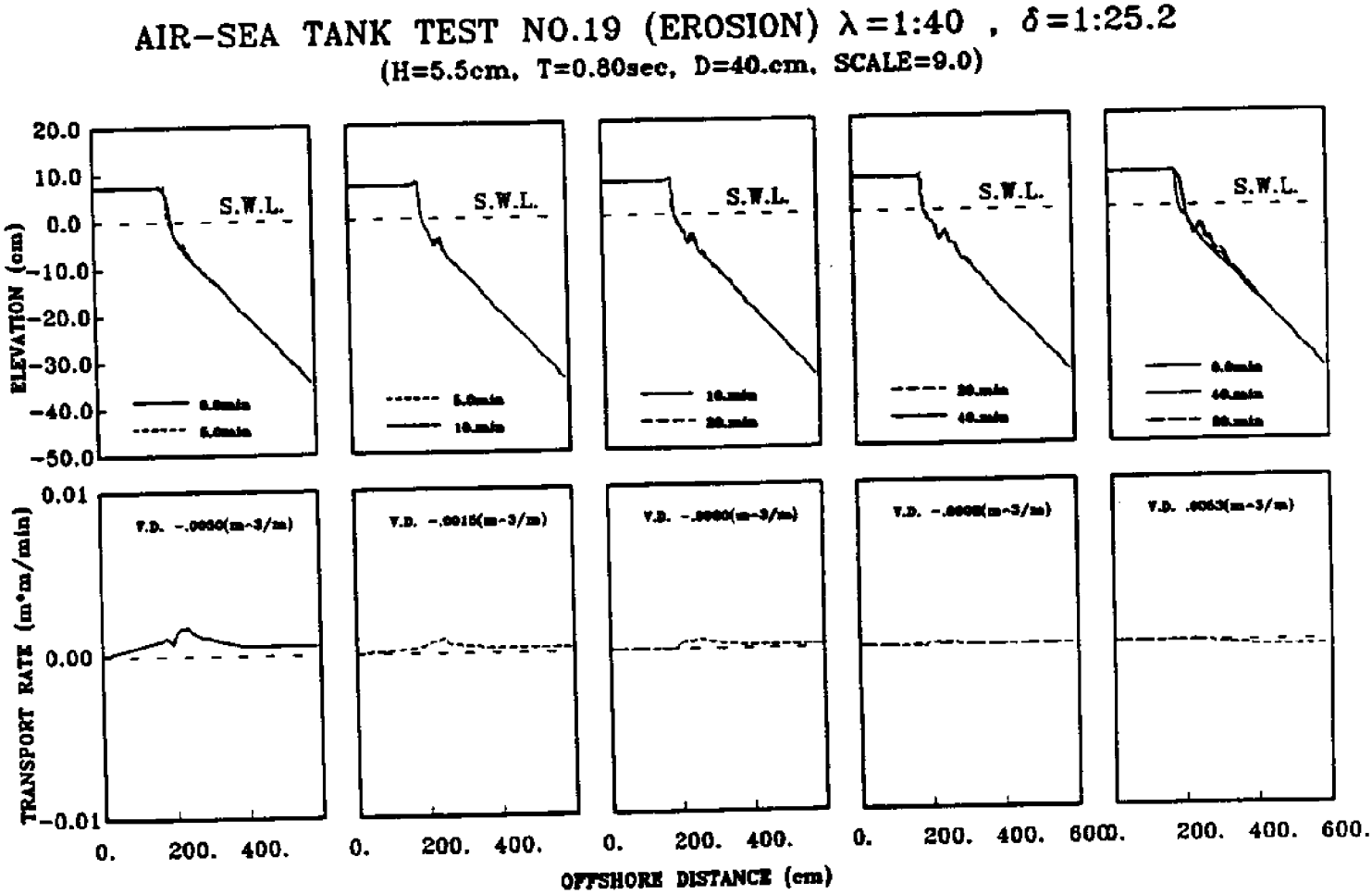

Figure A.18: Beach Profile Evolution and Sediment Transport Pattern of Test No.19

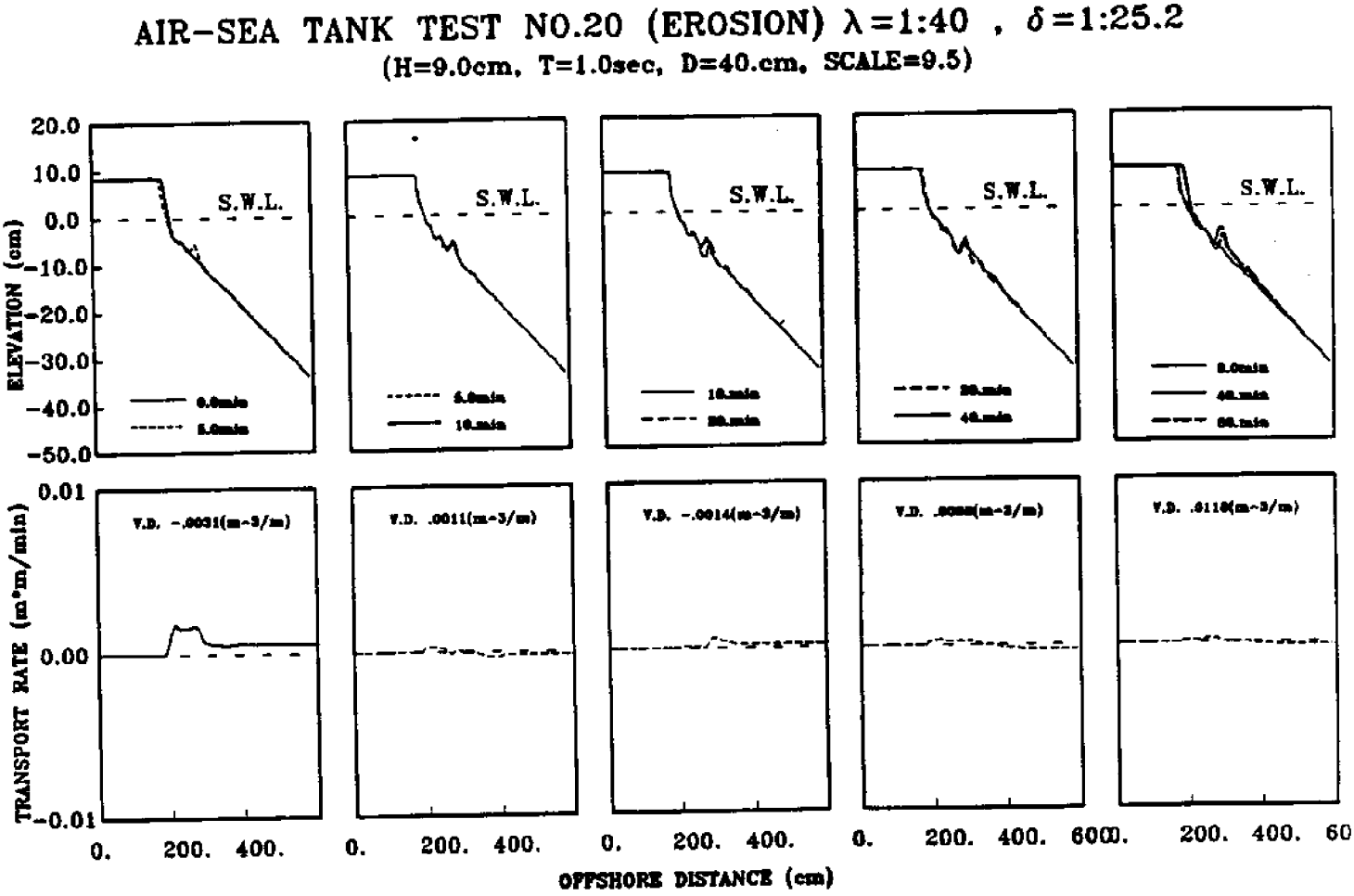

Figure A.19: Beach Profile Evolution and Sediment Transport Pattern of Test No.20

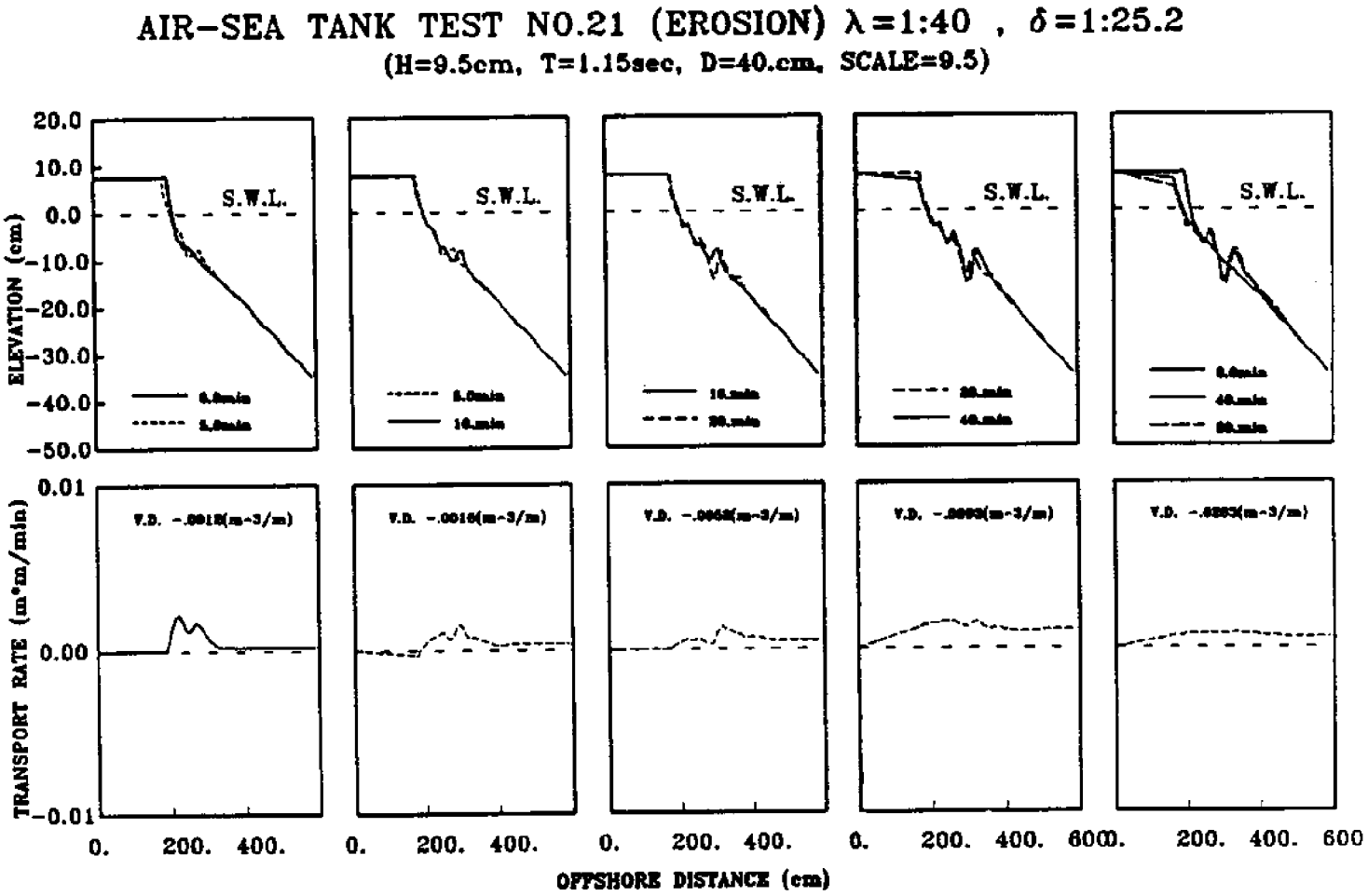

Figure A.20: Beach Profile Evolution and Sediment Transport Pattern of Test No.21

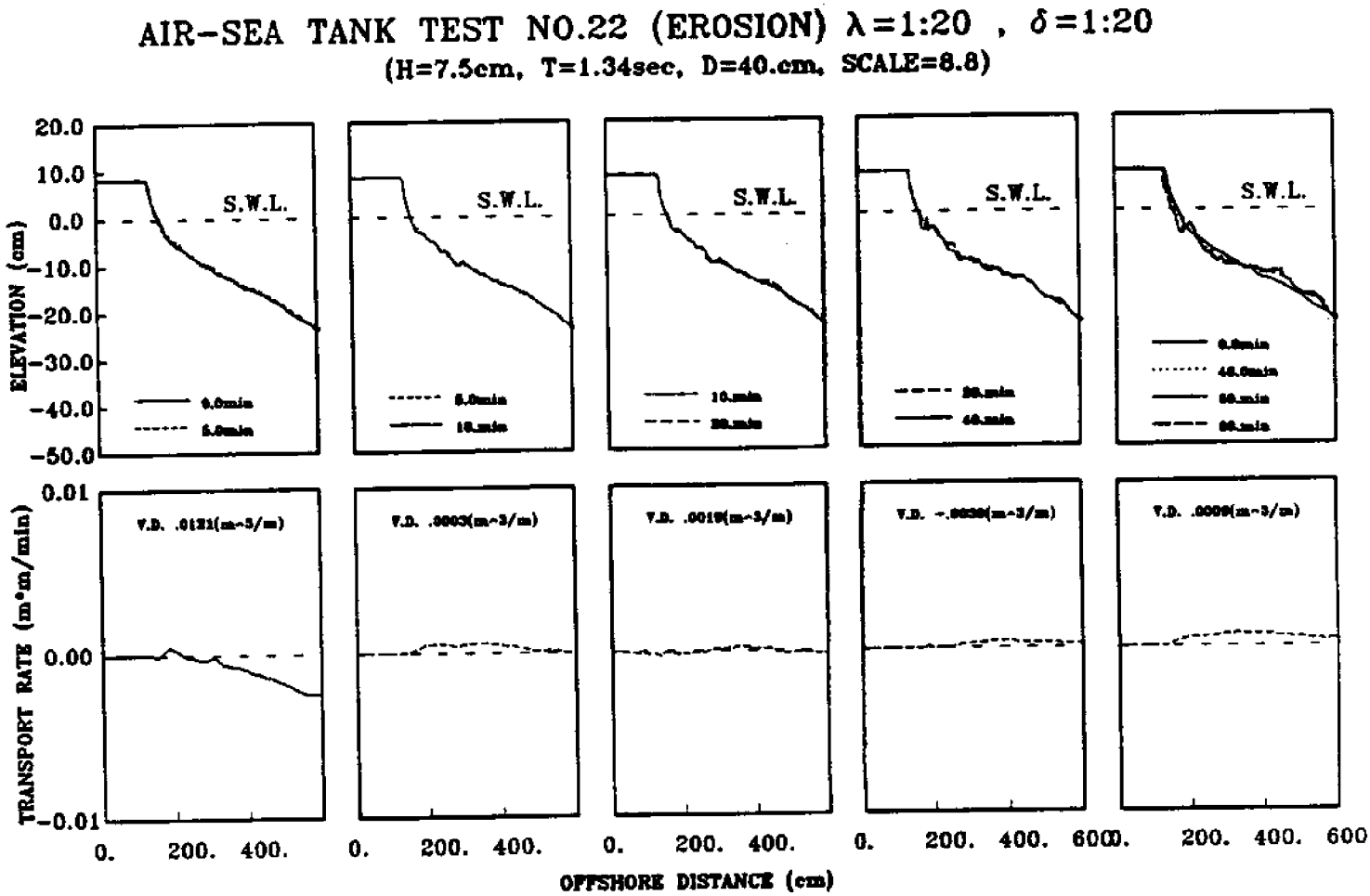

Figure A.21: Beach Profile Evolution and Sediment Transport Pattern of Test No.22

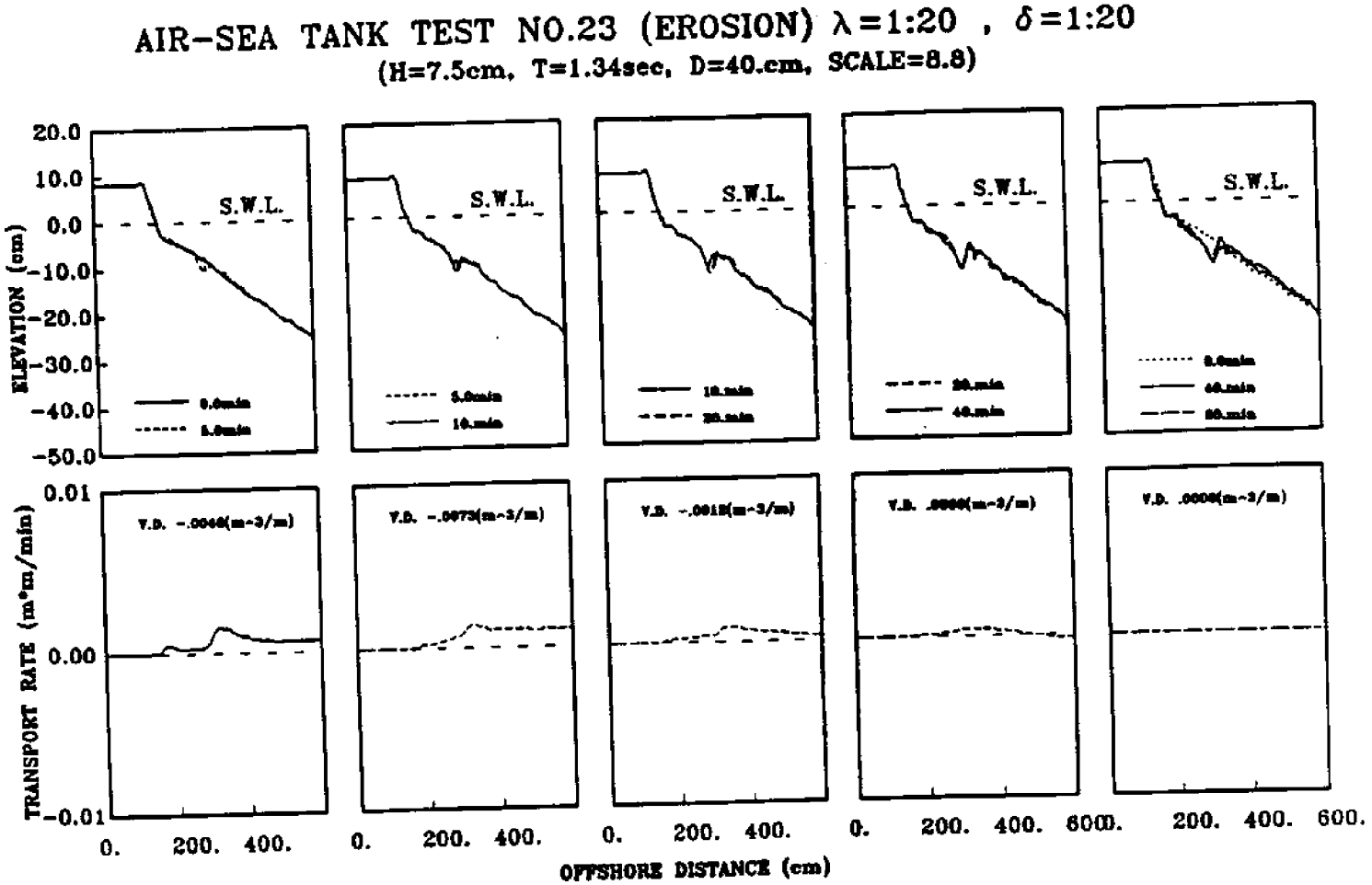

Figure A.22: Beach Profile Evolution and Sediment Transport Pattern of Test No.23

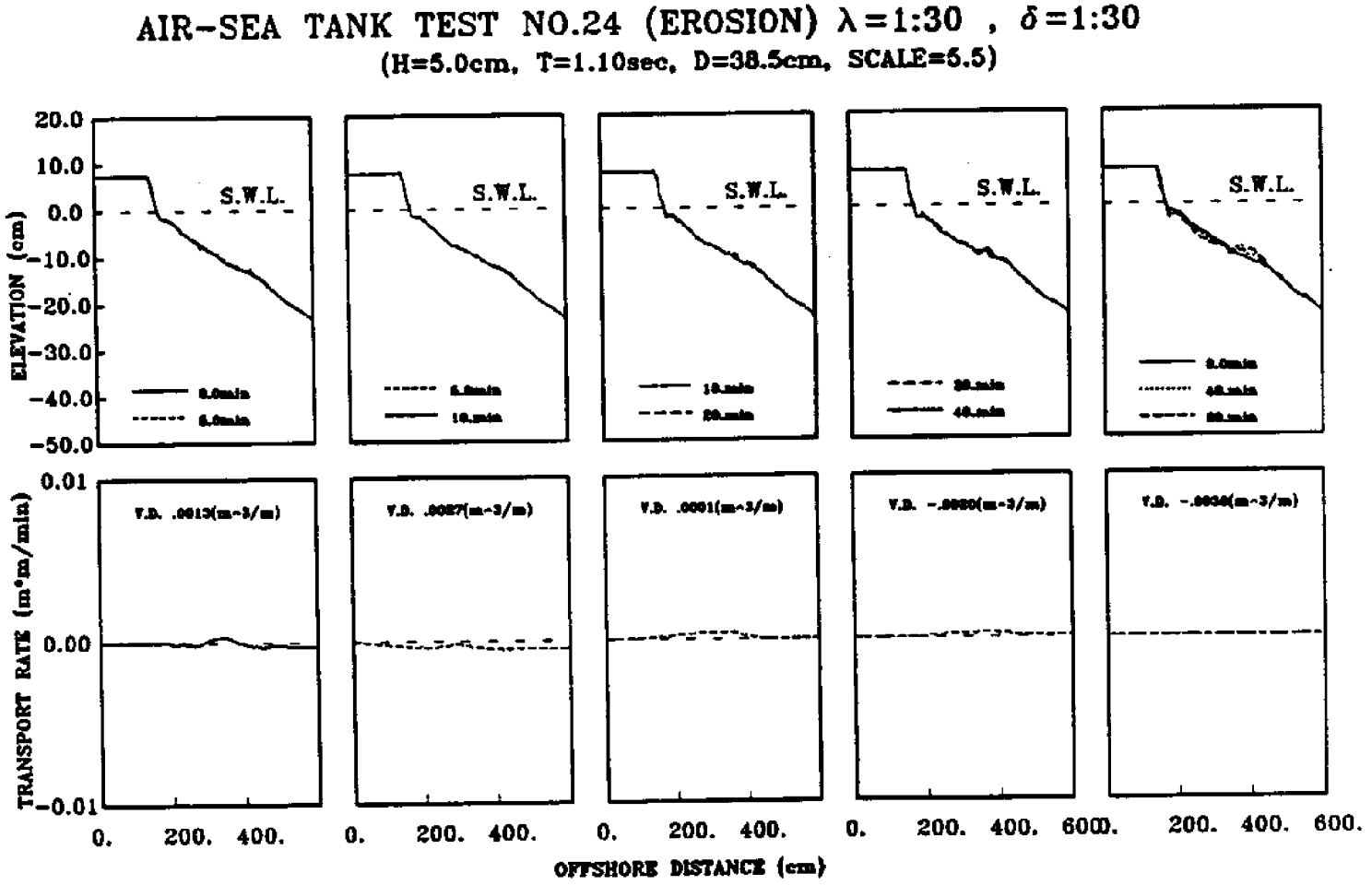

Figure A.23: Beach Profile Evolution and Sediment Transport Pattern of Test No.24

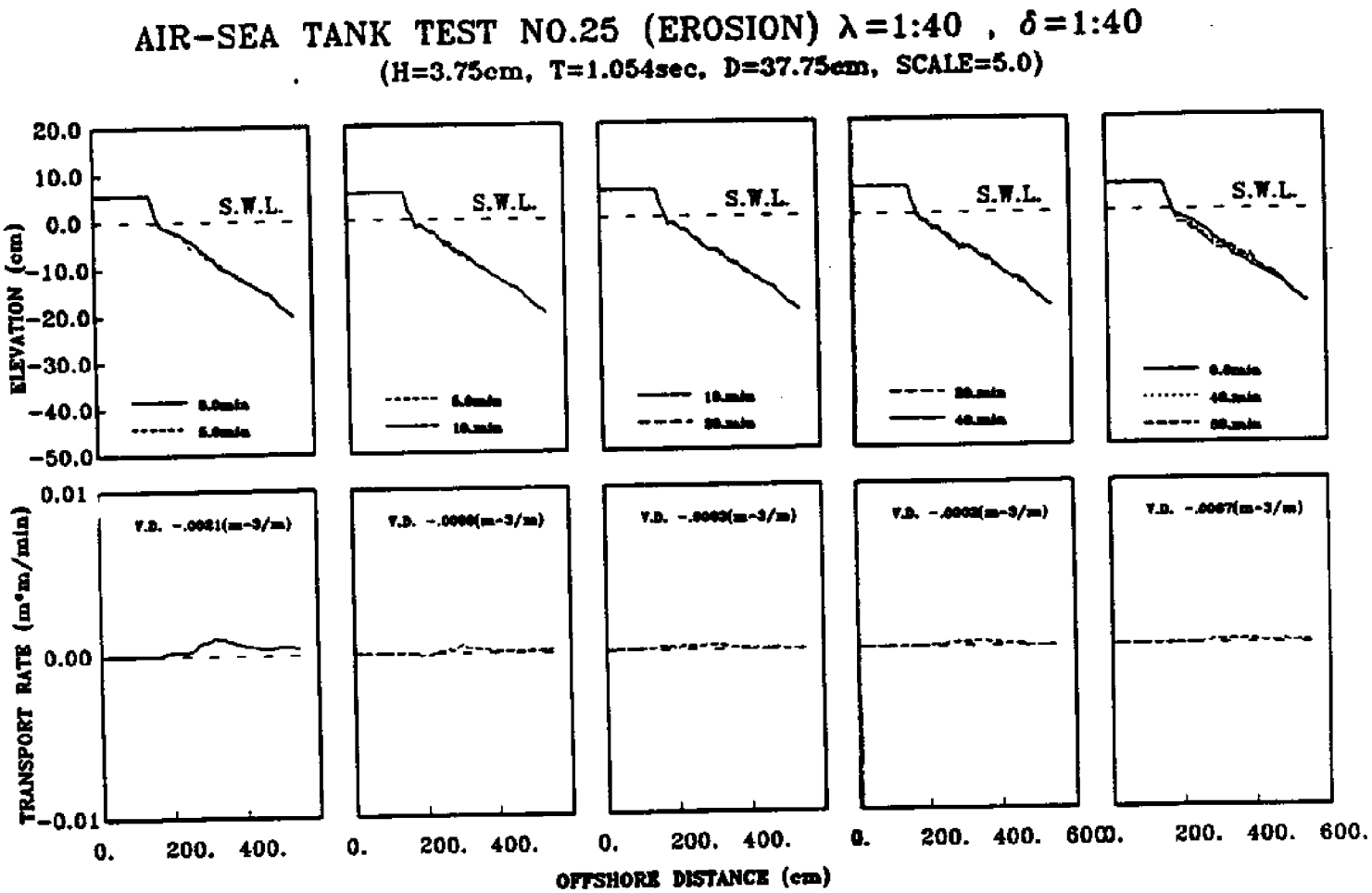

Figure A.24: Beach Profile Evolution and Sediment Transport Pattern of Test No.25

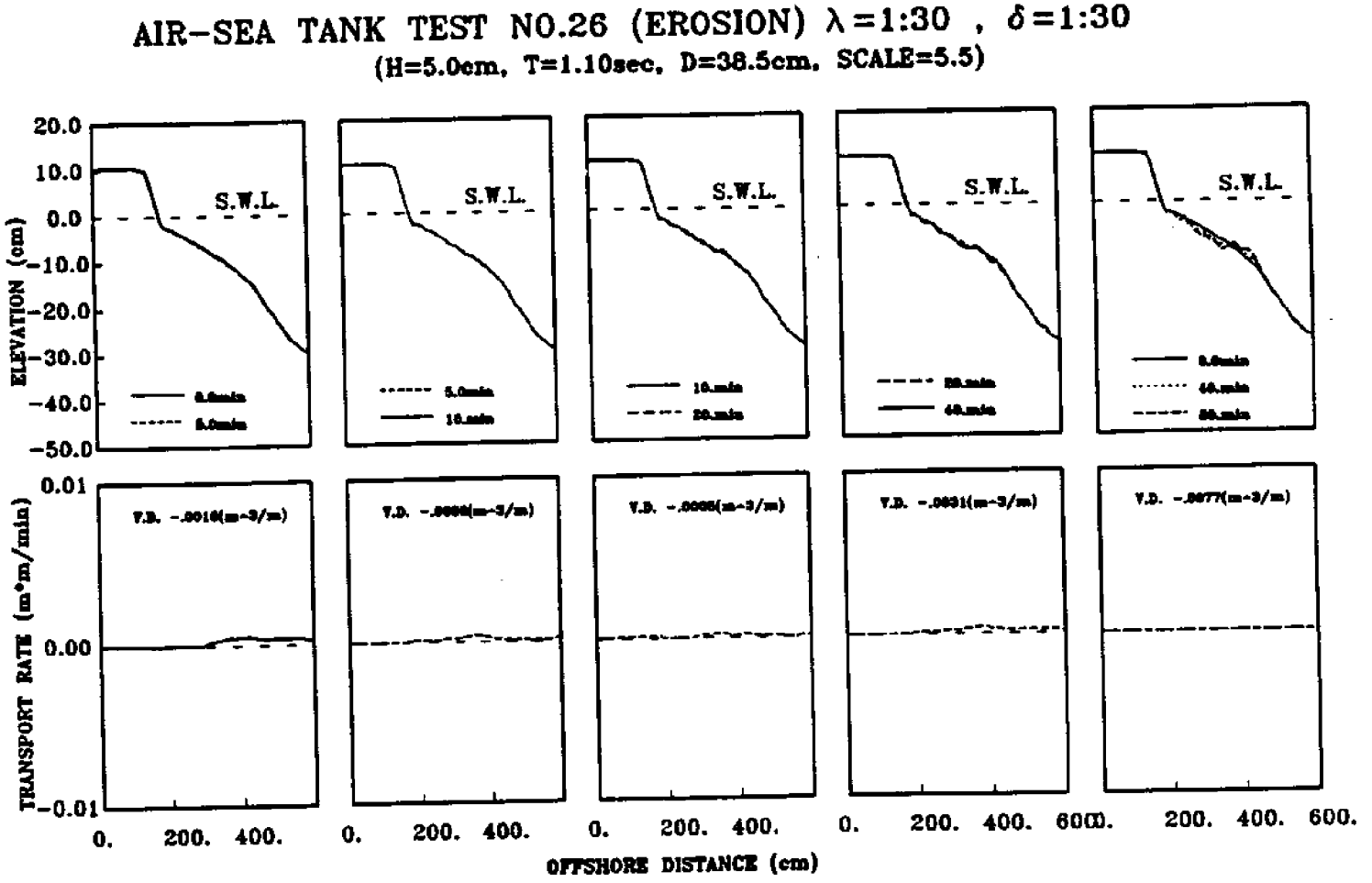

Figure A.25: Beach Profile Evolution and Sediment Transport Pattern of Test No.26

BIBLIOGRAPHY

Bagnold, R. A. 1940. "Beach Formation by Waves; Some Model- Experiments in a Wave Tank," Journal of the Institution of Civil Engineers, Vol 1, pp 27-52.

Bailard, J. A. 1981. "An Energetics Total Local Sediment Transport Model for a Fine Plane Sloping Beach," Journal of Geographical Research,Vol 80,no.c11,pp 10938-10954

Bailard, J. A. 1982. "Modeling on-offshore Sediment Transport in the Surfzone," Coastal Engineering Conference, American Society of Engineering, Cape Town, Republic of South Africa

Dalrymple, R. A. and Thompson, W. W. 1976. "Study of Equlibrium Beach Profiles," Proceedings of 15th Coastal Engineering Conference, American Society of Engineering, Honolulu, Hawaii, pp. 1277-1296.

Dean, R. G. 1973. "Heuristic Models of Sand Transport in the Surf Zone," Proceedings of the Conference on Engineering Dynamics in the Surf Zone, Sydney, Australia, pp. 208-214.

Dean, R. G., Dalrymple, R.A. 1985. "Physical Modeling of Littoral Processes," Physical Modelling in Coastal Engineering, The Netherlands, pp. 119-139.

Dette, H. H. and Uliczka, K. 1986. "Prototype and Model Evolution of Beach Profile," Proceedings of Symposium on Scale Effects in Modeling Sediment Transport Phanomena, Toronto, Canada.

Fan, L. N. and Le Mehaute, B. 1969. "Coastal Movable Bed Scale Model Technology," Tetra Tech, Inc. No. TC-131.

Graaff, J. V. 1977. "Dune Erosion During a Storm Surge," Journal of Coastal Engineering, Vol. 1, pp. 99-134.

Hughes, S. A. 1983. "Movable-Bed Modeling Law for Coastal Dune Erosion," Journal of Waterway, Port, Coastal and Ocean Engineering, New York,Vol. 109, No. 2, pp. 164-179.

Hughes, S. A. and Fowler, J. E. 1990. "Validation of Movable-Bed Modeling Guidance," Abstract, Proceedings of 22nd Coastal Engineering Conference, American Society of Engineering, Delft, Netherlands

Hudson, R., Herrmann, F., Sager, R., Whalin, R., Keulegan, G., Chatham, C. and Hales, L. 1979. "Coastal Hydraulic Models," SR-5, U.S. Army, Corps of Engineers, Coastal Research Center.

Kamphuis, J. W. 1974. "Practical Scaling of Coastal Models," Proceedings of 14th Coastal Engineering Conference, American Society of Engineering , New York, pp.2086-2101.

Kamphuis, J. W. 1975. "The Coastal Mobile Bed Model," Civil Engineering, Report No. 75, Queen's University, Kingston, Ontario, Canada, pp. 113.

Kamphuis, J. W. 1982. "Coastal Mobile Bed Modeling from a 1982 Perspective," Civil Engineering, Report No. 76, Queen's University, Kingston, Ontario, Canada.

Kriebel, D. L., Dally, W.R. and Dean, R.G. 1986. "Beach Profile Response Following Severe Erosion Events," UF/COEL-86/016,Coastal and Oceanographic Engineering Department, University of Florida,Gainesville,FL.

Kriebel, D. L., Dally, W.R. and Dean, R.G. 1986. "Undistorted Froude Model for Surf Zone Sediment Transport," Proceedings of 20th Coastal Engineering Conference, American Society of Engineering, Taipei, Taiwan, Vol. 2, pp. 1296-1310.

Larson, M. and Kraus, N. C. 1989. "SBEACH: Numerical Model for Simulating Storm-Induced Beach Change," Report 1, Technical Report CERC-89-9, U.S. Army Engineer Waterways Experiment Station, Coastal Engineering Research Center, Vicksburg, Mississippi.

Le Mehaute, B. 1970. "A Comparison of Fluvial and Coastal Similitude," Proceedings of the 12th Coastal Engineering Conference, Washington D.C. , pp. 1077-1095.

McCowan, J. 1894. "On the Gighest Wave of Permanent Type," Phil. Magazine, Series 5, 38.

Noda, E. K. 1972. "Equilibrium Beach Profile Scale-Model Relationship," Journal of the Waterways, Harbors and Coastal Engineering Division, Proceeding of the American Society of Civil Engineers, Vol. 98, No. WW4, pp. 511-528.

Noda, H. 1978. "Scale Relations for Equilibrium Beach Profiles," Proceedings of 16th Coastal Engineering Conference, American Society of Engineering, Hamburg, Germany, Vol. 2, pp. 1531-1541.

Saville, T. 1980. "Comparison of Scaled Beach Deformation Tests using Sand and Coal," Abstracts of the 17th Coastal Engineering Conference, American Society of Engineering, Sydney, Australia, pp.439.

"Shore Protection Manual", 1984. U.S. Army Corps of Engineers, Vol. 1, Department of the Army, Corps of Engineers, Washington, D.C.

Singamsetti, S. R. and Wind, H. G. 1980. "Characteristics of Shoaling And Breaking Periodic Waves Normally Incident To Plane Beaches Of Constant Slope ," University Of Florida, 1980.

Vellinga, P. 1978. " Movable Bed Model Tests on Dune Erosion," Proceedings of 16th Coastal Engineering Conference, American Society of Engineering , Hamburg, Germany, pp. 2020-2039.

Vellinga, P. 1982. " Beach and Dune Erosion During Storm Surges," Journal of Coastal Engineering , Vol. 6, pp. 361-389.

Wang, H. 1985. "A Note on Beach Profile Scale Modeling," Sorderdruck,aus Heft 88(1985) der Mitteilungeh der Leichtweiss-Instituls fur Wasserbau,der Technischen Universitat Braunschweig,pp.356-398.

Wang, H., Toue, T. and Dette, H. H. 1990. "Movable Bed Modeling Criteria for Beach Profile Response," Proceedings of the 22nd ICCE, American Society of Engineering, Deft, The Netherlands, Chapter 195,pp 2566.

Yalin, M. S. 1963. "Mehtod for Selecting Scales for Models with Movable Bed Involving Wave Motion and Tidal Currents," Proceedings of the 10th Congress of the International Association for Hydraulic Research, Vol. 1, pp. 221-229.